COMMISSION ON POWDER DIFFRACTION

INTERNATIONAL UNION OF CRYSTALLOGRAPHY

http://www.mpi-stuttgart.mpg.de/cpd/index.html

NEWSLETTER No. 31, May 2004

http://www.mpi-stuttgart.mpg.de/cpd/html/newsletter.html

IN THIS ISSUE

Powder Diffraction of Molecular Functional Materials

(Norberto Masciocchi, Editor)

CPD Chairman's Message

The present newsletter edited by Norberto Masciocchi nicely demonstrates that powder diffraction is an indispensable tool for the analysis of technically important molecular compounds. In this regard, I would like to draw your attention to our new section for "educational exercises" and "teaching pamphlets" at http://www.mpi-stuttgart.mpg.de/cpd/html/news.html. In particular the exercise on how to distinguish between the different isomers from Alq_3 (a "hot candidate" for blue LED's) using high resolution powder diffraction data is a nice one and I encourage all newcomers to the field to give it a try. The teaching section is still in its infancy and I strongly hope that some of you will send in their contributions which would be for the benefit of everyone in the community.

I have started to keep our address base up to date by removing false addresses etc. Therefore since the largest expenses are due to mailing costs, I urge you to report address changes to me in good time.

Although we try our best, Newsletter No. 30 did not appear on time for various reasons. We do not want to trade our high standard for speed and apologize for the delay. All issues of the scanned newsletters have finally been corrected for scanning and typographical errors and are now available for download at http://www.mpi-stuttgart.mpg.de/cpd/html/newsletter.html. Now, all newsletters easily fit on a "collectors" CD.

On a long term scale, I agreed to be the editor of a basic textbook on powder diffraction which will be published by the Royal Society of Chemistry. The entire CPD will be strongly involved in this project.

I encourage all readers of the newsletter to report any powder related news to me. In particular, Lachlan Cranswick and I are always interested in new or updated computer programs, scripts, macros or other solutions using graphics programs etc. To develop the latter, usually one spends a lot of time but after the project is finished they are quickly discarded and the wheel will be invented over and over. Sometimes, it turns out that software not specifically written for powder diffraction is very well suited for a particular problem related to powder diffraction and a little note on this would be very welcome. As a recent example from my own lab, I was looking for a program which quickly converts atomic coordinates between different space groups and reliably detects missing symmetry within a given tolerance. It turned out that KPLOT by Rudolf Hundt (available free of charge at http://www.crystalimpact.de/download/kplot.htm) does the job.

Robert Dinnebier

From the Editor of Newsletter 31

For decades, chemists, mineralogists and material scientists have been employing powder diffraction as the most powerful (analytical and structural) method in the characterization of metals, alloys, salts, rocks and ores, *i.e.* of *classic* **inorganic** compounds. Until the mid 90's, the realm of *molecular* materials (such as **organics** and pharmaceutically active species) was largely colonized by single crystal diffraction since their structural complexity and their weakly diffracting behavior at high angles seemed to restrict the use of powder diffraction to phase identification (which is, nevertheless, a highly profitable activity: indeed, quantification and detection of polymorphs and solvates have consequences of high economical value). Once the recent improvements in radiation sources, optics, instrumentation, detectors, computers and software were made available to the wide community of structural chemists, the derivation of a structural model for such species (*from powder diffraction data only*) came within reach. The increase of instrumental resolution and new efforts in devising indexing algorithms make its possible to detect, even from polyphasic mixtures, the correct unit cell of an unknown species, and, eventually, to solve (by a combination of direct- or reciprocal-space techniques, brutal force, and more advanced methods) their crystal *and* molecular structures. Recently, also the structures of a number of **organometallic** species and covalent **polymers** have been successfully retrieved, leading to the discovery of new stoichiometries, connectivities and geometries, unforeseen, unexpected or even badly postulated, throughout the years, on the basis of weak spectroscopic evidence. However, the recent progresses in the characterization of **molecular functional materials** are not limited to the *ab-initio* structure determination method only. As witnessed by the variety of the contributions collected in this Issue, the powder diffraction technique allowed to study a number of *smart 'exotic'* systems, such as glassy polymers, biological membranes, polymer electrolytes, nanoporous materials and low-dimensional magnetic or NLO active species, all being extremely **functional** in their very different miniaturized worlds.

Norberto Masciocchi

"*Science would soon come to a standstill if all scientists were of the same intellectual type. Science needs scholars with many different talents*."

Max von Laue

WWW sites related to powder diffraction

The Commission on Powder Diffraction (CPD): http://www.mpi-stuttgart.mpg.de/cpd/index.html
The International Union of Crystallography (IUCr): http://www.iucr.org/
The International Centre for Diffraction Data (ICDD): http://www.icdd.com/
The International X-ray Analysis Society (IXAS): http://www.ixas.org/
CCP 14: http://www.ccp14.ac.uk/

Submitting a proposal for neutron diffraction or synchrotron radiation X-ray diffraction is possible at many (publicly funded) large scale facilities in the world. It represents an important and frequently unique opportunity for powder diffraction experiments. A useful guide and information can be accessed through the following web-site, maintained by R. Dinnebier at http://www.pulverdiffraktometrie.de/

This list is far from being complete and needs input from users and readers of the CPD Newsletter. Please send comments to *R. Dinnebier* (r.dinnebier@fkf.mpg.de)

Call for contributions to the next CPD Newsletter (No 32)

The next issue of the CPD Newsletter will be edited by Rob Delhez, to appear in December 2004. Rob will greatly appreciate contributions from readers on matters of interest to the powder diffraction community, e.g. meeting reports, future meetings, developments in instruments, techniques, and news of general interest. Please contact him for sending articles and suggestions. Software developments can be directly addressed to Lachlan Cranswick or to the Editor of Newsletter No 32 (addresses are given below). For those wondering about the gap between newsletter No 29 and No 31, the winter issue (No 30) edited by Camden Hubbard is delayed but we expect publication shortly.

Dr. R. (Rob) Delhez
X-ray diffraction Laboratory of Materials Science
Rotterdamseweg 137, 2628 AL Delft, The Netherlands
Phone:+31 (0)15 278 22 61 Fax: +31 (0)15 278 67 30
e-mail: R.Delhez@tnw.tudelft.nl

Dr Lachlan M. D. Cranswick
Neutron Program for Materials Research, National Research Council Canada
Building 459, Chalk River Laboratories, Chalk River ON, Canada, K0J 1J0
Phone: +1 (613) 584-8811 ext 3719 ; C2: ext 3039 Fax: +1 (613) 584-4040
E-mail: lachlan.cranswick@nrc.gc.ca
http://neutron.nrc.gc.ca/

How to receive the IUCr CPD Newsletter

If you wish to be added to the mailing list for the Newsletter of the IUCr Commission on Powder Diffraction or have changed address, please contact the Chairman:

Robert Dinnebier (r.dinnebier@fkf.mpg.de).

The Newsletter can also be downloaded in electronic format, as a .pdf file, from the CPD web-site.

Companies

If you would like to advertise in this twice-yearly newsletter, please contact Robert Dinnebier

e-mail: r.dinnebier@fkf.mpg.de
Telephone: +49-711-689-1503
Fax: +49-711-689-1502

THE IUCR COMMISSION ON POWDER DIFFRACTION - TRIENNIUM 2002-2005

Chairman: Dr R. E. Dinnebier (Robert)
Max-Planck-Institut für Festkörperforschung,
Heisenbergstrasse 1, D-70569 Stuttgart, Germany
Telephone: +49-711-689-1503 | Fax: +49-711-689-1502
e-mail: r.dinnebier@fkf.mpg.de

Secretary: Prof. A. N. Fitch (Andy)
ESRF, BP220, F-38043 Grenoble Cedex, France
Telephone : +33 476 88 25 32 | Fax: +33 476 88 25 42
e-mail: fitch@esrf.fr

Dr R. Delhez (Rob)
Laboratory of Materials Science, Delft University of Technology, Rotterdamseweg 137 2628 AL Delft, The Netherlands
Telephone: +31 15 2782261 | Fax: +31 (15) 278 6730
e-mail: R.Delhez@tnw.tudelft.nl

Prof. N. Masciocchi (Norberto)
Dipartimento di Scienze Chimiche ed Ambientali,
Università dell'Insubria,
via Valleggio 11, 22100 Como (Italy)
Telephone: +39-031-326227 | Fax: +39-031-2386119
e-mail: norberto.masciocchi@uninsubria.it

Dr C. R. Hubbard (Cam)
Diffraction and Thermophysical Properties Group, MS 6064, Bldg 4515, High Temperature Materials Laboratory, Metals & Ceramics Division, Oak Ridge National Laboratory, Oak Ridge, TN 37831-6064
Telephone: 865-574-4472 | Fax: 865-574-3940
e-mail: hubbardcr@ornl.gov

Dr D. Balzar (Davor)
Department of Physics & Astronomy
University of Denver
2112 E Wesley Ave, Denver, CO 80208-0202
Telephone: 303-871-2137 | Fax: 303-871-4405
e-mail: balzar@du.edu

Prof. G. J. Kruger (Gert)
Department of Chemistry & Biochemistry, Rand Afrikaans University, P O Box 524, Aucklandpark, South Africa
Telephone: +27 11 489 2368 | Fax: +27 11 489 2360
e-mail: gjk@na.rau.ac.za

Dr. I. Madsen (Ian)
CSIRO Minerals
Box 312, Clayton South 3169
Victoria, Australia
Telephone: +61 3 9545 8785 | Fax: +61 3 9562 8919
e-mail; Ian.Madsen@csiro.au

Prof. W. I. F. David (Bill)
Rutherford Appleton Laboratory (CCLRC), Chilton, Oxon. OX11 OQX, United Kingdom
Telephone: +44 1235 445179 | Fax: +44 1235 445383
e-mail: bill.david@rl.ac.uk

Prof. M. Delgado (Miguel)
Laboratorio de Cristalografía, Departamento de Química, Núcleo Universitario Dr. Pedro Rincón Gutiérrez, Sector La Hechicera. Edif. "A". Nivel Patio. Universidad de Los Andes, Mérida, Venezuela
Telephone: +58 274240-1372
e-mail: migueld@ula.ve

ICDD Representative
Prof. R. L. Snyder (Bob)
Department of Materials Science & Engineering, Georgia Institute of Technology, Columbus, 771 Ferst Dr. N.W., Atlanta, GA 30332-0245, USA;
Telephone: +1 (404) 894-2888 | Fax: +1 (404) 894-2888
e-mail: bob.snyder@mse.gatech.edu

Consultants
Prof. P. Scardi (Paolo)
Dipartimento di Ingegneria dei Materiali e Tecnologie Industriali, Università di Trento, 38050 Mesiano (TN), Italy;
Telephone: +39 0461 882417/67 | Fax: +39 (461) 881977
e-mail: Paolo.Scardi@ing.unitn.it

Dr F. Izumi (Fujio)
National Institute for Research in Inorganic Materials
1-1 Namiki, Tsukuba, Ibaraki 305-0044, Japan
Telephone: +81-298-51-3354 (ext. 511); FAX: +81-298-52-7449
e-mail: izumi@nirim.go.jp

XRPD Characterization of Organics

Vladimir V. Chernyshev
The Laboratory of Structural Chemistry,
Department of Chemistry, Moscow State University
119992 Moscow (Russia)
Vladimir@struct.chem.msu.ru

Introduction

X-Ray powder diffraction (XRPD) is now one of the most widely used techniques available to materials scientists for studying the structure and microstructure of crystalline solids. XRPD is a routine tool for quali- and quantitative phase analysis, and an important method for material characterization, probing strain, stress, texture, defects and stacking faults in a large variety of structures. A major advance in recent years has occurred in the determination of crystal structure *ab initio* from powder diffraction data [1-9], in cases where suitable single crystals are not available. Numerous research groups working in universities and industrial laboratories actively use various methods for the structure determination by XRPD and obtain reliable three-dimensional structures (recent examples for organic compounds see in [10-21]).
In this paper we will focus mainly on a methodology used in our group in XRPD characterization of organic materials with the unknown crystal structure.

Indexing

XRPD characterization of new organic sample is always started from a special X-ray powder diffraction pattern measurement on a laboratory device - Guinier camera and/or Bragg-Brentano vertical powder diffractometer DRON-3. This pattern allows us estimate the degree of crystallinity of material under investigation. Sometimes, there are only 3-5 broad diffraction peaks in the pattern, or no peaks at all, so the sample needs to be re-crystallized.
The detection of peaks and the location of their positions, which may not coincide with their maxima, is carried out with the program MRIA [22], first by automatic peak search option and then by careful manual inspection. As a result the set of d-spacings (d's) and intensities (I's) of peaks can be derived from the pattern and used further in the search and identification of (possible) impurities in the sample. This search is based on a comparison of experimental data with standard d's and I's contained in the Powder Diffraction File (PDF) database [23] or with those calculated from the known crystal structures of organic and organo-metallic materials, contained in the Cambridge Structural Database, CSD [24]. The identification of an impurity, which is usually a small amount of the source or intermediate reagents, makes it possible to eliminate all its diffraction peaks from the data set.
For the indexing purposes we use TREOR [25], ITO [26] and AUTOX [27, 28]. Each of these programs is based on their own algorithms for indexing, so when processing the same data set, only one of the above programs, as sometimes happens, leads to the correct unit cell. Several unit cells, which provide the better figure of merit M_{20} [29], are tested further with the Pawley fit [30] in the appropriate space group without systematic extinctions. The main problem for the indexing is created by extra peaks from unknown impurities, which may often be present in the sample, obtained as a result of a new synthetic route. The chemists are always sure they obtained a pure compound, we have the same hope and, therefore, do not like the unit cell, which may be correct, but can not describe all diffraction peaks. The indexing of the pattern of non-pure compound becomes much more complicated procedure, when the unit cell content is different from the expected one, for example, due to the solvent co-crystallization.
An illustrative example is indexing of hydrated form of doxazosin mesylate. The crystal structures of two modifications of doxazosin mesylate $C_{23}H_{26}N_5O_5^+ \cdot CH_3SO_3^-$, 4-amino-2-[4-[(2,3-dihydro-1,4-benzodioxin-2-yl) carbonyl]piperazin-1-yl]-6,7-dimethoxyquinazoline methanesulfonate, a commonly used antihypertensive agent, have been determined by synchrotron X-ray powder diffraction [31]. An anhydrous form, **A**, crystallizes in monoclinic unit cell with the volume (V) of 5026 Å^3, Z = 8, so the volume increment of one structural unit, V/Z, is equal to 628 Å^3. The second studied modification of doxazosin mesylate, *d***G**, was obtained while preparing the another anhydrous form, **G**, following the method described in original patent [32].

Table 1. First 25 peaks, d's and I's, from the powder pattern of hydrated form *d***G** of doxazosin mesylate. Those of an unidentified impurity are starred.

d, Å	I, %	d, Å	I, %
16.108	21	6.260	5*
9.698	100	6.097	1
9.563	6*	5.646	1
8.596	11	5.431	39
8.496	2*	5.365	19
8.048	22	5.207	6
7.696	18	5.084	3
7.380	21	5.021	28
7.224	51	4.994	16
7.111	10	4.896	14
6.732	25	4.854	13
6.618	2*	4.785	16
6.374	20		

Therefore, we expected that correct indexing for the second modification, the positions of 25 peaks of which are shown in Table 1, will provide

approximately the same volume increment *V*/*Z*. However, no solution was found which could index all peaks from the Table 1. Two possible unit cells, orthorhombic with V = 5180 Å^3, M_{20} = 6, and monoclinic with V = 2716 Å^3, M_{20} = 36, left two and four unindexed peaks, respectively. The M_{20} criterion and the Pawley fit give preference to the monoclinic unit cell, while the volume increment consideration and comparison of numbers of unindexed lines support the orthorhombic unit cell. A visual comparison of powder pattern of *d***G** with the powder pattern for **G** published in original patent [32] shows their non-coincidence. It is known [33] also that form **G** is hygroscopic and at ambient conditions it tends to form a hydrate. Therefore, the presence of the solvent water molecules in the monoclinic unit cell could explain the increase of volume increment. However, an exhaustive answer on the question of which unit cell is correct for *d***G** was obtained only after the crystal structure determination [31] in the monoclinic unit cell, where two water oxygen positions were found in asymmetric unit.

Sometimes, when indexing programs [25-28] failed in a standard run with the non-primitive centered unit cells, a careful inspection of the output can give an idea, which may lead to the correct indexing. This was the case of anhydrous form **A** of doxazosin mesylate [31], when standard indexing "walked" around the two monoclinic unit cells with *a*, *b*, *c*, β equal to 31.18 Å, 7.77 Å, 10.46 Å, 97.36°, and 15.59 Å, 7.77 Å, 20.92 Å, 97.36°, respectively. Both these unit cells left a number of unindexed lines. However, the Pawley fit with the "combined" monoclinic unit cell - 31.18 Å, 7.77 Å, 20.92 Å, 97.36° - led to the perfect fitting and allowed establishing the space group of *I2/c*, which was further transformed into *C2/c* with β = 118.72°.

There are also examples of indexing, where the results of Pawley fit can not help to choose the correct unit cell between several possibilities, so only structure solving provides the unique answer. An illustrative example is indexing of nitroxoline [34] - 8-hydroxy-5-nitroquinoline, $C_9H_6N_2O_3$, from the pattern measured at DRON-3 diffractometer. Two unit cells, monoclinic - *a* = 14.07 Å, *b* = 15.60 Å, *c* = 3.845 Å, β = 94.57°, *V* = 842 Å^3, space group of $P2_1/c$, *Z* = 4, and orthorhombic - *a* = 28.05 Å, *b* = 31.20 Å, *c* = 3.727 Å, *V* = 3261 Å^3, space group of *Fdd2*, *Z* = 16, provided the close R_{wp} values after the Pawley fit - 0.056 and 0.051 for monoclinic and orthorhombic cells, respectively (see also Fig. 1).

All attempts to solve crystal structure of nitroxoline in the monoclinic unit cell failed, after that the solution was found in the orthorhombic cell. Extrapolating this example to the high-resolution patterns we expect the same problems with the indexing of unit cell with the higher volume, when the crystal structure determination only will allow to choose between several possible unit cell dimensions.

The indexing is becoming more and more important stage in the full structural characterization of powder substances. We estimate our success rate in crystal structure determination from powder diffraction data in case of correct indexing as 98%, so just indexing rather than structure solution is now more challenging task for us.

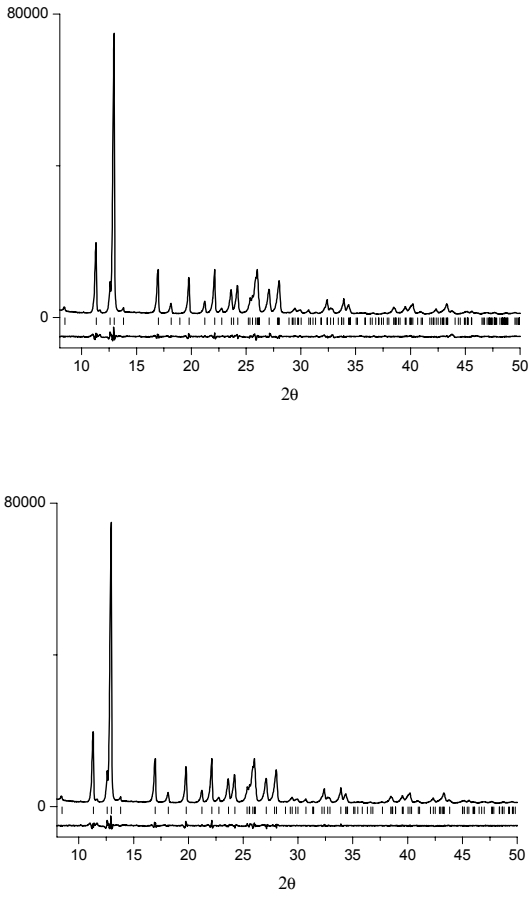

Figure 1. *The results of Pawley fit of nitroxoline in monoclinic (top) and orthorhombic (bottom) unit cells.*

Structure determination.

In the crystal structure determination we use the grid search [35] and simulated annealing [36] techniques developed in our group in close cooperation with the Laboratory for Crystallography (headed now by Dr. R. Peschar and earlier - by Prof. Dr. H. Schenk), University of Amsterdam. Both these techniques are incorporated into the MRIA program [22]. Although simulated annealing consumes essentially less computing time we still prefer the grid search technique, which allows an exhaustive exploration of all possible positions of the molecule(s) in the crystal structure and effectively helps us to avoid a false solution. The starting molecular models are usually taken from the Cambridge Structural Database [24] or constructed by DFT, program PRIRODA [37], or semi-empirical quantum chemical calculations, programs PCMODEL [38] and MOPAC [39], using the preliminary data of IR and NMR spectroscopy and mass spectrometry.

In the direct-space approach for solving crystal structures from powder diffraction data, the suitability of each position and orientation of the molecule(s) in the crystal lattice is quantified using an appropriate figure-of-merit, for instance, the weighted profile R factor R_{wp}, which takes peak overlap into account implicitly. We prefer to work with another R factor, *R(X)* [35]

$$R(X) = \Sigma |X_{exp,j} - Scale\ X_{calc,j}| / \Sigma X_{exp,j} \quad (1)$$

where $$X_{calc} = \Sigma m_i Y_i F^2_{calc,i} \quad (2)$$

and m_i, Y_i ,$F_{calc,i}$ are the multiplicity, texture correction multiplier and structure factor of the reflection i, respectively. $X_{exp,j}$ in (1) corresponds to the integrated intensities of the peaks in the pattern. Their values are defined during the Pawley fit. In the case of overlapping reflections, X_{exp} contains the F^2 of several reflections, so in (2) i = 1, 2 etc. One can see, the set of $\{X_{exp}\}$ contains the same structural information like the whole pattern $\{y_{exp}\}$. At the same time, the essential advantage in the use of $\{X_{exp}\}$ set, without separation of the intensities of overlapping reflections into individual components, instead of $\{y_{exp}\}$ set is a sharp decrease in the number of experimental values, and, subsequently, in the computing time. For instance, the powder pattern of dichlorobis(2-methylquinoline-*N*-oxide)zinc(II), $ZnCl_2(C_{10}H_9NO)_2$ [40], contains 6001 experimental points $\{y_{exp}\}$, while the total number of X_{exp} values is equal to 221. Actually, computing *R(X)* (1) with the grid search or simulated annealing techniques, we do not use the whole set of $\{X_{exp}\}$, but rather several of tens, usually around 100, of low-angle values.

The polycrystalline samples of various compounds have a tendency for preferred orientation, or texture, which can have a pronounced influence on the course of structure determination. To take texture effects into account properly at the stage of crystal structure solution, additional patterns are measured either in opposite (transmission/reflection) mode or in the same mode with the specimen prepared in a different way. The comparison of two patterns with different degrees of texture allows us to identify the direction of preferred orientation and the principal value of the March-Dollase [41] texture parameter r (r>1 or r<1). During the subsequent calculation of X_{calc} (2), the approximate values of texture correction multipliers Y_i can be calculated for each reflection.

The less number of variable degrees of freedom used in the structural motif search the more reliable results provide both techniques - grid search and simulated annealing. Therefore, the possibility to decrease this number is always carefully investigated. Sometimes the powder data allow to locate first the position of heavy atom, say Cl [42, 43], by the Patterson method and then determine the position and orientation of the remaining molecular fragment(s). In the other cases [31, 44] the number of trial models can be sharply decreased by performing simple geometric analysis.

The X-ray powder data, particularly those measured on laboratory devices, are virtually insensitive to the positions of hydrogens. So H atoms are usually excluded from the initial molecular models used in *R(X)* calculations and positioned later geometrically in the solved structures. Solving the crystal structure from the neutron powder data [45, 46] requires the presence of H atoms in the initial models.

The Rietveld refinement, realized in the MRIA program, is often used in combination with the grid search to test several trial structures, which provide the minimal values of *R(X)* (1). In the final Rietveld refinement of definitely solved structures we always use the restraints to the intramolecular bond lengths and contacts and to the planarity of particular structural fragments. Texture is usually taken into account with the March-Dollase [41] formalism, but sometimes it requires more flexible symmetrized harmonics expansion [47, 48]. Anisotropic line-broadening is often observed in the high-resolution powder patterns and needs proper calculation [49, 50] too.

Structure validation

How can one estimate the reliability of the solution obtained from powder data? The question also arises as to whether this solution corresponds to the global or local minimum. The answer to these questions is not obvious as demonstrates the crystal structure determination of *p*-phenylazoaniline hydrochloride, $C_{12}H_{12}N_3^+ \cdot Cl^-$ [42]. The objective of this study was the identification of protonation site in the cation (Fig. 2), choosing between two possibilities - N2 or N3.

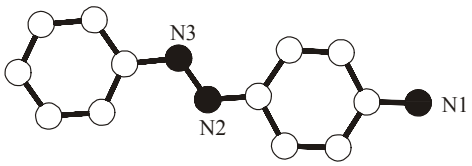

Figure 2. *(4-Aminophenyl)phenyldiazenium. The possible protonation sites are N2 and N3*

p-Phenylazoaniline hydrochloride crystallizes in a monoclinic unit cell with the one structural unit per asymmetric part [42]. The Patterson method applied to X-ray powder data measured at DRON-3 diffractometer allowed us find a position of anion, Cl^-. The position and orientation of cation were then searched by the grid search and simulated annealing techniques, which found the only solution, **1**. The subsequent bond-restrained Rietveld refinement led to R_{wp}=0.068 (Fig. 3a) and N2 protonation with the N2···Cl contact of 3.08(2) Å.

The crystal packing of solution **1** (Fig. 4a) is reasonable, there are no short intermolecular contacts, though one of amino H atoms is not involved in hydrogen bonding. Does the solution **1** corresponds to the global minimum or not?

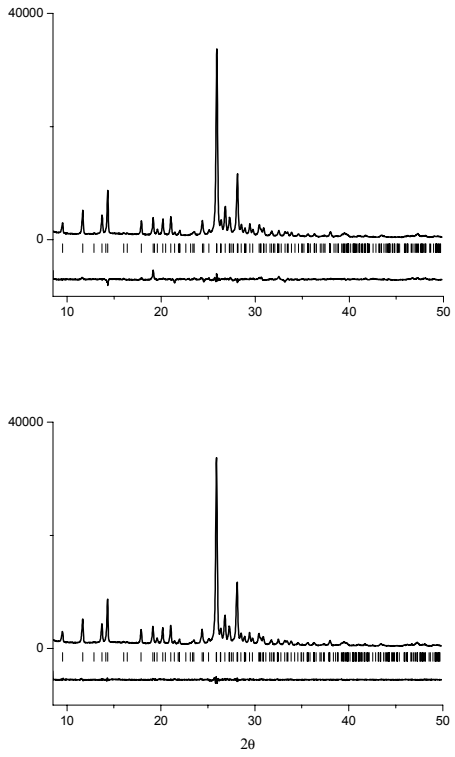

Figure 3: *The results of Rietveld refinements for solution **1** (top, R_{wp}=0.068) and solution **2** (bottom, R_{wp}=0.040).*

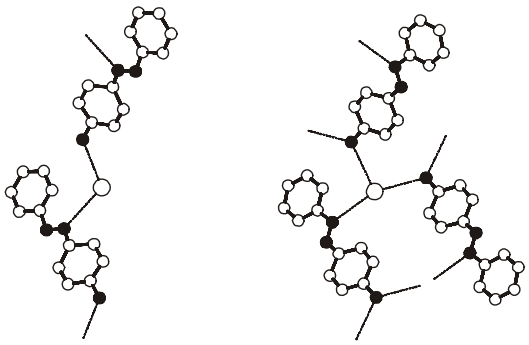

Figure 4: *Crystal packings of p-phenylazoaniline hydrochloride in the cases of (a) solution **1** and (b) solution **2**. The N···Cl contacts less than 3.3 Å are shown as thin lines.*

In our practice of crystal structure determination we use three empirical rules [9], which help in estimating the reliability of the solution obtained: 1) the solution must be in complete agreement with the results of other physicochemical studies; 2) the relationship $(R_{wp})_{RR}/(R_{wp})_{PF} < 1.3$ must be fulfilled for the solution to be correct, $(R_{wp})_{RR}$ and $(R_{wp})_{PF}$ obtained in the Rietveld refinement and Pawley fit, respectively; 3) the Rietveld refinement of the structure without fixation of structural fragments must converge and may not lead to crucial changes in the atomic parameters. In the case of *p*-phenylazoaniline hydrochloride the Pawley fit gave R_{wp}=0.037. Therefore, the relationship $(R_{wp})_{RR}/(R_{wp})_{PF}$ = 1.8 does not correspond to the global minimum. Moreover, the third condition - the convergence of the Rietveld refinement without restraints - was not fulfilled for the solution **1**. This situation gave an impulse for the search for new solution **2**, which was found with the orientational grid search using the smaller, 5° instead of 10°, grids and fixed position of the cation. The subsequent bond-restrained Rietveld refinement led to R_{wp} = 0.040 (Fig. 3b) and N3 protonation with the N3···Cl contact of 3.27(2) Å (Fig. 4b). Interestingly, we were unable to obtain this orientation using simulated annealing search [36].

To clarify the reasons why both search algorithms prefer solution **1**, but not solution **2**, we calculated two sets of *R(X)* (Table 2) using 100 X_{obs} values and varying the orientation of the cation in the vicinities of the two solutions. Table 2 clearly shows that global minimum (solution **2**) is very sharp and is not essentially deeper than the wide local minimum (solution **1**).

Table 2. The ten lowest values of *R(X)* in the vicinities of two solutions calculated for 100 X_{obs} values. The positions of Cl^- (0.25, 0.15, 0.25) and geometric center of cation (0.45, 0.5, 0.23) were fixed. The orientational grid for the polar angles φ, ψ, κ of the cation is 5°.

Solution **1**				Solution **2**			
φ, °	ψ, °	κ, °	*R(X)*	φ, °	ψ, °	κ, °	*R(X)*
0	120	20	0.33	165	135	170	0.28
5	120	20	0.33	165	135	175	0.29
5	115	20	0.34	165	135	165	0.32
0	115	20	0.34	165	140	170	0.40
0	125	20	0.34	165	140	165	0.40
5	125	20	0.34	165	140	175	0.42
-5	120	20	0.35	160	140	170	0.52
-5	125	20	0.36	160	140	165	0.52
-5	115	20	0.36	160	140	175	0.55
0	115	25	0.38	165	130	170	0.56

The crystal structure and N3 protonation of *p*-phenylazoaniline hydrochloride was further confirmed by neutron powder diffraction measurements [42] and single-crystal structure determination [51]. To validate the new crystal structure we use either the various powder patterns measured at different diffractometers [42, 45, 52] or a set of crystal structures from the same family solved from powder patterns measured at one device [43, 53, 54].

Examples

As soon as the crystal structure of powder organic compound is determined, though with the lower accuracy than that obtained in single-crystal studies, it can help to find the answers to many questions and some examples of this are given below.

Molecular structure validation

The preliminary information about the structure of the molecule of a new compound can be obtained usually from the IR and NMR spectroscopy and mass-spectrometry, which may result in several possible molecular structures with equal probability. In the cases when several isomers are indistinguishable by spectroscopic or quantum chemical methods, and there is no suitable single crystal, the crystal structure solution from powder data can help to determine a correct molecular structure.

In the framework of the study of pyrazolo[1,5-a]pyrimidine derivatives several compounds were synthesized, among those were 3-amino-4-nitro-6-methyl-8-oxopyrazolo[1,5-a]pyrimidine, $C_7H_7N_5O_3$ (**I**), and 1-amino-4-methoxycarbonyl-3-methyl-8-oxopyrazolo[1,5-a]pyrimidine, $C_9H_{10}N_4O_3$ (**II**). The preliminary studies revealed two possible molecular structures for **I** and **II** (Fig. 5).

The Guinier X-ray powder patterns of **I** and **II** were indexed in monoclinic unit cells, the crystal structures of **I** and **II** were successfully determined. As a consequence of crystal structure determinations the molecular structures **Ia** for **I** [52] and **IIa** for **II** (Fig. 5), which crystallizes as a monohydrate [55], were revealed. The crystal and molecular structures of **I** were also confirmed with X-ray powder data measured in reflection mode and neutron powder data [52].

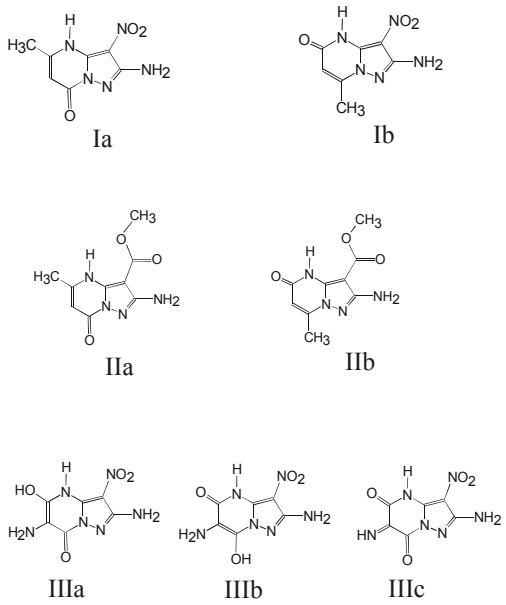

Figure 5: *Chemical diagrams of possible molecular structures of compounds **I** , **II** and **III**.*

In the case of 2,6-diamino-5-hydroxy-3-nitro-4*H*-pyrazolo[1,5-a]pyrimidin-7-one, $C_6H_6N_6O_4$ (**III**), the preliminary studies allowed three possible molecular structures (Fig. 5), which are qualitatively equivalent and hardly distinguished by R_{wp} with X-ray powder data. The monoclinic unit cell dimensions and structural motif of **III** were determined from the Guinier X-ray powder data, which allowed also to find the position of solvent water oxygen. The positions of the two H atoms of the water molecule were found in a difference Fourier map with the synchrotron data. The correct molecular structure, **IIIa** (Fig. 5), was chosen on the basis of careful analysis of crystal packing and intermolecular hydrogen bonds (Fig. 6), and confirmed with the neutron powder data [45].

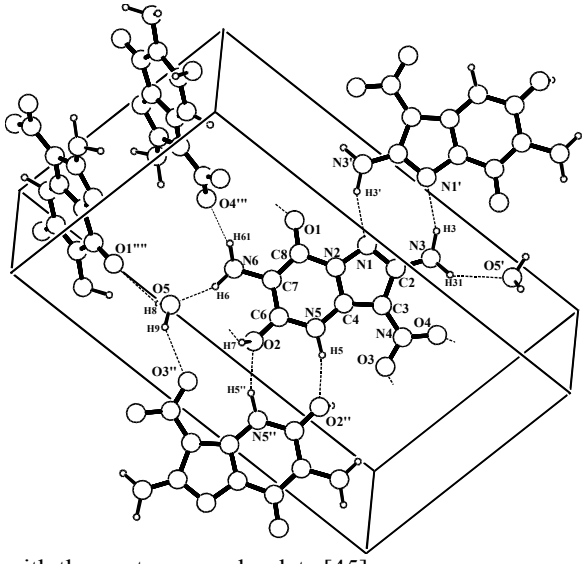

Figure 6: *The crystal packing and intermolecular hydrogen bonds in **III.***

Unexpected molecular structure

An important prerequisite for the above, and many others, structure determinations was the knowledge of the two-dimensional molecular structure. However, there are cases when the list of possible molecular structures does not contain the true one. This situation is usual for the single-crystal direct methods, which can successfully be applied sometimes to the high-resolution powder data [15]. Nevertheless, the low-resolution powder data can also lead to the correct molecular structure starting from erroneous two-dimensional models. An illustrative example is structure determination of 2,4-dinitro-*N*-phenyl-6-(phenylazo)benzamide, $C_{19}H_{13}N_5O_5$ (**IV**) [54].

The interaction of 2,4,6-trinitrobenzaldehyde and its azomethine derivatives with aromatic amines in boiling acetic acid was investigated in the 1930s by Secareanu & Lupas, who assigned structures *A* and *B* (Fig. 7) to the products of this reaction. Recently, the above reaction was investigated in more detail in the framework of a research project concerning the reactions of *C*-(2,4,6-trinitrophenyl)azomethines with various nucleophiles [56]. Modern spectroscopic methods disqualified structures *A* and *B*, but allowed *C* and *D* (Fig. 7), which were used as starting models in the crystal structure determination of compound **IV**.

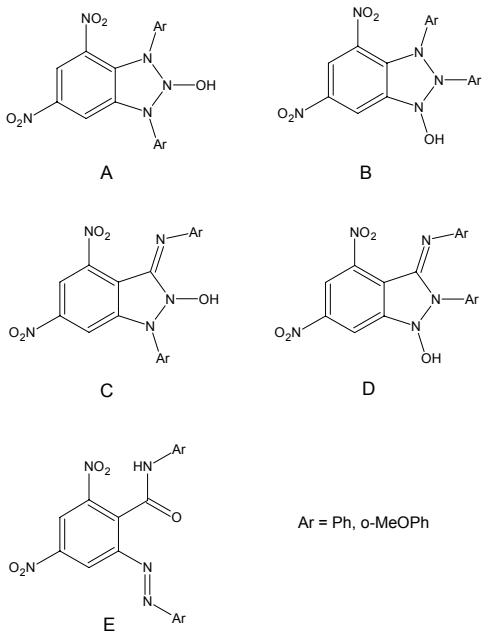

Figure 7: *The initial erroneous (A-D) and obtained as a result of crystal structure determination (E) molecular structures of **IV**.*

All patterns for indexing, structure determination and refinement were measured at room temperature on a DRON-3 diffractometer. The specimen was prepared by pressing the powder onto the sample holder. Because of this preparation procedure, preferred orientation was observed. To take preferred orientation effects into account properly at the stage of crystal structure solution, additional pattern was measured. For this new measurement in a short range of 2θ diffraction angles, the specimen was interground with amorphous starch to reduce texture. The subsequent comparison of two patterns with different degrees of texture allowed us to identify the direction of preferred orientation and the principal value of the texture parameter *r*, which was assigned to 1.3 during the grid-search calculations.
A number of initial models of **IV** were built up on the basis of the two-dimensional structures *C* and *D* (Fig. 7). All these models were tested with the grid search procedure and 100 low-angle X_{obs} values. No model of **IV** could provide low value of *R(X)*. The inspection of obtained crystal packings with PLATON [57] showed unrealistically close intermolecular contacts. No significant improvements, neither in *R(X)* values nor in crystal packings, were obtained after subsequent bond-restrained Rietveld refinements. The decision was taken that the two-dimensional structures *C* and *D* were incorrect.
The crystal structure of **IV** was solved using a combination of grid search technique and subsequent bond-restrained Rietveld refinement. Initially, two of the models providing the lowest *R(X)* were selected for further investigation. Structure determination was then continued with the rigid structural fragments of these models, which were unambiguously present in **IV** in accordance with spectroscopic data. These structural fragments were removed from the selected models and used in a grid search one by one with the subsequent Rietveld refinement of each new obtained model. Finally, the crystal structure of **IV** was solved, and the correct molecular structure *E* (Fig. 7) was determined. One can see here the correlations with the crystal structure determination by direct methods. However, the positions and orientations of rigid structural fragments rather than positions of single atoms have been looked for. This situation leads to an essential decrease in the number of degrees of freedom, which lets us effectively solve crystal structures from low-resolution powder data.
Two additional structures - *N*-(2-methoxyphenyl)-2-(2-methoxyphenylazo)-4,6-dinitro-benzamide, $C_{21}H_{17}N_5O_7$, and *N*-methyl-2,4-dinitro-*N*-phenyl-6-(phenylazo)benzamide, $C_{20}H_{15}N_5O_5$, from the same family as **IV** - have been determined to confirm the correctness of crystal structure of **IV** [54].

Organic dyes

Upon transfer from solutions to the solid state, many organic dyes demonstrate considerable changes in their visible spectra, and hence, in their color. The dependence of color on crystal packing motif has been prominently illustrated by differently colored pairs of polymorphs [58, 59]. For these objects, the powder diffraction technique complements single-crystal methods, because single crystals of many interesting compounds (i.e. those demonstrating the largest spectral changes) are not available, whereas powder diffraction allows the unambiguous determination of crystal structures even with laboratory data. Because the molecular structures of the majority of organic dyes are predictable *a priori*, except for few intramolecular degrees of freedom, their models can be efficiently used in grid search and simulated annealing techniques.
The chemical diagrams of selected compounds **V** - **IX** are shown in Fig. 8. The compounds **V** - sodium 4-(2-pyridinyldiazenyl)resorcinolate monohydrate, $Na^+ \cdot C_{11}H_8N_3O_2^- \cdot H_2O$ - and **VI** -ammonium 2,4-dinitro-1-naphthalenolate, $NH_4^+ \cdot C_{10}H_5N_2O_5^-$ - are widely used colorants: **V** is a metallochromic indicator (PAR) and **VI** is an anionic dye (Acid Yellow 24). A comparison of the diffuse reflectance spectra of crystalline **V** and **VI** with the absorption spectra of their aqueous solutions demonstrates that the geometry of their anions does not change significantly upon transfer from crystalline to the solution state. The correct conformations of the anions in **V** and **VI** were obtained as a result of their crystal structure determinations from laboratory X-ray powder diffraction data [60].
In the framework of the quantitative study of the effect of the crystal environment on the molecular electronic structure [61], the crystal structures of compounds **VII** - 1-[(2-nitrophenyl)hydrazono]-1H-naphthalen-2-one (Pigment Orange 2), $C_{16}H_{11}N_3O_3$ - and **VIII** - 4-(phenyldiazenyl)naphthalen-1-amine hydrochloride, $C_{16}H_{14}N_3^+ \cdot Cl^-$ - have been determined [62, 63] from laboratory powder data.

The impact of crystal packing on visible spectra of crystalline anthraquinone colorants was carefully investigated in [64], were the crystal structure of 1,4-dihydroxy-5,8-di-*p*-toluidinoanthraquinone, $C_{21}H_{21}N_2O_4$, **IX**, was determined from laboratory powder data. This study [64] concluded that, for some of the 18 investigated compounds, the differences in color between crystals and solutions are ascribable to the changes in molecular conformations or to the impact of hydrogen bonds.

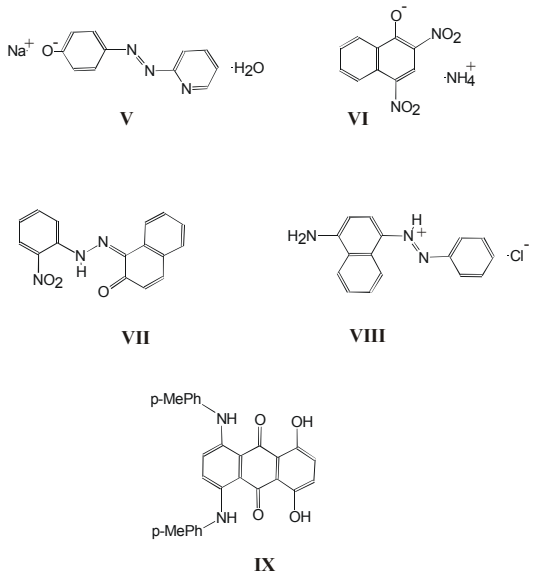

Figure 8: *Chemical diagrams of compounds **V** – **IX.***

Alternative metabolic pathway validation

Dithiocarbamoyl derivatives of diverse heterocycles demonstrate a broad range of physiological activity; antifilarial, antiviral and antifungal agents, oncolytic and lipoprotein disorder drugs are known among this group of compounds. Therefore, the question of the possible metabolic pathways of such compounds is a hot topic in medicinal chemistry. It has been demonstrated that the thermolysis of dithiocarbamoyl derivatives of pyridines and pyrimidines containing a nitro group *ortho* to the dithiocarbamoyl moiety can result in the formation of disulfide compounds with elimination of the nitro group [65] (Fig. 9, (a)).

Recently, an alternative thermolysis pathway involving the elimination of carbon disulfide (Fig. 9, (b)) has been proposed and validated by the powder crystal structure determinations of three compounds [43] - 6-dimethylamino-5-nitropyrimidin-4-yl *N,N*-diethyl-dithiocarbamate, $C_{11}H_{17}N_5O_2S_2$ (**X**), and 6-methylamino-5-nitropyrimidin-4-yl *N,N*-diethyldithio-carbamate, $C_{10}H_{15}N_5O_2S_2$ (**XI**), and 4-dimethylamino-6-methylamino-5-nitropyrimidinium chloride mono-hydrate, $C_9H_{16}N_5O_2^+ \cdot Cl^- \cdot H_2O$. All patterns for indexing, structure determination and refinement were measured at room temperature in a Guinier camera.

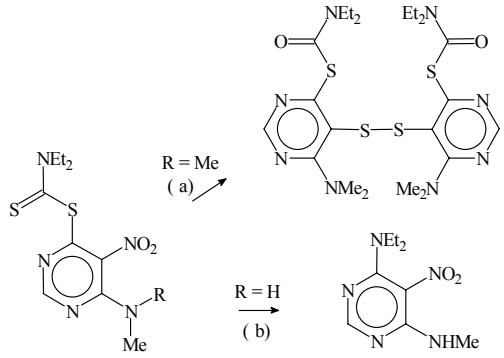

Figure 9: *A traditional (a) and an alternative (b) metabolic pathways of dithiocarbamates.*

The molecular structures of **X** and **XI** and their conformations, revealed by the crystal structure determinations, are shown on Fig. 10. The different reactivity of **X** and **XI** can be interpreted in terms of the differences in their molecular structures (Table 3). The twist of the nitro group out of the plane of the pyrimidine ring in **X** should lower its affinity for nucleophilic substitution compared with **XI**. Besides this, the twist of the nitro group in **X** breaks the secondary S···O contact, which is present in **XI**. Short intramolecular S···O contacts arise fom the σ-interaction between the non-bonding orbital of the O atom and the *p* and *d* orbitals of the S atom, and this interaction affects the spectral and chemical properties of the corresponding compounds.

Table 3. Experimental and DFT-calculated geometric parameters (Å, °) defining the conformations of **V** and **VI**.

	X-ray	DFT
V		
C5 - C4 - S4 - C9	103.9(5)	164
C4 - C5 - N5 - O51	62.6(7)	34
S3 - C9 - S4 - C4	-17.1(5)	-103
S4···O51	2.964(7)	2.687
VI		
C5 - C4 - S4 - C9	148.9(7)	169
C4 - C5 - N5 - O51	14.3(9)	2
S3 - C9 - S4 - C4	-93.8(5)	-105
S4···O52	2.636(7)	2.591

The density functional theory (DFT) calculations were performed with the program PRIRODA [37] employing the BLYP (Becke-Lee-Yang-Parr) exchange-correlation functional [66, 67].

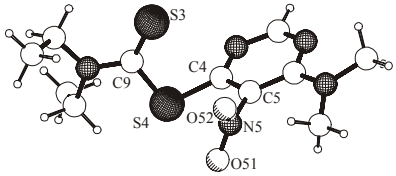

X

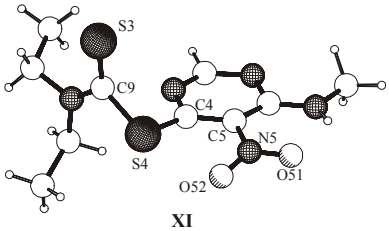

XI

Figure 10: *The molecular structures of **X** and **XI**.*

The evidence of thermal isomerization

During the systematic development of new approaches to the functionalization of δ-carboline derivatives [68] the interesting phenomenon was observed - the compound **XII**, 1-(4-nitrophenyl)-2-phenylimino-2,5-dihydro-1*H*-pyrido[3,2-*b*]indole-3-carbonitrile, $C_{24}H_{15}N_5O_2$ (Fig. 11), irreversibly transforms into a new isomer **XIII** with distinct properties on increasing the temperature to greater than 603 K, or after boiling in a solution of N,N-dimethylformamide in the presence of ^{t}BuOK.

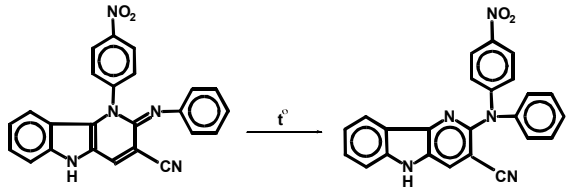

XII **XIII**

Figure 11: *Thermal isomerization pathway of **XII** into **XIII.***

The ^{1}H NMR spectra of compounds **XII** and **XIII** differ in the chemical shifts of like protons (the proton signals for the fused benzene ring were assigned based on the COSY spectrum). The obtained information indicated that the aryl substituents in **XII** are spatially separated, while in **XIII** they are brought close in space. The differential NOE spectra of both types of isomers exhibit responces of signals of the protons in positions 4 and 6 upon pre-saturation of the N(5)H protons; this indicates unambiguously that the molecule contains an aromatic indole system. Finally, the addition of acids to **XII** results in protonation at the exocyclic N atom. Compound **XIII**, unlike **XII**, cannot be protonated and form no hydrochloride. An important difference between the electronic spectra of the isomers is that the long-wavelength band of **XII** undergoes a strong bathochromic shift (by about 100 nm) compared to that of **XIII**, indicating that the chromophore is much more extended in the former type of compound. This altogether indicates that structural changes involve predominantly the pyridine fragment of the molecule. It was assumed that this distinction in properties of the two isomers can be explained either by the unexpected transformation shown on Fig. 11 or by the strong conformational changes of **XII**. To prove unambiguously the structures of compounds **XII** and **XIII**, a powder X-ray diffraction study was undertaken [53].

All patterns for indexing, structure determination and refinement were measured at room temperature in a Guinier camera. The indexing and Pawley fit showed that **XII** crystallizes in a monoclinic unit cell with the volume of 4180(3) Å^3, space group $P2_1/n$, D_x = 1.288 Mg m^{-3}, and **XIII** crystallizes in a orthorhombic unit cell with the volume of 3857(3) Å^3, space group *Pbca*, D_x = 1.396 Mg m^{-3}. There are two independent molecules in the crystal structure of **XII**. However, careful inspection of the results of Pawley fit shows the presence of pseudo-C centering. The Pawley fit was undertaken again in space group *C2/c* to take into account the intensities of most of the peaks, though gave a worse profile *R* factor, R_{wp} = 0.089 compared with R_{wp} = 0.064 for $P2_1/n$. The crystal structure of **XII** was solved in space group *C2/c* and refined in the correct space group $P2_1/n$. The asymmetric unit of **XII** contains two independent molecules, which are connected into chains *via* N-H···N hydrogen bonds between the imino H atoms and the azomethyne N atoms of adjacent molecules (Fig. 12a).

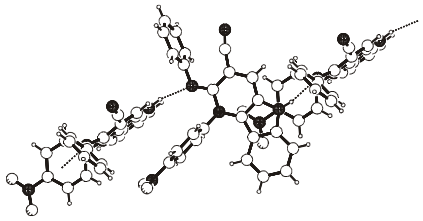

(a)

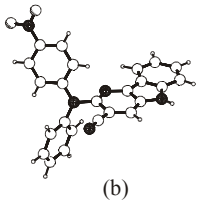

(b)

Figure 12: *The chain of H- bonded adjacent molecules in **XII** (a) and molecular structure of **XIII** (b).*

Protonation site validation

Synchrotron radiation, because of its high brightness and excellent vertical collimation, provides high-resolution X-ray powder data with minimal peak overlap. The combination of high energy operation and narrow peak widths means that problems with the high level of complexity can now be solved with the use of synchrotron powder data. One of such problems was the protonation site identification in two crystalline modifications of doxazosin mesylate [31].

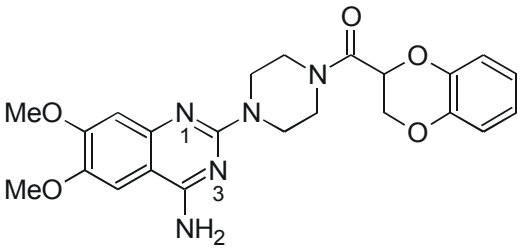

Figure 13: *Doxazosin*.

The selective α_1-adrenoceptor antagonist doxazosin (Fig. 13) is an effective antihypertensive agent used either by itself or in combination with agents from other antihypertensive classes. Drug-delivery forms of doxazosin are usually prepared as solid-state forms of doxazosin mesylate, $C_{23}H_{26}N_5O_5^+ \cdot CH_3SO_3^-$, seven polymorphic modifications of which, designed as forms **A**, **D**, **E**, **F**, **G**, **H** and **I**, are known [33]. It is also known that form **G** is hygroscopic [33] and at ambient conditions it tends to form a hydrate. A molecule of doxazosin has several alternative protonation sites - N1, N3 and exocyclic N atoms (Fig. 13). It was suggested previously [69] that the key pharmacophore for initial α_1-receptor recognition by doxazosin was the N1 protonation. Therefore, in the case of anhydrous and hydrated solid forms of doxazosin mesylate it is important to clearly identify the protonation site responsible for the biopharmaceutical properties of doxazosin. However, no crystal structure of any form of doxazosin or doxazosin mesylate has been reported so far, because of problems with producing crystals of sufficient size and quality suitable for single-crystal X-ray diffraction.

High-resolution synchrotron powder diffraction data for two forms of doxazosin mesylate - the anhydrous form **A** and the hydrated form *d***G** - were collected at the powder diffraction beamlines BM1B and ID31 at the ESRF, Grenoble, France. The monoclinic unit cell dimensions were determined for both compounds (some details of indexing are given above). The crystal structures were solved with the systematic grid search procedure. The details of structure solutions and refinements are given in [31].

A special attention was paid to the correct establishment of the protonation site of doxazosin in forms **A** and *d***G**. The position of the H1 atom, attached to N1, could be found in a difference-Fourier map among the ten highest positive peaks. However, we could not consider this finding as evidence of N1 protonation, because the five highest positive peaks concentrated around the mesylate ion. The accuracy of that powder study [31] was not sufficient for the reliable location from a difference-Fourier map of only one H atom, which introduces 0.3% to the total scattering power. The unambiguous identification of N1 protonation in both structures (Fig. 14) was established based on the close N1···O contacts - 2.76(1) Å in **A** and 2.89(1) Å in *d***G**. Finally, the definitive detection of the N1 protonation site in anhydrous and hydrated solid forms of doxazosin mesylate was obtained as a result of crystal structure determination from powder data.

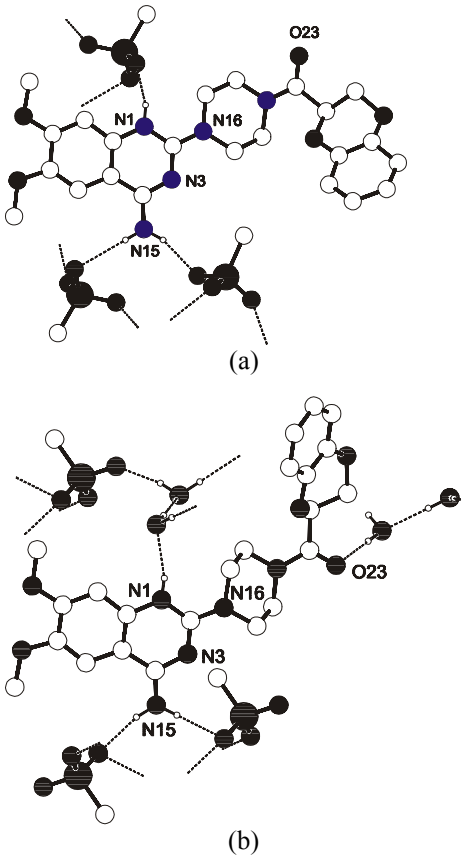

Figure 14*: Conformations of the protonated form of doxazosin and hydrogen bonding in (a)* ***A*** *and (b) d***G***.*

Concluding remarks

The examples presented here for structure determination from powder diffraction data show that powder diffraction today can be routinely used not only for quali- and quantitative phase analysis, material characterization, probing strain, stress, texture etc., but for crystal structure determination as well. Based on our experience now we confirm the validity of the seven year old statement [4] that "XRPD is no longer bound to validate (or reject) prefigured hypothesis but, being a valuable, sometimes irreplaceable, active structural tool, can be profitably used to discover new structural features".

The results highlighted in this article were obtained in close cooperation with many our colleagues. We acknowledge the great contribution of chemists-synthetics from the Department of Medicinal Chemistry under Prof. V.G. Granik, State Scientific Center of Antibiotics, Moscow, Russia; the staff of Laboratory for Crystallography, University of Amsterdam, The Netherlands; Prof. A.N. Fitch and Prof. H.-P. Weber, ESRF, Grenoble, France; Prof. P. Stephens, Department of Physics and Astronomy, Stony Brook University, USA; Prof. V.A. Trounov and Dr. A.I. Kurbakov, St.-Petersburg Nuclear Physics Institute, Gatchina, Russia.

References

[1] W.I.F. David, K. Shankland, L.B. McCusker, Ch. Baerlocher. (2002). Editors. *Structure Determination from Powder Diffraction Data*. New York: Oxford University Press.

[2] A. Le Bail. (1994-2004). *Structure Determination from Powder Diffraction Database*. http://www.cristal.org/iniref.html.

[3] J.I. Langford, D. Louër. (1996). *Rep. Prog. Phys*. **59**, 131-234.

[4] N. Masciocchi, A. Sironi. (1997). *J. Chem. Soc., Dalton Trans*., 4643-4650.

[5] R.B. Hammond, K.J. Roberts, R. Docherty, M. Edmondson. (1997). *J. Phys. Chem.* **B101**, 6532-6536.

[6] D.M. Poojary, A. Clearfield. (1997). *Acc. Chem. Res.* **30**, 414.

[7] Y.G. Andreev, P.G. Bruce. (1998). *J. Chem. Soc., Dalton Trans.,* 4071-4080.

[8] K.D.M. Harris, M. Tremayne, B.M. Kariuki. (2001). *Angew. Chem. Int. Ed. Engl.* **40**, 1626-1651.

[9] V.V. Chernyshev. (2001). *Russ. Chem. Bull. Int. Ed.* **50**, 2273-2292.

[10] E.Y. Cheung, K.D.M. Harris, R.L. Johnston, K.L. Hadden, M. Zakrzewski. (2003). *J. Pharm. Sci.* **92**, 2017-2026.

[11] E. Tedesco, F. Della Sala, L. Favaretto, G. Barbarella, D. Albesa-Jove, D. Pisignano, G. Gigli, R. Cingolani, K.D.M. Harris. (2003). *J. Am. Chem. Soc.* **125**, 12277-12283.

[12] Y.-H. Kiang, A. Huq, P.W. Stephens, W. Xu. (2003). *J. Pharm. Sci.* **92**, 1844-1853.

[13] H.M. Colquhoun, P.L. Aldred, Z. Zhu, D.J. Williams. (2003). *Macromol.*, **36**, 6416-6421.

[14] C. De Rosa. (2003). *Macromol.*, **36**, 6087-6094.

[15] M. Brunelli, J.P. Wright, G.B.M. Vaughan, A.J. Mora, A.N. Fitch. (2003). *Angew. Chem. Int. Ed. Engl.* **42**, 2029-2032.

[16] H. Nowell, N. Shan, J.P. Attfield, W. Jones, W.D.S. Motherwell. (2003). *Cryst. Eng.* **6**, 57-67.

[17] M. Wunschel, R.E. Dinnebier, S. Carlson, P. Bernatowicz, S. van Smaalen. (2003). *Acta Cryst. B*, **B59**, 60-71.

[18] C.E. Botez, P.W. Stephens, C. Nunes, R. Suryanarayanan. (2003). *Powder Diffr.* **18**, 214-218.

[19] V. Brodski, R. Peschar, H. Schenk. (2003). *J. Appl. Cryst.* **36**, 239-243.

[20] J. Giovannini, L. Ter Minassian, R. Ceolin, S. Toscani, M.-A. Perrin, D. Louër, F. Leveiller. (2001). *J. de Physique IV: Proceedings*, **11**, 123-126.

[21] W. Lasocha, J. Czapkiewicz, P. Milart, H. Schenk. (2001). *Z. Kristallogr.* **216**, 291-294.

[22] V.B. Zlokazov, V.V. Chernyshev. (1992). *J. Appl. Cryst.* **25**, 447-451.

[23] *PDF-2 Powder Diffraction File Database*, Release 2003, International Centre for Diffraction Data, Newtown Square, Pennsylvania, USA, 2003.

[24] The Cambridge Structural Database,Version 5.25, November 2003. (2003). The Cambridge Crystallographic Data Center, Cambridge, UK.

[25] P.-E. Werner, L. Eriksson, M. Westdahl. (1985). *J. Appl. Cryst.* **18**, 367-370.

[26] J.W. Visser. (1969). *J. Appl. Cryst.* **2**, 89-95.

[27] V.B. Zlokazov. (1992). *J. Appl. Cryst.* **25**, 69-72.

[28] V.B. Zlokazov. (1995). *Comput. Phys. Commun.* **85**, 414-422.

[29] P.M. de Wolff. (1968). *J. Appl. Cryst.* **1**, 108-113.

[30] G.S. Pawley. (1981). *J. Appl. Cryst.* **14**, 357-361.

[31] V.V. Chernyshev, D. Machon, A.N. Fitch, S.A. Zaitsev, A.V. Yatsenko, A.N. Shmakov, H.-P. Weber. (2003). *Acta Cryst. B*, **B59**, 787-793.

[32] I. Grafe, J.P. Moersdorf. (2000). US Patent 6130218.

[33] M. Grčman, F. Vrečer, A. Meden. (2002). *J. Therm. Anal. Calorim.* **68**, 373-387.

[34] A.V. Yatsenko, K.A. Paseshnichenko, V.V. Chernyshev, H. Schenk. (2002). *Acta Cryst. C*, **C58**, o19-o21.

[35] V.V. Chernyshev, H. Schenk. (1998). *Z. Kristallogr.* **213**, 1-3.

[36] S.G. Zhukov, V.V. Chernyshev, E.V. Babaev, E.J. Sonneveld, H. Schenk. (2001). *Z. Kristallogr.* **216**, 5-9.

[37] D.N. Laikov (1997) *Chem.Phys.Lett.* **281**, 151-154.

[38] *PCMODEL for Windows*, Version 7.0, Serena Software, Bloomington, USA, 1999.

[39] J.J.P. Stewart, MOPAC 7.2, QCPE Program No. 455, 1993.

[40] S.N. Ivashevskaja, L.A. Aleshina, V.P. Andreev, Y.P. Nizhnik, V.V. Chernyshev, H. Schenk. (2002). *Acta Cryst. C*, **C58**, m300-m301.

[41] W.A. Dollase. (1986). *J. Appl. Cryst.* **19**, 267-272.

[42] A.V. Yatsenko, V.V. Chernyshev, A.I. Kurbakov, H. Schenk. (2000). *Acta Cryst. C*, **C56**, 892-894.

[43] V.V.Chernyshev, K.A. Paseshnichenko, V.A. Makarov, E.J. Sonneveld, H. Schenk. (2001). *Acta Cryst. C*, **C57**, 72-75.

[44] A.V. Yatsenko, V.V. Chernyshev, S.G. Zhukov, E.J. Sonneveld, H. Schenk. (1999). *Powder Diffraction*, **14**, 133-135.

[45] V.V. Chernyshev, A.N. Fitch, E.J. Sonneveld, A.I. Kurbakov, V.A. Makarov, V.A. Tafeenko. (1999). *Acta Cryst. B*, **B55**, 554-562.

[46] V.B. Rybakov, V.V. Chernyshev, V.A. Tafeenko, A.D. Shutalev, A.I. Kurbakov, V.A. Trounov. (2001). *Z. Kristallogr.* **216**, 629-632.

[47] M. Ahtee, M. Nurmela, P. Suortti, M. Järvinen. (1989). *J. Appl. Cryst.* **22**, 261-268.

[48] M. Järvinen. (1993). *J. Appl. Cryst.* **26**, 525-531.

[49] N.C. Popa. (1998). *J. Appl. Cryst.* **31**, 176-180.

[50] P. Stephens. (1999). *J. Appl. Cryst.* **32**, 281-289.

[51] A.H. Mahmoudkhani, V. Langer. (2001). *Acta Cryst. E*, **E57**, o839-o841.

[52] V.V. Chernsyhev, A.V. Yatsenko, V.A. Tafeenko, S.G. Zhukov, L.A. Aslanov, E.J. Sonneveld, H. Schenk, V.A. Makarov, V.G. Granik, V.A. Trounov, A.I. Kurbakov. (1998). *Z. Kristallogr.* **213**, 477-482.

[53] V.V. Chernyshev, V.A. Tafeenko, S.Yu. Ryabova, E.J. Sonneveld, H. Schenk. (2001). *Acta Cryst. C*, **C57**, 982-984.

[54] V.V. Chernyshev, A.V. Yatsenko, A.M. Kuvshinov, S.A. Shevelev. (2002). *J. Appl. Cryst.* **35**, 669-673.

[55] V.V. Chernyshev, A.V. Yatsenko, V.A. Tafeenko, E.J. Sonneveld, H. Schenk, V.A. Makarov. (1999). *Powder Diffraction*, **14**, 289-292.
[56] A.M. Kuvshinov. (2001). PhD thesis, Zelinski Institute of Organic Chemistry, Moscow, Russia.
[57] A.L. Spek. (2000). *PLATON for Windows*, University of Utrecht, The Netherlands.
[58] D.T. Cromer, K.-Y. Lee, R.R. Ryan. (1988). *Acta Cryst. C*, **C44**, 1673-1675.
[59] A. Jacobson, A. Petric, D. Hogenkamp, A. Sinur, J.R. Barrio. (1996). *J. Am. Chem. Soc.* **118**, 5572-5579.
[60] A.V. Yatsenko, K.A. Paseshnichenko, V.V. Chernyshev, H. Schenk. (2001). *Acta Cryst. C*, **C57**, 397-399.
[61] A.V. Yatsenko. (2003). *J. Mol. Model.* **9**, 207-216.
[62] A.V. Yatsenko, K.A. Paseshnichenko, V.V. Chernyshev, H. Schenk. (2001). *Acta Cryst. E*, **E57**, o1152-o1153.
[63] A.V. Yatsenko, V.V. Chernyshev, K.A. Paseshnichenko, H. Schenk. (2001). *Acta Cryst. C*, **C57**, 295-297.
[64] A.V. Yatsenko, V.V. Chernyshev, S.I. Popov, E.J. Sonneveld, H. Schenk. (2000). *Dyes and Pigments*, **45**, 169-176.
[65] K. Rasheed, J.D. Warkentin. (1977). *J. Org. Chem*. **42**, 1265.
[66] A.D. Becke. (1988). *Phys. Rev. A*, **38**, 3098-3100.
[67] C. Lee, W. Yang, R.G. Parr. (1988). *Phys. Rev. B*, **37**, 785-789.
[68] S.Yu. Ryabova, L.M. Alekseeva, E.A. Lisitza, A.S. Shashkov, V.V. Chernyshev, G.B. Tichomirova, M.S. Goyzman, V.G. Granik. (2001). *Russ. Chem. Bull. Int. Ed.* **50**, 1449-1456.
[69] S.F. Campbell, M.J. Davey, J.D. Hardstone, B.N. Lewis, M.J. Palmer. (1987). *J. Med. Chem.* **30**, 49-57.

XRPD and Polymorphism in Pharmaceuticals

Harry G. Brittain
Center for Pharmaceutical Physics
10 Charles Road; Milford, NJ 08848 USA
hbrittain@centerpharmphysics.com

Introduction

Since the structure of pharmaceutical solids has become a very important aspect of drug development, the technique of x-ray powder diffraction (XRPD) is now exceedingly important to pharmaceutical research. Without doubt, XRPD is the primary method whereby one can obtain fundamental structural information on the structure of a crystalline substance material on a routine basis. Typical applications of x-ray diffraction methodology include the determination of crystal structures, evaluation of polymorphism and solvatomorphism, evaluation of degrees of crystallinity, and the study of phase transitions [1].

The XRPD technique has become exceedingly important to pharmaceutical scientists, since it represents the easiest and fastest method to obtain fundamental information on the structure of a crystalline substance in its ordinarily obtained form. Since the majority of drug substances are obtained as crystalline powders, the powder pattern of these substances is often used as a readily obtainable fingerprint for determination of its structural type. In fact, it is only by pure coincidence that two compounds might form crystals for which the ensemble of molecular planes happened to be identical in all space. One such example is provided by the respective trihydrate phases of ampicillin and amoxicillin [2], but such instances are uncommon. The most commonly encountered applications of XRPD methodology in pharmaceutics include the phase identification of pharmaceutical substances, the study of polymorphic and solvatomorphic materials, and the evaluation of degrees of crystallinity. Variable temperature XRPD is finding substantial use in the study of phase transitions, and the use of XRPD as a stability-indicating method of analysis has extended its use into drug substance and dosage form stability studies.

Phase Identity of Materials

The most recent USP general chapter on x-ray powder diffraction [3] provides a general criterion for the equivalence of two powder patterns. Prior to the analysis, one must establish the calibrated precision of the diffractometer, which typically is reproducible to within ±0.1 or ±0.2 degrees 2θ. The XRPD data of a sample and reference standard are acquired over a range of scattering angles that range from as close to zero as possible to 40 degrees 2θ, and values for the ten strongest peaks are tabulated. It should be noted that inorganic materials, which have smaller d-spacings, will need to be scanned to well beyond 40 degrees 2θ. The agreement between the corresponding peak angles of the sample and the reference should be within the calibrated precision range of the diffractometer.

The general chapter states that the relative intensities between the sample and reference may vary considerably, and does not place an acceptance criteria on relative intensities. Older versions of the general method had an acceptance criteria of ±20% for the relative intensities of corresponding peaks, but this is now recognized as being impractical.

To illustrate the use of a USP acceptance test for XRPD, consider the powder pattern of (*L*)-malic acid to have been obtained on a diffractometer whose calibrated precision had been determined to be ±0.2 degrees 2θ. These data [4] lead to the acceptance criteria summarized in Table 1. For a given (*L*)-malic acid sample to pass an XRPD identity test would require that the scattering peaks of the sample fall within the boundaries defined in the Table.

Table 1: *XRPD Identity Test Criteria for (L)-Malic Acid; angles given in units of degrees 2θ.*

Reference Scattering Angle	Lower Limit on Scattering Angle	Upper Limit on Scattering Angle
19.327	19.127	19.527
20.752	20.552	20.952
21.031	20.831	21.231
22.310	22.111	22.511
24.426	24.226	24.626
27.710	27.510	27.910
29.380	29.180	29.580
29.714	29.514	29.914
34.000	33.800	34.200
39.455	39.255	39.655

Study of Polymorphism and Solvatomorphism

One of the most important uses of XRPD in pharmaceuticals concerns its application as the primary determinant of polymorphic or solvatomorphic identity [5]. Polymorphic crystal forms are those for which the two or more crystalline forms exhibit identical elemental analyses, while solvatomorphic crystal forms exhibit differing elemental analyses due to the inclusion of solvent molecules in the crystal structure. Since these effects are purely crystallographic phenomena, it is self-evident that x-ray diffraction techniques would represent the essential method of determination. Owing to its ease of data acquisition, XRPD is particularly useful as a screening technique for batch characterization, and the criteria already described for phase identification can serve to differentiate polymorphs or solvatomorphs. It is prudent, however, to support the results of an XRPD study with a confirmatory technique, such as polarizing light microscopy, differential scanning calorimetry, solid-state vibrational spectroscopy, or solid-state nuclear magnetic resonance [6].

To illustrate the utility of XRPD as a means to characterize polymorphs, we will consider the polymorphism associated with ranitidine hydrochloride. The substance is known to crystallize in two anhydrous polymorphs, and the XRPD patterns [7] of the two forms are shown in Figure 1.

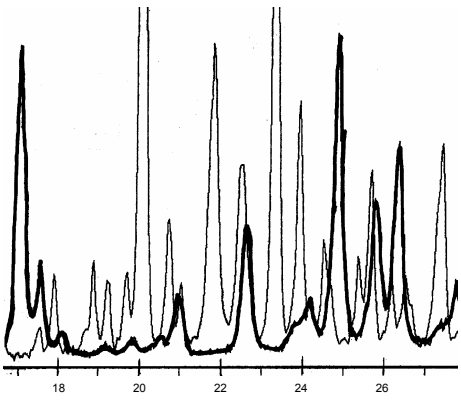

Figure 1: *XRPD patterns of ranitidine hydrochloride, Form I (thick trace) and form II (thin trace).*

For a variety of reasons, most workers need to determine the quantity of Form II in a sample of Form I, and it is clear from the figure that the scattering peaks around 20 and 23.5 degrees 2θ would be particularly useful for this purpose. Conversely, if there were a reason to determine the level of Form I in a bulk Form II sample, then the scattering peaks around 9 and 25 degrees 2-θ would suffice.

Magnesium stearate is known to form in a variety of crystal forms, chiefly an anhydrate phase, a dihydrate, and a trihydrate. The ability of this substance to function as a tablet lubricant appears to be related to its crystal form, and these forms are readily distinguished on the basis of their XRPD powder patterns [8]. The observed scattering peaks all appeared to be derived from multiple scattering off the long (001) crystal spacing. The various phases differed primarily in the magnitude of the long crystal spacing, suggesting that the hydration water was present between the molecular planes and was not an integral part of the crystal lattice.

Degree of Crystallinity

When reference samples of the pure amorphous and pure crystalline phases of a substance are available, it is possible to prepare calibration samples of known degrees of crystallinity through the careful mixing of the reference materials. The preparation of a calibration curve (expressed as XRPD response *vs*. degree of crystallinity) permits the evaluation of unknown samples to be performed.

In one study, a XRPD procedure was described for estimation of the degree of crystallinity in digoxin samples [9]. Crystalline product was obtained commercially, and the amorphous phase was obtained through ball-milling of this substance. Calibration mixtures were prepared as a variety of blends prepared from the 100% crystalline and 0% crystalline materials, and acceptable linearity and precision was obtained in the calibration curve of XRPD intensity *vs.* actual crystallinity. Figure 2 shows the powder pattern of an approximately 40% crystalline material, illustrating how these workers separated out the scattering contributions from the amorphous and crystalline phases.

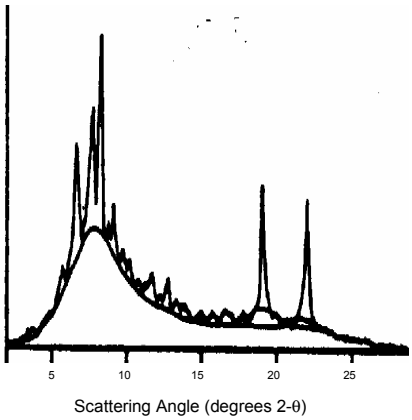

Figure 2: *XRPD pattern of digoxin, whose degree of crystallinity was reduced to 40% by ball-milling. The figure was adapted from data contained in ref. [9].*

In another example, a study of partially crystalline indomethacin has been reported [10]. The crystalline substance was obtained from commercial sources, and the amorphous phase subsequently generated by quench-cooling the melted drug substance. Calibration mixtures were prepared as a variety of blends from the 100% crystalline and 0% crystalline materials, and acceptable linearity (r^2 = 0.988) was obtained in the calibration curve of XRPD intensity (based on three peaks) *vs*. actual crystallinity.

Thermodiffractometry

The performance of XRPD on a hot stage enables one to obtain powder patterns at elevated temperatures and permits one to deduce structural assignments for thermally induced phase transitions. Determination of the origin of thermal events taking place during the conduct of differential thermal analysis or differential scanning calorimetry is not always straight-forward, and the use of supplementary XRPD technology can be extremely valuable. By conducting XRPD studies on a stage capable of being heated, one can bring the system to positions where a DSC thermogram indicates the existence of an interesting point of thermal equilibrium. One of the obvious uses thermodiffractometry that immediately comes to mind entails the desolvation of solvatomorphs. For instance, after the dehydration of a hydrate phase, one may obtain either a crystalline anhydrate phase or an amorphous phase. The XRPD pattern of a dehydrated hydrate will clearly indicate the difference. In addition, should one encounter an equivalence in powder patterns between the hydrate phase and its dehydrated form, this would indicate the existence of channel-type water (as opposed to genuine lattice water) [11].

For instance, the commercially available form of Aspartame is hemihydrate Form II, which transforms into hemihydrate Form I when milled [12]. Also known is a 2.5-hydrate species, and VT-XRPD has been used to study the desolvation and ultimate decomposition of the various hydrate forms. When heated to 150º C, both hemihydrate forms dehydrate into the same anhydrous phase, which then cyclizes to 3-(carboxy-methyl)-6-benzyl-2,5-dioxopiperazine if that material is heated to 200º C. The 2.5-hydrate was shown to dehydrate to hemihydrate Form II when heated to 70º C, and this product was then shown to undergo the same decomposition sequence as directly crystallized hemihydrate Form II. Various XRPD patterns obtained during the heating sequence of the 2.5-hydrate are shown in Figure 3.

XRPD in Accelerated Stability Studies

The requirement to establish the physical quality of a drug substance during the conduct of stability studies is now well recognized, and XRPD is certainly capable of being validated to the status of a stability-indicating assay. The crystallographic stability of a drug substance can be studied using XRPD as part of the protocol, and this is especially important when either a metastable or an amorphous form of the drug substance has been chosen for development. This work is especially important if either a metastable or amorphous form of the drug substance has been chosen for development purposes. One may conduct such work either on samples that have been stored at various conditions and pulled at designated time points, or on substances that are maintained isothermally and the XRPD periodically measured.

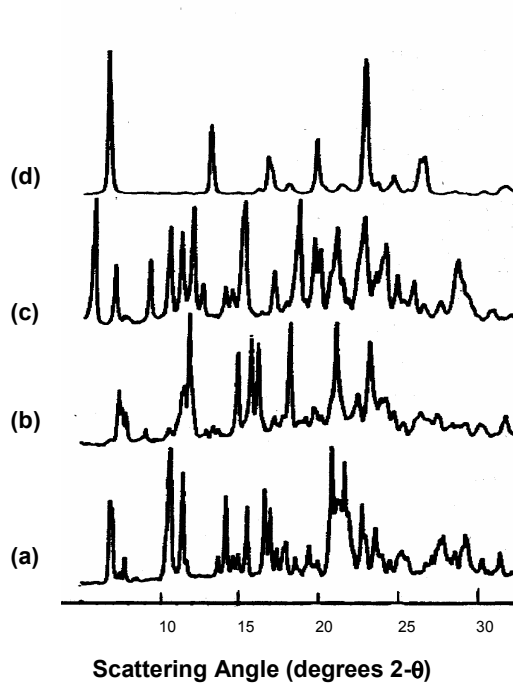

Figure 3: *XRPD patterns of aspartame (a) 2.5-hydrate, (b) hemihydrate, (c) anhydrate, and (d) dioxopiperazine degradant. The data were adapted from ref. [12].*

Amorphous clarithromycin was prepared by grind and spray drying processes, and XRPD was used to follow changes in crystallinity upon exposure to elevated temperature and relative humidity [13]. Exposure of either substance to a combined 40° C and 82% relative humidity environment for seven days led to formation of the crystalline form, but the spray-dried material yielded more crystalline product than did the ground material. This finding, when supported with thermal analysis studies, led to the conclusion that the amorphous substances produced by the different processing methods were not equivalent.

Summary

X-ray powder diffraction represents the methodology of choice for the crystallographic characterization of drug substances produced on a routine, batch-type basis. Properly prepared samples yield powder patterns that contain a scattering peak for each crystal plane / face, and therefore constitute an identification test for a given crystalline phase. When the data are of suitable quality, XRPD can be used to deduce details of the unit

cell and the crystal structure. With the generation of appropriate calibration data, XRPD can be used as a means to deduce the degree of crystallinity in a given sample, of the composition of a physically heterogeneous mixture. Since polymorphism and solvatomorphism are crystallographic occurrences, XRPD will always be the primary determinant of the existence of such phenomena. Variable temperature XRPD is a valuable tool to understand thermally induced reactions, and to characterize materials during the conduct of stability studies.

References

[1] Suryanarayanan, R. (1995) X-ray powder diffractometry. In: Physical Characterization of Pharmaceutical Solids (ed Brittain, H.G.), pp. 187-221. Marcel Dekker, New York.

[2] Boles, M.O., Girven R.J., & Gane, P.A.C. (1978) The structure of amoxicillin trihydrate and a compatrison with the structures of ampicillin. Acta Cryst., B34, 461-466.

[3] General test <941>, X-ray diffraction (2004) In: United States Pharmacopoeia 27, pp. 2401-2402. The U.S. Pharmacopoeial Convention, Rockville, MD.

[4] Brittain, H.G. (1999) Malic acid. In: Analytical Profiles of Drug Substances and Excipients, Volume 28 (ed Brittain, H.G.), pp. 168-174. Academic Press, San Diego.

[5] Brittain, H.G. (1999) Methods for the characterization of polymorphs and solvates. In: Polymorphism of Pharmaceutical Solids (ed Brittain, H.G.), pp. 227-278. Marcel Dekker, New York.

[6] Byrn, S., Pfeiffer, R., Ganey, M., Hoiberg, C. & Poochikian, G. (1995) Pharmaceutical solids: A strategic approach to regulatory considerations. Pharm. Res., 12, 945-954.

[7] Brittain, H.G. (2002) Unpublished results.

[8] Sharpe, S.A., Celik, M., Newman, A.W. & Brittain, H.G. (1997) Physical characterization of the polymorphic variations of magnesium stearate and magnesium palmitate hydrate species. Struct. Chem., 8, 73-84.

[9] Black, D.B. & Lovering, E.G. (1977) Estimation of the degree of crystallinity in digoxin by x-ray and infrared methods. J. Pharm. Pharmacol., 29, 684-687.

[10] Otsuka, M., Kato, F. & Matsuda, Y. (2000) Comparative evaluation of the degree of indomethacin crystallinity by chemoinfometrical fourier-transformed near-infrared spectroscopy and conventional powder x-ray diffractometry. AAPS-PharmSci., 2, issue 1, no. 9.

[11] Stephenson, G.A., Groleau, E.G., Kleemann, R.L., Xu, W. & Rigsbee, D.R. (1998) Formation of isomorphic desolvates: Creating a molecular vacuum. J. Pharm. Sci., 87, 536-542.

[12] Rastogi, S., Zakrzewski, M. & Suryanarayanan, R. (2001) Investigation of solid-state reactions using variable x-ray powder diffractometry. 1. Aspartame hemihydrate. Pharm. Res., 18, 267-273.

[13] Yonemochi, E., Kitahara, S., Maeda, S., Yamamura, S., Oguchi, T. & Yamamoto, K. (1999) Physicochemical properties of amorphous clarithromycin obtained by grinding and spray drying. Eur. J. Pharm. Sci., 7, 331-338.

XRPD of Low-dimensional Organometallic Systems

Norberto Masciocchi[a] and Angelo Sironi[b]

[a]Dipartimento di Scienze Chimiche ed Ambientali, Università dell'Insubria
via Valleggio 11, 22100 Como (Italy)
norberto.masciocchi@uninsubria.it
[b]Dipartimento di Chimica Strutturale e Stereochimica Inorganica, Università di Milano
via G.Venezian 21, 20133 Milano (Italy)
angelo.sironi@istm.cnr.it

Introduction

The search for new materials for tailor-made applications and new devices does not anymore involve only solid-state chemists, physicists or material engineers but also synthetic and structural organometallic chemists. In a recent review [1] we have argued that *ab-initio* X-ray powder diffraction (XRPD) may be a powerful structural tool when dealing with *i)* insoluble, thermally unstable, compounds which cannot be (re)crystallised from solution or from the melt; *ii)* metastable phases destroyed or modified upon manipulation; *iii)* twins; *iv)* very small crystals and/or crystal aggregates; *v)* gas/solid, liquid/solid and solid state reactions fragmenting and misorienting the coherent domains of the starting crystals but conserving the (poly)crystalline nature of the sample. In the following, we will show how organometallic and hybrid organic-inorganic systems fit into the above mentioned categories thus promoting XRPD to a principal tool for the characterisation of organometallic materials.

Molecular compounds (and 'salts' containing *large* polyatomic ions) are bound by weak intermolecular forces hence have high thermal parameters, large peak widths and a rapid fall-off of the scattering power with the scattering angle. In addition, even if the presence of a few metal atoms often simplifies the process of structure solution, their dominant scattering power masks information in the diffraction data concerning the organic component, thus modelling and refining of that part of the structure may be more difficult (however, conformationally rigid ligands may simplify structure refinements if rigid body refinements are used). Accordingly, the obtained structural 'details' are rather blurred; nevertheless, XRPD still affords a

plenty of useful, otherwise inaccessible, information such as paracrystallinity, molecular shape, heavy atoms stereochemisty, rough bonding parameters and crystal packing.
In the following, the contribution of XRPD to the comprehension of the structure of different materials of 'molecular' origin, although polymeric, will be presented. Their low-dimensional nature typically hampers the growth of suitable crystals and low-quality diffraction patterns are normally observed; however, their (often faulted) structural anisotropy lies at the very basis of their functional properties.

Organometallic molecular wires based on M-M or M-H-M bonds

One-dimensional and 'pseudo' one-dimensional materials have long fascinated physicists and chemists because of their unusual properties. There is a recent renaissance of research in the area of 1D polymers with metal-containing backbones possibly in the light of the explosion of interest in nanoscale electronic devices [2]. Here we discuss the structure of three polymers, namely $[ReH(CO)_4]_n$ [3], $[Ru(CO)_4]_n$ [4] and $[Ru(CO)_2bipy]_n$ [5], for which the representative XRPD patterns are drawn in Figure 1.

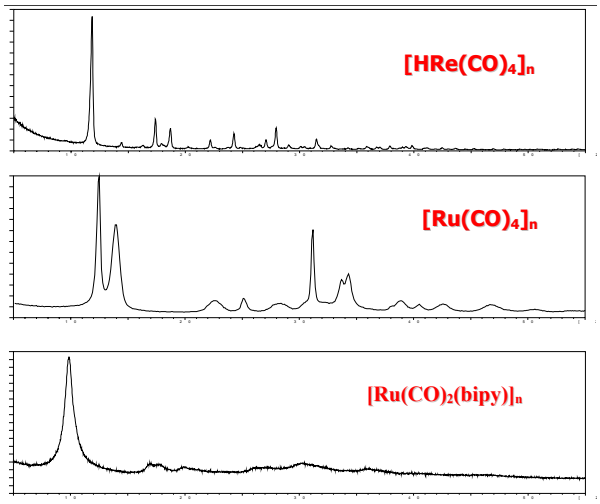

Figure 1: *Raw XRPD patterns for three 1D organometallic polymers, showing different degrees of crystallinit, and markedly anisotropic peak widths, up to 1.5° 2θ.*

In all three cases there are two kinds of problems which are deeply entangled: i) the structural complexity of the materials, for which XRPD alone is not able to afford accurate atomic positions, particularly when strong scatterers are present (Re, Ru), and ii) the sample contribution, which is a clear manifestation of the presence of defects, inherent in the actual phase; interestingly, and at variance from conventional single-crystal studies, XRPD affords, in some cases, some extra-information of microstructure and coherence length, normally overlooked.

The analyses of the XRPD traces of very different 'quality' (as shown above) clearly resulted in structural models of different accuracy; modelling and geometrical restraints were necessary in the first two cases to help convergence in the final Rietveld refinement cycles; differently, the very limited amount of information present in the bottom trace of Figure 1 required the knowledge of the previously determined ruthenium carbonyl structure in order to assess a few 'accessible' structural features (cell parameters, hence crystal packing) of the ruthenium polymers containing diazaaromatic ligands.

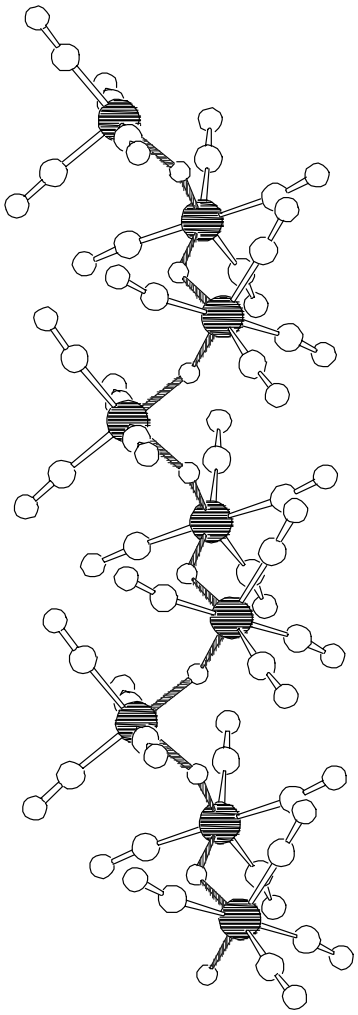

Figure 2: *A fragment of the 3_1 helix of $[HRe(CO)_4]_n$. Rhenium atoms in black.*

In the first of our examples, the $[HRe(CO)_4]_n$ polymer, the three independent metal atoms, defining infinite 3_1 helices, were unambiguously located by direct methods; however, due to the intrinsic limitations of XRPD, we were unable to complete the starting model by Fourier methods; thus, we had to rely on molecular mechanics and some previous stereochemical knowledge to obtain the bulk structure. It is of particular interest that the preliminary information afforded by powder diffraction (*i.e.* lattice constants, space group symmetry and 'good' heavy atom locations) uniquely determined the shape of the 'cavity' containing the molecule, and, hence, the

overall stereochemistry of the polymer. Finally, even the hydrogen locations were assessed (within the helical metal core, screened by the carbonyl ligands).
In this species, as well as in the related $[HRe(CO)_4]_6$ hexamer, it might be considered odd to speak about hydrogen locations when we barely see the metal centers; however, it is well known that the location of the hydrides may be determined, at the molecular level, from those of the other atoms [6].
From the much poorer XRPD trace of $[Ru(CO)_4]_n$, we still managed to determine its crystal and molecular structure, which was unexpectedly different from that guessed by IR spectroscopy [7]: instead of a zig-zag polymer built by *cis*-C_{2v} fragment, linear chains, containing the staggered, *trans* D_{4h} monomers (2.94 Å apart) were found. In addition, its microstructural analysis allowed the determination of the average chain length and of their lateral strain.

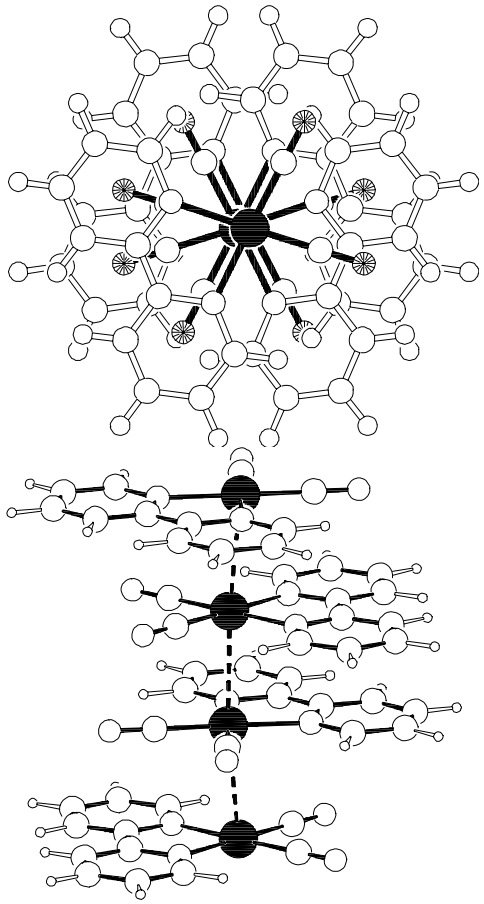

Figure 3: *Stacking of staggered $Ru(CO)_2(bipy)$ fragments in the 1D polymer. Top: view down c, the chain axis. Bottom: lateral view. Nearly collinear ruthenium atoms (in black) are ca. 3.0 Å apart. For the crystal disorder, see text.*

The structural features determined for $[Ru(CO)_4]_n$ significantly helped in unravelling the nature, and the crystal packing, of the nearly amorphous $[Ru(CO)_2(bipy)]_n$ polymer, an efficient catalyst for electrochemical oxygen evolution. In this case, we had to 'manually' guess the lattice parameters by observing the systematicity of the d* ratios of the few observable bumps, as well as by detecting their subtle splitting.

Once the correct cell centering was detected, model building and interpretation of a highly disordered structure allowed a rather decent matching between observed and calculated XRPD traces. The final model confirms the polymeric nature of the sample, which shows stacking of C_{2v}-$Ru(CO)_2(bipy)$ fragments (*ca.* 3.0 Å apart), staggered (as in $[Ru(CO)_4]_n$), but disordered in four equivalent orientations about *z*.

Layered Organic - Inorganic Hybrid Materials

The class of hybrid inorganic-organic materials has recently received a wide interest because the spatial organisation of the metals and their intrinsic properties (magnetism, luminescence, etc.) can be controlled, and finely tuned, by the proper choice of ligands.
Two-dimensional systems are common to many aspects of material chemistry. The variety of the available organic ligands (and the tendency of certain inorganic substrates to afford well defined layers) can be used to design low-dimensional systems with a high stereochemical control, exploiting (strong) covalent bonding, weaker dipolar effects, segregation or intercalation processes.
More than ever, preferential orientation effects are likely at work. This is a rather annoying problem, both in the indexing, but particularly in the structure solution (and refinement) stages. If possible, the side-loading technique should be used, unless only a small quantity of material is available (in such case, the capillary mounting is desirable). Even in the most careful preparation, texture effects will be present, and must be accounted for during data analysis.
In the following, two representative examples from this class of compounds are described.

Magnetic Cobalt Soaps. Their crystal morphology, as shown in Figure 4, speaks for itself. Nevertheless, careful sample preparation, the use of a highly monochromatized soft radiation (Co-Kα_1), and particularly the metric information gathered from SAED on a single platelet (Figure 4) allowed the structural analyses of a number of (monoclinic) cobalt soaps with cell parameters as large as 58 Å. Due to their structural complexity, neither direct nor Patterson methods afforded unique (refinable) cobalt atom location, that could be later used for model completion by Fourier methods. However, direct space *simulated annealing* techniques, using two independent rigid *all-trans* alkanoate groups and one *cis*-$Co(H_2O)_2$ fragments, eventually afforded a reasonable starting model [8].
Mono- and di-carboxylato(diaqua)cobalt(II) species belong to the same structural class, with long chain organic ligands segregated from the polar heads and metal ions connected by RCO_2 bridges in the rare *anti-anti* conformation (see Figure 5). Based on the structures determined from XRPD data, the interpretation of the low-temperature magnetic

behaviour and the magnetic coupling constants of two-dimensional lattice were then possible.

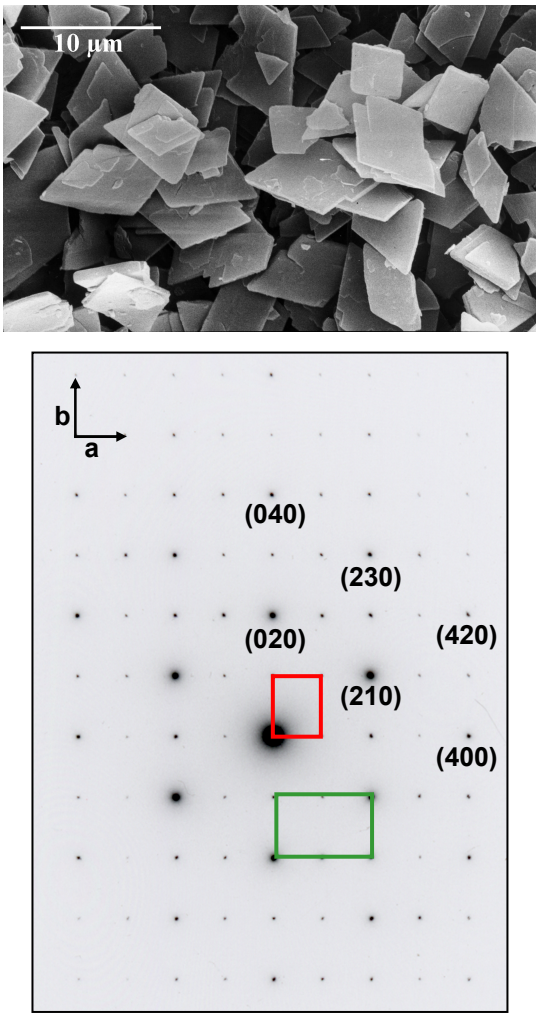

Figure 4. *Top: Crystal morphology from SEM micrographs. Bottom: characteristic electron diffraction pattern as recorded with the platelets oriented perpendicularly to the electron beam. The rectangles correspond to the (a*,b*) cell of the present compounds (small) and of the paraffin–like subcell (large).*

$[DAMS^+][Cu_5I_6]$: This species shows a very simple XRPD pattern corresponding to a rhombohedral lattice, with approximate cell volume of 600 $Å^3$, whose asymmetric unit cannot obviously host the large $[DAMS^+]$ cation. What conventional diffraction sees is the stacking (along the trigonal axis with a spacing of *ca.* 12.75 Å) of CuI slabs formed by two parallel slightly corrugated sheets (similar to those present in the room temperature CuI γ phase but with a certain amount of Cu^I vacancies in order to balance the charges of the *guest* anions) which are suitably translated in order to grant the tetrahedral co-ordination of the Cu^I ion. The 'empty' space within the slabs (*per* slab, *per* unit cell) is 96 $Å^3$. This implies that each $[DAMS^+]$ cation (estimated volume 262 $Å^3$, length *ca.* 17 Å) extends over three unit cells, does not conform to any translational or point symmetry operator of the host lattice and does not actually contribute to Bragg intensities except for low angle 00ℓ reflections. Nevertheless, by coupling structural, optical and spectroscopic information we were able to suggest that, within two *host* Cu-defective slabs, the intercalated $[DAMS^+]$ cations must be: *i)* 'edge-on' oriented (the interslab spacing being 12.75 Å); *ii)* dipole ordered (given the observed SHG activity); *iii)* densely packed (as J-aggregates); but *iv)* translationally disordered (see Figure 6 in next page). Finally, we were also able to propose a physical explanation for the highly crystalline rhombohedral stacking of the *host* lattice by observing that anion alignment of adjacent slabs must be due to favorable coupling of charges $(I^-)(^{\oplus}[DAMS^+]^{\oplus})(^-I)$ originated by the substantial bilateral symmetry of $[DAMS^+]$ nearby the charged N atom; thus, the factor controlling the formation of a macroscopic ordering is the intrinsic polarity of the 'first' $[DAMS^+]$ *guest* layer that imparts a definite 'order' to the *host* vacancies, which eventually determines the orientation of the next *guest* add-layer.

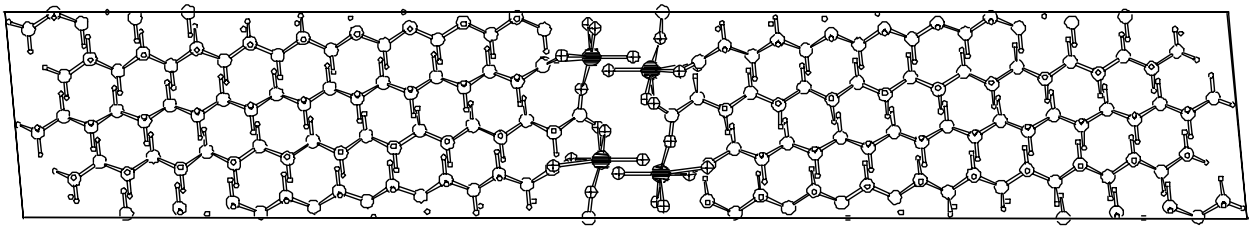

Figure 5. *Schematic plot (down* ***b****, horizontal axis =* ***c****) of the crystal structure of cis-*$Co(H_2O)_2(C_{20}H_{39}O_2)_2$*, showing the elongated organic ligands running nearly parallel to the* ***c*** *axis; cobalt atoms in black, oxygen atoms cross-hatched.*

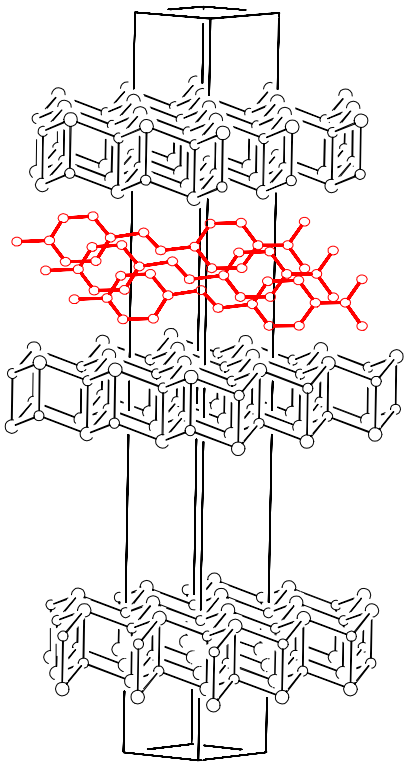

Figure 6: *Unit cell diagram for [DAMS$^+$][Cu_5I_6] (or DAMS$^+$@CuI), showing the defective (see text) CuI layers and the intercalated DAMS$^+$ ions. The latter are edge-on, with respect to the layers, and translationally disordered over three adjacent cells.*

Summary

It would be unfortunate if the stereochemistry of important organometallic species, or of entire classes of compounds, would remain unknown because of the lacking of suitable well-diffracting specimens. Thus, as demonstrated above on a selected subset of examples, we succesfully employed powder diffraction in fully characterizing a number of species of low-dimensional nature, which did not afford single crystals for conventional structural analysis.

Noteworthy, a number of stereochemical features have been addressed by a combination of techniques, like simulated-annealing methods, 'partially flexible' rigid body treatment of fragments of 'known' geometry, SAED and packing energy analysis. Further examples can be found in the realm of truly molecular systems, which we characterized also by coupling neutron diffraction of polycrystalline samples [9] or low-temperature ^{1}H-NMR experiments [10] (not cited above), both acting as a unvaluable *lenses* for addressing structural subtelties.

Acknowledgements.

We thank all co-workers who have participated in this project for their continuous support and helpful discussions. Funding from the Italian MURST and CNR is also acknowledged.

References

[1] N. Masciocchi and A. Sironi, *J. Chem. Soc. Dalton Trans.* **1997**, 4643.
[2] J. K. Bera and K. R. Dunbar, *Angew. Chem. Int. Ed.* **2002**, *41*, 4453.
[3] N .Masciocchi, G. D'Alfonso, L. Garavaglia and A. Sironi, *Angew. Chem. Int. Ed.* **2000**, *39*, 4478.
[4] N .Masciocchi, M. Moret, P. Cairati, F. Ragaini and A. Sironi, *J. Chem. Soc., Dalton Trans.*, **1993**, 471.
[5] N. Masciocchi, A. Sironi, S. Chardon-Noblat and A. Deronzier, *Organometallics*, **2002**, *21*, 4009.
[6] G.Orpen, *J. Chem. Soc., Dalton Trans.*, 1980, 2509.
[7] W.R.Hastings and M.C.Baird *Inorg.Chem.* **1986,** *25***,** 2913.
[8] J.M. Rueff, N. Masciocchi, P. Rabu, A. Sironi, and A. Skoulios, *Chem.Eur.J.,* **2002**, *8*, 1813
[9] N. Masciocchi, G. D'Alfonso, W. Kockelmann, W. Schäfer and A. Sironi *Chem.Commun.* **1997**, 1903.
[10] M. Muccini, M.A. Loi, K. Keveney, R. Zamboni, N. Masciocchi and A. Sironi. *Adv. Mater.,* **2004**, *16*, in press.

XRPD Characterization of Metal(IV) Phosphonates

Riccardo Vivani and Ferdinando Costantino
Department of Chemistry - University of Perugia
via Elce di Sotto, 8 - 06123 Perugia (Italy)
ric@unipg.it

Introduction

In recent years, zirconium phosphonates have been widely investigated because they offer to the materials chemistry a large toolkit for the preparation of tailor made compounds, with structure and reactivity that can be tuned for application in many fields, such as molecular and ionic recognition, catalysis, protonic conduction and so on. They are easily obtained as low-dimensional, especially layered, solids having different structures, corresponding to different chemical behaviors [1-4]. They are generally very insoluble compounds. This feature, although attractive for many potential applications, makes it difficult to deduce their structural characteristics. Large crystals prepared from zirconium phosphates or phosphonates are very rare. Therefore, the recent use of new instrumental apparatus and numerical strategies for the analysis of powder diffraction data has been very fruitful in this field [5]. In many cases, these structural studies were crucial for the development of the chemistry of a given compound. For example, zirconium phosphates and phosphonates with a layered structure of γ-type were first prepared in the 1960s, and have been the object of growing interest since 1990 [1], just after the publication of the structure of γ-zirconium phosphate

[6]. Recently, especially thanks to Clearfield and co-workers, a number of different layered zirconium phosphonates has been solved using powder diffraction methods [3,7,8]. We recently reported the synthesis and characterization of a series of zirconium phosphonates whose structures were solved by XRPD methods using a conventional X-ray source (CuKα radiation) [9-11]. The objective of this research was the preparation of layered compounds with an available space in a poorly hindered interlayer region, as depicted in Fig. 1.

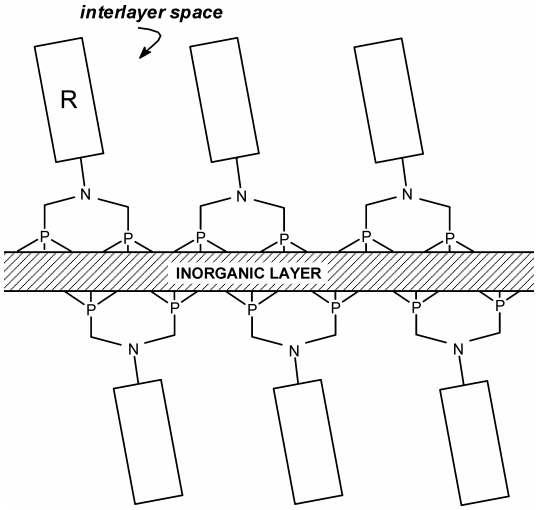

Figure 1. *Scheme of a layered diphosphonate in which both phosphonic groups are bonded to the same face of the inorganic layer.*

Selected R-amino-N,N-bis-methylphosphonic acids, in which R was an alkyl chain of various lengths, a butanoic or a benzyl group, were thus prepared. In these building blocks only one organic residue is associated to each two phosphonate tetrahedra. Synthesis of microcrystalline zirconium derivatives of these diphosphonic acids was accomplished using the so-called HF-method, in which the rate of precipitation was controlled by the slow release of zirconium ions in a solution containing the diphosphonic acid. Release of zirconium was obtained by the thermal decomposition of soluble zirconium fluorocomplexes. Compounds with the general formula $ZrF(O_3PCH_2)_2NH$-R were thus obtained. Despite the presence of different organic groups, these compounds have shown similar structural features, and even though these structures have been solved using data from a conventional Bragg-Brentano diffractometer, several structural details, such as weak interactions, conformational changes due to phase transitions and small geometrical differencies between them, have been described with good accuracy.

The pentylamino derivative, $ZrF(O_3PCH_2)_2NH C_5H_{11}$, 1a

This compound belongs to a series of omologous alkylamino derivatives with different chain lengths (no. of C atoms in the alkyl chain = 3, 4, 5, 6, 8, 9, and 10). They showed similar composition and chemicophysical characteristics. Although the structure was solved for the pentylamino derivative, which was the most crystalline sample of the series, it is likely that all other samples may have the same kind of structure.

1a crystallizes in the monoclinic system, space group $P2_1/c$, unit cell: a = 13.1874(3) Å, b = 8.8723(3) Å, c = 10.9793(3) Å, β = 96.594(3)°, Z = 4. The structure was solved by direct methods with the EXPO program [12], by which ten of the eighteen atoms of the asymmetric unit were detected. A series of Rietveld refinements alternated with Fourier difference maps, performed with the GSAS program [13] revealed the positions of the remaining three oxygen atoms and all carbon atoms of the alkyl chain.

Structure **1a** (Fig. 2) arises from the packing of hybrid inorgano-organic layers interacting by van der Waals forces. Each layer is made of corner sharing ZrO_5F octahedra and O_3PC tetrahedra. Zr octahedra are placed in two parallel planes that are about 2.2 Å apart. Pairs of phosphonate tetrahedra, facing the same side of the layers, belong to the same diphosphonate moiety, and are bridged together by the benzylamino group, via the nitrogen atom.

The two phosphonate groups of each diphosphonic unit are crystallographically and chemically non-equivalent, since one of them is triply connected to three zirconium atoms, while the second one is connected to only two zirconium atoms. The third P-OH group points toward the nitrogen atom of an adjacent diphosphonic group. The PO···N distance is only 2.48(1) Å indicating that a strong hydrogen bond is present between them. Very likely the amino group is protonated by the phosphonate, and therefore the system has a zwitter ionic character. This is in agreement with IR absorption spectra and with previous works found in the recent literature on similar systems reporting single crystal X-ray structural data [14-16]. This zwitter ionic structural motif has been found on all the R-aminodiphosphonates investigated. We believe that it acts as a structure orienting factor, inducing the formation of the atypical layer framework observed: the P-O···N interaction forces the phosphonate group to be external to the inorganic layer and tends to exclude one P-O group from the zirconium coordination, with the consequent insertion of an additional anionic ligand, F^- in this case, to complete zirconium valence and coordination.

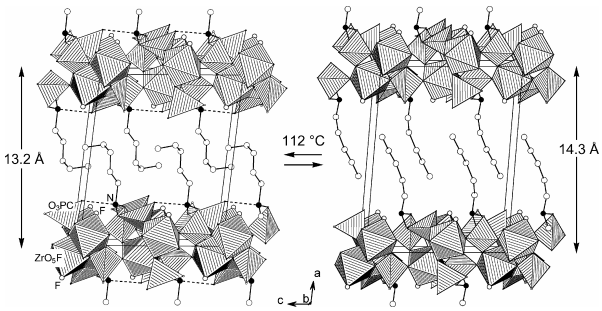

Figure 2. *Structures of **1** before (left) and after (right) the phase transition at 112°C. Hydrogen bonds are represented as dashed lines.*

The aminoalkyl tails point towards the interlayer regions from both sides of the inorganic layers. In this structure the free area associated to each organic pendant group is about 48.6 Å^2 ($a \times b/2$), a large value if compared with those of α- and γ-type structures (about 24.0 and 35.7 Å^2, respectively). This value is more than twice the estimated van der Waals cross section of an alkyl chain (about 18.6 Å^2). Due to this, the packing of the layers generates an interdigitated arrangement of organic groups coming from adjacent layers. To the best of our knowledge, this unusual feature has not been observed in any other zirconium phosphonate. In these alkyl chains, the nitrogen and the first three carbon atoms are close to a trans-trans conformation, while the last two carbon atoms are bent back probably to fill the whole space available.

TG and DSC analysis for **1a** showed a sharp and reversible endothermic peak at 112 °C with no weight loss, and therefore due to a reversible phase transition. The XRPD pattern taken at 150 °C showed that the interlayer distance of the compound increased by more than 1 Å, from 13.2 to 14.3 Å. A structural model of the phase formed (phase **1b**) was obtained by the Rietveld refinement of the room temperature structure (Fig. 2). Unit cell parameters for **1b** are a = 14.341(2) Å, b = 8.869(2) Å, c = 10.932(1) Å, β = 94.51(1)°. In **1b**, the a axis (the direction of layer packing) is longer and the b and c axes (parallel to the layers) are shorter than in **1a**. The increased PO···N distance (2.92(5) Å) suggests that the thermal effect observed by DSC is associated with the loss of PO···N interaction, which produces a relaxation of the whole alkylamino residue, and a consequent conformational change of alkyl chains, that are now close to their extended conformation.

Preliminary studies have shown that compounds of this series, especially the long-chain terms, are able to easily intercalate long-chain alkanols, azobenzene and other large non-polar or low-polar molecules.

The aminobutanoic derivative, $ZrHF(O_3PCH_2)_2NHC_3H_6CO_2$, **2**

Similarly to sample **1a**, structure of **2** has been determined "ab initio" with EXPO, by which eleven of the nineteen atoms of the asymmetric unit were detected. A series of Rietveld refinements alternated with Fourier difference maps, performed with GSAS, revealed the positions of the remaining two oxygen atoms of the layer framework, all four carbon atoms of the alkyl chain and the two oxygen atoms of the carboxylic group. **2** crystallizes in the monoclinic space group $P2_1/c$ with a = 12.9640(3) Å, b = 8.9900(4) Å, c = 10.7924(4) Å, β = 101.854(4)°, and Z = 4. The connectivity of the inorganic part of layers is very similar to **1**, and also in this case, the organic groups are interdigitated in the interlayer region (see Fig. 3).

Two strong non-covalent interactions were detected in the structure. One of them involves neighbouring P-OH and amino groups (PO···N distance = 2.83(2) Å), as observed for **1a**; the other interaction engages terminal carboxylic groups and fluorine atoms belonging to adjacent layers (COO···F = 2.65(2) Å). IR absorption spectra seem to indicate that fluorine atoms are protonated by the carboxylic group.

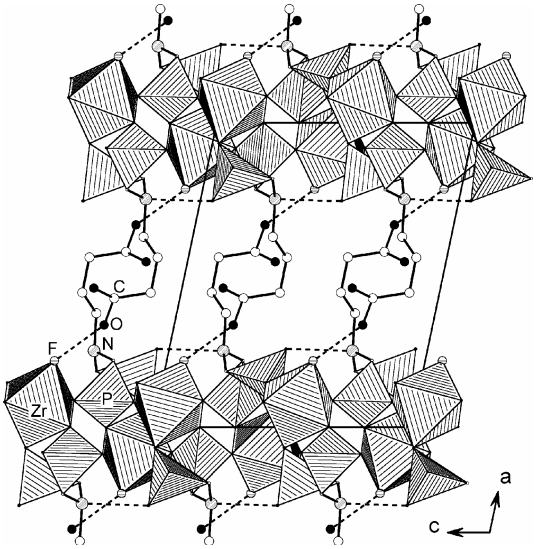

Figure 3: *Structure of **2** viewed along the b axis. Hydrogen bonds are represented as dashed lines.*

Two strong non-covalent interactions were detected in the structure. One of them involves neighbouring P-OH and amino groups (PO···N distance = 2.83(2) Å), as observed for **1a**; the other interaction engages terminal carboxylic groups and fluorine atoms belonging to adjacent layers (COO···F = 2.65(2) Å). IR absorption spectra seem to indicate that fluorine atoms are protonated by the carboxylic group.

Thermal treatment at 240°C caused a change of the interlayer distance from 12.7 to 11.9 Å, due to the loss of one mol of HF per mol of zirconium, with the formation of a stable compound of composition $Zr(O_3PCH_2)_2NHC_3H_6CO_2$. In this compound carboxylate groups are probably coordinated to the zirconium atoms belonging to adjacent layers (Fig. 4), as suggested by the red-shift of the C=O antisymmetric stretching band in the IR spectrum. Unfortunately, our attempts to refine the structure of this phase with the Rietveld method were unsuccessful, because of a global loss of crystallinity.

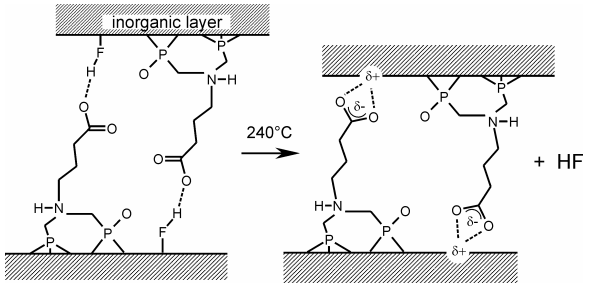

Figure 4: *Scheme of the transformation of **2** after heating at 240°C. Zirconium - carboxylate interaction is represented as intermediate between an ionic interaction and a coordination bond.*

Preliminary experiments have shown that **2** is able to intercalate ammonia and short *n*-alkylamines from ethanol solutions, with the formation of compounds with an increased interlayer distance. When these intercalation compounds are put in water, or when the intercalation reactions are carried out in water, the solid spontaneously exfoliate, and stable colloidal dispersions are obtained. This may be due to the interposition of the guest species between carboxylic groups and fluorine atoms, with the consequent breackage of COO···F interactions between adjacent layers. This feature discloses intriguing potentialities of **2** for application in materials chemistry.

***The benzyl derivative, $ZrF(O_3PCH_2)_2NHCH_2C_6H_5$,* 3.**

This compound crystallizes in the orthorhombic system, *Pbca* space group, a = 8.9429(2) Å, b = 9.1746(2) Å, c = 31.5654(7) Å, Z = 8. The structure was solved in direct space with a "Reverse Monte Carlo" method implemented in the FOX program [17]. The program is able to optimise a structural model described by the use of building blocks defined in terms of their internal coordinates, such as bond lengths, bond angles, and dihedral angles. Trial structures were generated using the "Parallel Tempering" algorithm [18]. The structure was described using one ZrO_5F octahedron and one diphosphonate molecule as building blocks. Benzyl ring lengths and angles were not optimised. All other dihedral angles were left to change freely. In short, (about one million trials, 20 min.) the program found a stable configuration, with a connectivity similar to that previously observed in analogous systems, and a sufficiently low R_{wp} value (0.12). Fig. 5 shows a screenshot of the program interface during the optimisation procedure. The model was then refined with GSAS.

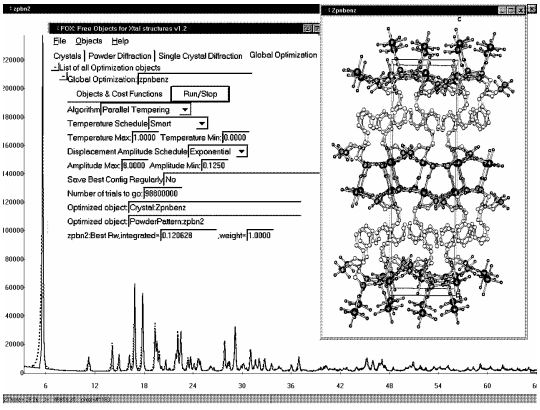

Figure 5: *Screenshot from the FOX program during the structure optimisation of **3**. The trial structure shown on the right is close to the final model. The observed XRD pattern (dashed line) and the calculated one (solid line) are also shown.*

Structure of **3** is similar to that of aminopentyl and aminobutanoic derivatives for many features, such as the atomic connectivity inside the inorganic layers, the interdigitated arrangement of the interlayer organic groups, their zwitterionic character (see Fig. 6).

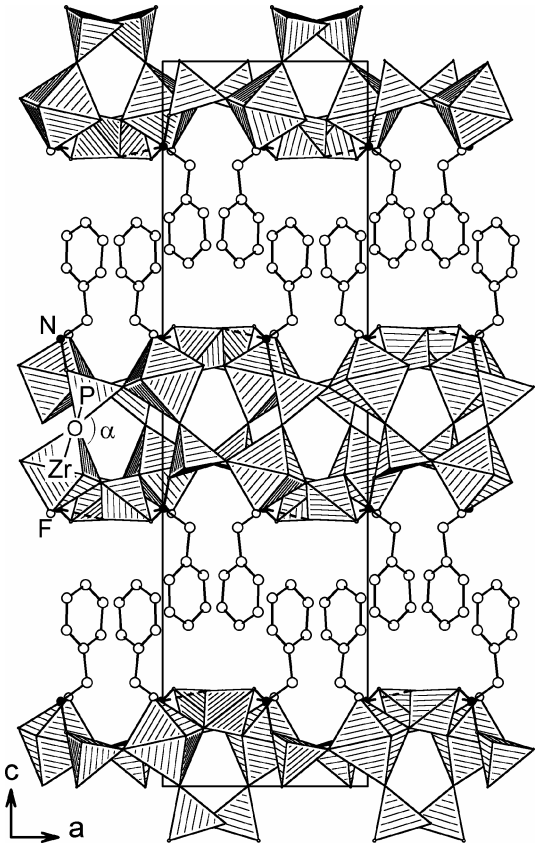

Figure 6: *Structure of **3**, viewed along the b axis. Hydrogen bonds are as dashed lines.*

However, the b axis of **3**, parallel to the layers, is considerably shorter than the corresponding axis (the c axis) in the previously described compounds (9.1746(2) Å for **3**, 10.9793(3) Å for **1a** and 10.7924(4) Å for **2**), while on the other direction parallel to the layers, the a axis of **3** is close to b axis of the other two structures (8.9429(2) Å for **3** vs. 8.8723(3) Å for **1a** and 8.9900(4) Å for **2**). Furthermore the structure of benzylamino derivative is stretched along the c axis, perpendicular to the layer plane, with a larger thickness of the inorganic layers. Parallel planes containing zirconium atoms inside a layer are now 4 Å apart, and the Zr-O-P angle indicated with α in Fig. 6 has an unusual large value of 178.6(7)°. These changes seem to be due to the steric requirements for obtaining a close packed arrangement of benzyl groups. Optimization of the interlayer space, with the probable formation of π-π interactions between benzene rings, should produce a reduction of free area per each benzyl group, which is obtained by the compression of the structure in a direction parallel to the layers (b axis). As a consequence of this, the layer framework is expanded along the c axis.

On the contrary, in the alkyl derivatives the best reciprocal interlayer contacts can be simply found by a conformational change of alkyl chains.

Conclusion

Investigation on zirconium R-amino N,N-bis methylphosphonates started with the aim of finding new layered structures with a poorly hindered interlayer region, that is a free area per each organic group larger than those of traditional α- and γ-zirconium phosphonates. These studies led to the preparation and characterization of a new class of zirconium fluoride diphosphonates with a common layer framework. Their structure has been solved *ab initio* by X-ray powder data from a conventional Bragg-Brentano diffractometer. It is likely that many other hybrid inorgano-organic derivatives can be similarly prepared. In this layer framework the large free area potentially available for each organic group is doubly occupied by two interdigitated moieties. Future investigation will be devoted to finding out whether the whole space could be recovered to accommodate larger functional groups. This study confirms the potential of XRPD technique, even when laboratory equipments are used, for structural investigations of insoluble compounds or for studies when single-crystals are not available.

References

[1] G. Alberti, in *Comprehensive Supramolecular Chemistry,* ed. G. Alberti and T. Bein, Pergamon Press, Oxford, 1996, vol. 7, Chap. 5.
[2] A. Clearfield and U. Costantino, in *Comprehensive Supramolecular Chemistry,* ed. G. Alberti and T. Bein, Pergamon Press, Oxford, 1996, vol. 7, Chap. 4.
[3] A. Clearfield, in *Progress in Inorganic Chemistry*; ed. K. D. Karlin, John Wiley & sons, New York, 1998, vol. 47, pp. 374-510.
[4] G. Alberti, M. Casciola, U. Costantino and R. Vivani, *Adv. Mater.*, **1996,** *8***,** 291.
[5] D. M. Poojary, A. Clearfield, *Acc. Chem. Res.* **1997**, *30*, 414
[6] D. M. Poojary, B. Zhang, Y. Dong, G. Peng, A. Clearfield, *J. Phys. Chem.* **1994**, *98*, 13616.
[7] G. Alberti, R. Vivani and S. M. Mascaròs, *J. Mol. Struct.,* **1998**, *35,* 357.
[8] C. Serre and G. Feréy, *J. Mater. Chem.*, **2002**, *12*, 2367.
[9] U. Costantino, M. Nocchetti, R. Vivani, *J. Am. Chem. Soc.,* **2002**, *124*, 8428.
[10] R. Vivani, U. Costantino, M. Nocchetti, *J. Mater. Chem.,* **2002**, *12*, 3254.
[11] R. Vivani, F. Costantino, M. Nocchetti, G. D. Gatta, *J. Chem Soc.Dalton Trans.,* in press
[12] A. Altomare, M. C. Burla, G. Cascarano, C. Giacovazzo, A. Guagliardi, A. G. G. Moliterni, G. Polidori, *J. Appl. Cryst.* **1995**, *28*, 842.
[13] A. Larson, R. B. Von Dreele, *GSAS, Generalized Structure Analysis System*, Los Alamos National Laboratory, 1988.
[14] J.-G. Mao, Z. Wang and A. Clearfield, *Inorg. Chem.,* **2002**, *41*, 2334.
[15] J.-G. Mao, Z. Wang and A. Clearfield, *J. Chem. Soc. Dalton Trans.,* **2002**, 4457.
[16] Z.-M. Sun, B. -P. Yang, Y. -Q. Sun, J. -G. Mao and A. Clearfield, *J. Solid State Chem.,* **2003**, *176*, 62.
[17] V. Favre-Nicolin and R. Cerny, *J. Appl. Crystallogr.*, **2002**, *35*, 734.
[18] M. Falcioni and M. W. Deem, *J. Chem. Phys.*, **1999**, *110*, 1754

Solving Structures of Polymer Electrolytes. When Single Crystals Are Not Enough.

Yuri G. Andreev and Peter G. Bruce
School of Chemistry, University of St. Andrews, St. Andrews KY16 9ST, (Scotland)
ya@st-and.ac.uk; p.g.bruce@st-and.ac.uk

Introduction

Polymer electrolytes consist of salts e.g. $LiN(SO_2CF_3)_2$, $NaClO_4$, KCF_3SO_3 dissolved in solid polymers such as poly(ethylene oxide) [PEO, $(-CH_2CH_2O-)_n$] [1]. The resulting materials are in fact coordination compounds in the solid state and are analogous to crown ether complexes. They are of considerable interest because of their ability to support ionic conductivity in a solid yet flexible membrane, rendering them key to the realisation of all-solid-state electrochemical devices such as lithium batteries for medical, consumer electronics or other energy storage applications.

Polymer:salt complexes form crystalline phases only at certain discrete compositions characterised by the number of ether oxygens per cation, e.g. 1:1, 3:1, 8:1. For years only amorphous phases of the complexes were considered to be conductors. As a result, the *raison d'être* for elucidating the structures of the crystalline phases was to provide information about the short-range order that is preserved on passing from the crystalline to the amorphous state [2]. However, the discovery of ionic conductivity in the crystalline polymer electrolytes, while previously they had been assumed to be insulators, has heightened interest in the structures of crystalline polymer electrolytes. In fact this discovery was a direct result of crystallographic studies of polymer:salt complexes. Furthemore, many polymer electrolytes have been prepared that contain cations other than Li^+ (including transition metals, lanthanides and actinides) yet their wealth of potential properties has remained unexplored and unexploited in part because of a lack of knowledge concerning the crystal structure of polymer electrolytes.
Until a few years ago the structural chemistry remained a closed book. The paucity of knowledge concerning the crystal structure of polymer electrolytes may be

traced to the difficulty in solving the structures using single crystal techniques applied to stretched fibres. But for a very few notable exceptions this approach has proved fruitless. Indeed pursuing this approach has yielded incorrect structures which have later been solved using superior powder diffraction data, e.g. PEO_4:KSCN [3]. Because powder diffraction yields superior data to that from stretched fibres for the vast majority of polymer electrolytes this has been the approach of choice for several years.

The first structures of crystalline polymer electrolytes, which contained relatively simple anions I^- [4] and SCN^- [5] and a short fragment of the chain (1 or 3 EO units) in the asymmetric unit, were solved from powder data using a combination of techniques ranging from trial-and-error and geometrical considerations to the Patterson method. The arrival of the Rietveld method and adaptation of Direct methods to powder data allowed elucidation of structures containing more complex anions, like $CF_3SO_3^-$, and slightly longer chain fragments either by a combination of refinement and difference Fourier synthesis, using the previously established structures as a starting model [6], or *ab initio* [7]. The development of direct-space methods for *ab initio* structure determination from powders which utilise global optimisation techniques [8,9], following the early idea of Deem, Newsam and Freeman [10], has revolutionised this field of powder diffraction. Remarkably, the first previously unknown structure solved by the direct space approach was that of a polymer electrolyte. All earlier attempts of solving the structure of PEO_3:$LiN(SO_2CF_3)_2$ using Direct methods or refinement, the latter based on structures of the previously determined 3:1 complexes, failed. The original algorithm and the computer program "Simulated Annealing" which incorporates global minimisation by simulated annealing (SA) and a versatile geometrical description of flexible molecules [8,11] not only enabled us to solve the structure which contained a flexible anion as complex as imide, $N(SO_2CF_3)_2^-$, but also promoted the development of other computer programs for *ab initio* structure determination in direct space [12]. Today, a number of polymer electrolyte structures of varying complexity have been solved *ab initio* by "Simulated Annealing" culminating in the solution of PEO_6:$LiAsF_6$ [13]. With 3 independent fragments comprising 26 non-H atoms, and a highly flexible long (6 EO units, 15 variable torsion angles) polymer chain fragment in the asymmetric unit and a total of 79 variables during SA, this structure still remains one of the most complex structures to be determined *ab initio* from powder diffraction data. The solution of the first 6:1 structure also made a dramatic impact on the field of polymer electrolytes, overturning the long-held view that crystalline polymer:salt complexes are insulators. The unusual features of the structure (Fig. 1a), where Li^+ ions reside within cylindrical channels formed by two PEO chains and coordinated only by ether oxygens, suggested that the PEO_6:$LiAsF_6$ complex (as well as isostructural PEO_6:$LiXF_6$, X=P, Sb) might conduct. Subsequent studies not only confirmed the presence of ionic conductivity in the crystalline 6:1 complex but also proved that it conducts better than the amorphous complex of the same composition [14]. Thus today the value of structural studies of crystalline polymer electrolytes stretches far beyond establishing the short-range order in these materials.

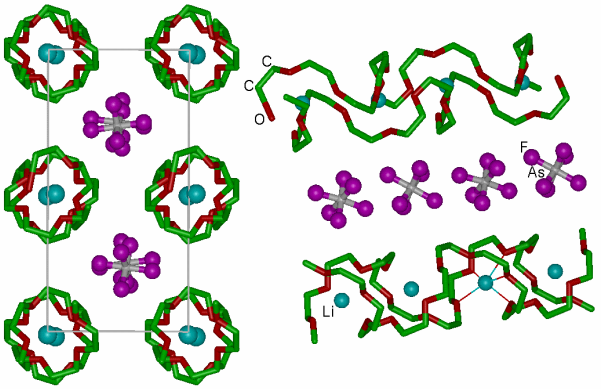

Figure 1: *The structure of PEO_6:$LiAsF_6$. Left, view of the structure along a showing rows of Li^+ ions perpendicular to the page. Right, view of the structure showing the relative position of the chains and their conformation (hydrogens not shown). Thin lines indicate coordination around the Li^+ cation.*

Although powder diffraction alone has proved, in recent years, to be a powerful tool for elucidation of polymer electrolyte structures, nevertheless the possibility of making use of single crystal methods remained tantalising. Here we describe the growth of single crystals of polymer:salt complexes that in combination with powder methods opens the way to accessing a range of polymer electrolyte structures not previously accessible.

Structural variations with molecular weight

In order to grow single crystals of polymer electrolytes the molecular weight (Mw) of PEO must be reduced. The crystal structure of polymer electrolytes appears to be invariant with Mw of PEO in the region 10^3-10^6 Da (Fig.2), while the crystallite size usually increases with the decreasing -Mw, reaching values in excess of 2000 Å [15]. The polymer chains in PEO:salt complexes turn out to be "crystallographically continuous" over much greater distance than the average length of individual chains. In the case of Mw=1000 Da each chain comprises on average only 21 EO units, when terminated by $-CH_3$ groups at both ends, and, depending on the conformation, this stretches over 3-4 unit cells and is typically not more than 40-50 Å in total length, which is ~50 times shorter than the size of the coherently scattering domains. Thus, a near-perfect translation symmetry is maintained over the disruptive regions where the methyl-capped ends of the neighbouring individual polymer chains meet. If this was not so then reducing the Mw from ~100,000, at which the chain length exceeds the coherence length, to 1000 at which it is significantly less, would result in a change of structure.

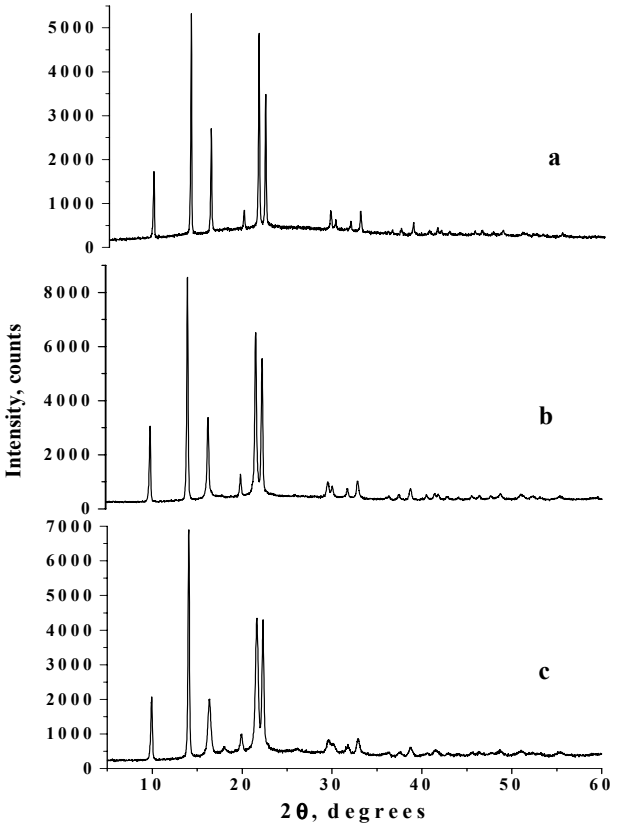

Figure 2: *X-ray powder diffraction patterns (Cu $K_{\alpha 1}$) of PEO_6:$LiSbF_6$, synthesized with Mw of PEO 1000 (a), 1500 (b) and 2000 (c).*

At the lower end of the Mw scale, glymes [$CH_3O(CH_2CH_2O)_nCH_3$, n=1,4] are known to form single crystals when complexed with salts [16]. In this case the chain is not sufficiently long even to mimic the continuity while maintaining the coordination of the cations. However, as can be seen from Fig. 3, the overall motif of the structure is the same as in the PEO complex with the same number of ether oxygens per cation.

New challenges and the new approach

PEO_8:$NaBPh_4$

A powder of an 8:1 crystalline complex with $NaBPh_4$ (Ph – phenyl C_6H_5) was prepared using PEO of Mw=1000. The X-ray pattern (STOE STADI/P) was readily indexed in a monoclinic cell with the space group identified as $P2_1/n$ and the asymmetric unit comprising one formula unit. *Ab initio* structure determination was attempted by the SA method using our "Simulated Annealing" program. Multiple runs of the program using a fully flexible 8-EO chain fragment (72 variable parameters, including 21 torsion angles) and various degrees of the flexibility of the BPh_4^- anion produced a number of structural models. Although each model provided a very good fit to the experimental data none of the models was chemically reasonable in terms of the cation coordination and did not ensure the continuity of the PEO chain at the junctions of neighbouring asymmetric units. Since the number of observable reflections in the powder pattern was in excess of the number of variables by a factor of at least 12 (for the most flexible model) we had to conclude that the multi-dimensional (>90D) parameter space in this case is too complex for a global optimisation algorithm to find the true minimum in a complex landscape of the figure-of-merit function.

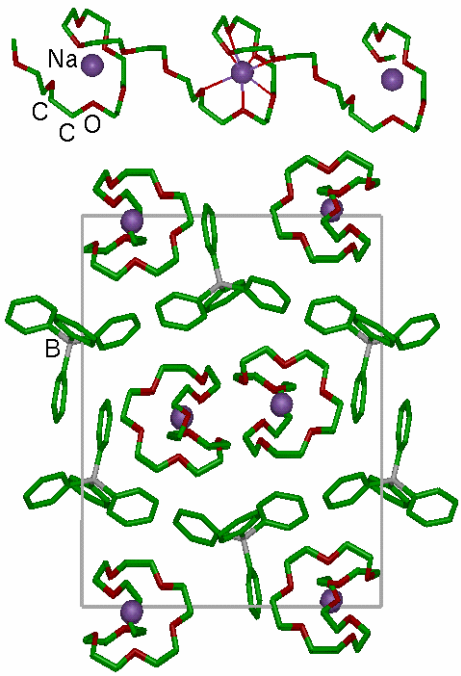

Figure 3: *The structures of diglyme$_2$:$LiSbF_6$ (left) and PEO_6:$LiSbF_6$ (right). Diglyme: $CH_3O(CH_2CH_2O)_2CH_3$; PEO - $CH_3O(CH_2CH_2O)_{20}CH_3$.*

In order to elucidate the structure of PEO_8:$NaBPh_4$ we attempted to grow single crystals of the complex using PEO with a Mw lower than 1000 (to promote the single crystal growth) but higher than that of the glymes (to avoid a possible change in the structure). Single crystals, ~0.1 mm in size, were formed with methoxy-end-capped PEO of average molar mass 500 [$CH_3O(CH_2CH_2O)_{10}CH_3$]. Single crystal data were collected at 125K using Mo K_α on a Bruker SMART diffractometer equipped with a fine-focus sealed tube, a graphite monochromator and a CCD detector. The data confirmed the cell and the space group previously determined from powder diffraction. The structure was solved by Direct Methods and subsequently refined using the SHELXL-97 code [17] using 2699 independently observed reflections with $I>2\sigma(I)$. The refinement converged to an R factor of 10%. Although the basic structure was evident from the single crystal solution, examination of the bond lengths and angles revealed some unrealistic values; for example, C-O distances as high as 1.72 Å and C-C distances as low as 1.14 Å were seen for some of the bonds, compared with typical values for PEO of 1.41-1.46 Å (C-O) and 1.52 -1.56 Å (C-C). This remained so despite

collecting data on several crystals and attempts to improve the refinement, including modelling the disorder by introducing multiple chains with partial occupancies. The origin of this problem lies in the short EO chains of the 500 Mw polymer. The structure determined by single crystal diffraction does not identify discrete chains, instead the chains appear continuous. Where two chain ends meet, two CH_3 groups are adjacent to each other instead of a C-C bond. The separation of two covalently bonded carbons and two CH_3 groups are of course different. This introduces disorder along the chains within the average crystal structure. This disorder is not sufficient to disrupt the translational symmetry of the chains but it does result in abnormal distances observed from the single crystal diffraction data.

Since the effect of chain ends may be reduced significantly by increasing the average molar mass of the PEO, our strategy has been to use the single crystal structure of the short-chain polymer as a starting model for refinement using powder diffraction data collected from a high Mw PEO. A new set of diffraction data was collected from the powder sample prepared with PEO of Mw=100,000. The GSAS program package was used for refinement [18]. The powder pattern consisted of 2869 points and contained 1159 reflections. The refinement involved 164 variables with 121 bond length and bond angle restraints. The final R_{wp} was 0.07 and corresponded to a good fit, as seen in Fig 4. All bond lengths and bond angles in the refined structure were within the acceptable ranges.

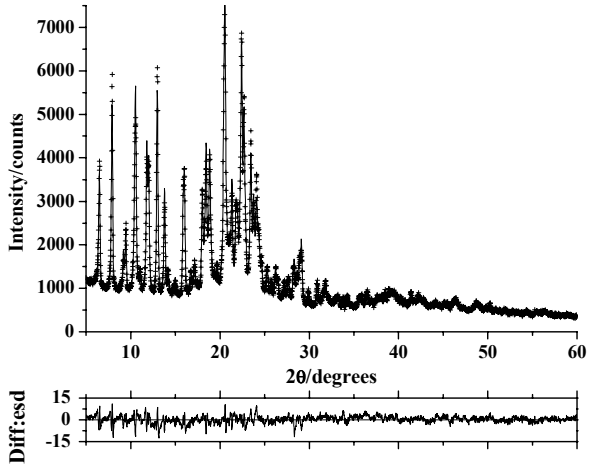

Figure 4: *Fitted X-ray powder diffraction pattern of PEO_8:$NaBPh_4$. Crosses, observed profile; solid lines, calculated (upper) and difference (lower) profiles.*

The final structure obtained by refinement using the powder diffraction data is shown in Fig 5. Each PEO chain folds such as to present a ring of 5 ether oxygens with one ether oxygen above and another below the plane of the ring. The Na^+ ions are located within this ring and are therefore coordinated by 7 ether oxygens. The BPh_4^- anions are located between the chains and do not coordinate to the cations.

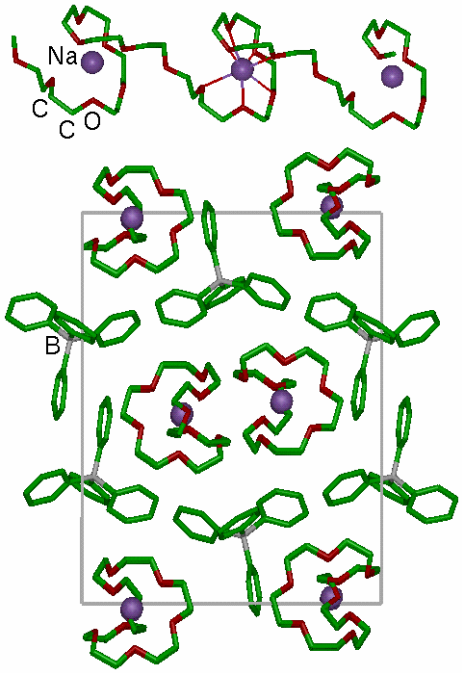

Figure 5: *The structure of PEO_8:$NaBPh_4$.; Top: view showing the conformation of the PEO chain and the coordination around the Na^+ cation (thin lines) (H atoms not shown); Bottom: view along the chain axis.*

The structure is quite different from all previously known polymer electrolyte crystal structures [19]. Only one chain is involved in coordinating the cations whereas in the 6:1 structures each PEO chain folds to form a half cylinder with pairs of chains interlocking to generate tunnels within which the Li^+ cations reside; again there is no coordination of the cations by the anions. As the salt content is increased and we reach the 4:1 and 3:1 complexes, each chain folds to form a helix with a cation being located in each loop of the helix. At these salt concentrations the anions also coordinate the cations unlike the situation in the 6:1 or 8:1 complexes. In the case of the even more concentrated 1:1 complexes the PEO chains adopt a zig-zag confirmation with the cations being coordinated by only 2 ether oxygens and either 4 or 5 anions depending on the particular salt, the anions bridge to cations associated with neighbouring chains thus generating a 3-dimensional network. We see that extending the boundaries of our polymer electrolyte structure to include the 8:1 complexes has revealed quite new polymer chain conformations. Also for the first time we observe a chain that describes two conformations which repeat alternately along its length. One involves chain folding to form a coordination site for the cation and the other links these coordination sites along the chain. This is in contrast to structures determined previously that exhibit the same single repeating confirmation throughout the structure.

PEO_4:$ZnCl_2$

A powder of a 4:1 crystalline complex with $ZnCl_2$ was first prepared using PEO of Mw=1000. Indexing of the X-ray powder pattern (STOE STADI/P) suggested a number of monoclinic cells and space groups with the asymmetric unit comprising either one or two formula units, depending on the cell volume. *Ab inito* structure determination was attempted using our "Simulated Annealing" program in all the possible cells and space groups. As in the case of PEO_8:$NaBPh_4$, the structural models produced by the SA procedure provided good fits to the experimental data but lacked chemical sense.

Single crystals of PEO_4:$ZnCl_2$ were grown using methoxy-end-capped PEO, Mw=500. The data from a single crystal ~0.1 mm in size were collected at 125K using Mo K_α on a Bruker SMART diffractometer. The volume of the unit cell appeared to be much smaller, 2-4 times, compared to the cells previously suggested by indexing the powder data. The space group was identified as C2/c with Zn^{2+} occupying a special position. The structure was solved and refined using 1196 independently observed reflections. Similar to the single-crystal model of PEO_8:$NaBPh_4$, the short chains in PEO_4:$ZnCl_2$ did not reveal any ordering of the CH_3 ends (as expected given the polydispersity) and appeared to be continuous with a number of bond lengths and bond angles lying well outside the acceptable limits. In order to this hurdle a new powder sample was prepared with PEO of Mw=2000. This average chain length reduces the number of the chain ends four-fold while at the same time preserving sufficient crystallinity for a powder refinement to succeed. The powder pattern (STOE STADI/P) consisted of 2498 points and contained 194 reflections. The refinement involved 30 variables with 15 bond length and bond angle restraints. The final χ^2 was 2.6 and corresponded to a good fit as seen in Fig 6.

The structure of PEO_4:$ZnCl_2$ is shown in Fig. 7 (left). The PEO chains are located in sets of planes parallel to the *bc* plane of the unit cell. As can be seen in Fig. 7 the chains are remarkably flat within these planes. A single chain is shown in Fig. 6 (right). It describes large loops within each of which a Zn^{2+} ion is located. Each Zn^{2+} ion is coordinated by two neighbouring ether oxygens along the chain and two Cl^- ions, the coordination around Zn^{2+} is therefore four forming a slightly distorted tetrahedron. There are two non-coordinating ether oxygens between each Zn^{2+} along the chain. Each chain is isolated from its neighbours. The Cl^- ions protrude from each chain but are more than 2.5Å from the atoms of the neighbouring chains, therefore there is no evidence of interaction between the Cl^- ions, or indeed any other parts of the chain, with neighbouring chains. The chains are held together in the solid state by only weak Van der Waals forces.

As might have been anticipated for the first structure of a polymer electrolyte containing divalent cations, the structure is completely different from any of the previously known polymer electrolytes containing monovalent cations. It would not have been possible to establish the structure of the present material starting from any known monovalent structure.

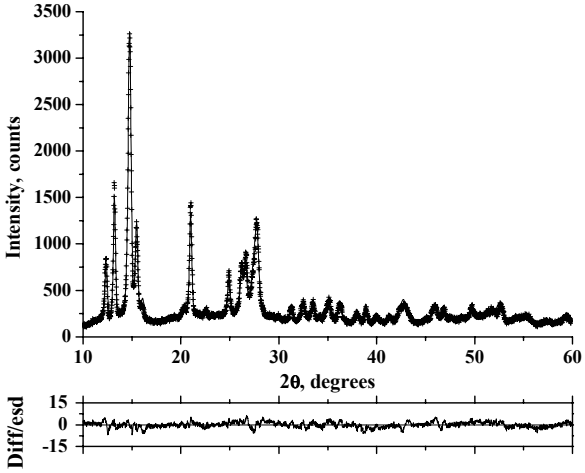

Figure 6: *Fitted X-ray powder diffraction pattern of PEO_4:$ZnCl_2$. Crosses, observed profile; solid lines, calculated (upper) and difference (lower) profiles.*

Conclusion

It is possible to grow single crystals of polymer electrolytes using PEO chains that are sufficiently short to promote single crystal growth but sufficiently long to retain the structure of the higher Mw analogues. Although the structures obtained from single crystal diffraction are essentially the same as the high Mw structures preserving the same translational symmetry, the effect of chain ends is sufficiently high to lead to unrealistic average bond lengths. However the single crystal determination does provide a sufficiently good model with which to carry out refinement of the structure using powder data collected on high molecular weight analogues. By this means we eliminate the problems introduced into the single crystal polymers by random chain ends. The approach described here has removed a major barrier to the establishment of the many polymer electrolyte structures that were impossible to access by other means.

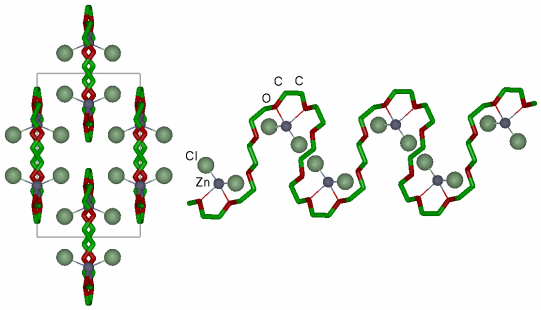

Figure 7: *(Left) View of the structure of PEO_4:$ZnCl_2$ showing the stacking of 4 PEO chains in the unit cell. The chains are located within the bc plane and run along b. (Right) The conformation of an individual chain and the coordination around the Zn^+ cation (thin lines) (hydrogens not shown).*

References

[1] "Solid State Electrochemistry", Ed. P. G. Bruce. Cambridge University Press, 1995.
[2] R. Frech, S. Chintapalli, P. G. Bruce, C. A. Vincent, J. Chem. Soc. Chem. Commun., 1997, 157.
[3] T. Hibma, Solid State Ionics, 1983, 9/10, 1101.
[4] Y. Chatani, S. Okamura, Polymer, 1987, 28, 1815.
[5] Y. Chatani, Y. Fujii, T. Takayanagi, A. Honma, Polymer, 1990, 31, 2238.
[6] P. Lightfoot, M. A. Mehta, P. G. Bruce, Science, 1993, 262, 883.
[7] P. Lightfoot, J. L. Nowinski, P. G. Bruce, J. Am. Chem. Soc, 1994, 116, 7469.
[8] Y. G. Andreev, P. Lightfoot, P. G. Bruce, J. Chem. Soc. Chem. Commun., 1996, 2169.
[9] K. Shankland, W. I. F. David, T. Csoka, Z. Kristallogr., 1997, 220, 550.
[10] J. M. Newsam, M. W. Deem, C. M. Freeman, Accuracy in Powder Diffraction II, NIST Spec. Publ. No. 846, 1992, 80.
[11] Y. G. Andreev, P. Lightfoot, P. G. Bruce, J. Appl. Cryst., 1997, 30, 294.
[12] W. I. F. David, K. Shankland, N. Shankland. J. Chem. Soc. Chem. Commun., 1998, 931; K.D.M. Harris, R.L. Johnston, B.M. Kariuki, Acta Cryst. A, 1998, 54, 632; H. Putz, J.C. Schoen, M. Jansen, J. Appl. Cryst., 1999, 32, 864; G.E. Engel, S. Wilke, O.Koenig, K.D.M. Harris, F.J.J. Leusen, J. Appl. Cryst., 1999, 32,1169; S. Pagola, P. W. Stephens, D. S. Bohle, A. D. Kosar, S., K. Madsen, Nature, 2000, 404, 307; A. Le Bail, Mat. Sci. Forum, 2001, 378-381, 65; S. Brenner, L. B. McCusker, C. Baerlocher, J. Appl. Cryst., 2002, 35, 243; V. Favre-Nicolin, R. Cerny, J. Appl. Cryst., 2002, 35, 734.
[13] G. S. MacGlashan, Y. G. Andreev, P. G. Bruce, Nature, 1999, 398, 792.
[14] Z. Gadjourova, Y. G. Andreev, D. P. Tunstall, P. G. Bruce, Nature, 2001, 412, 520.
[15] Z. Stoeva, I. Martin-Litas, E. Staunton, Y. G. Andreev, P. G. Bruce, J. Am. Chem. Soc., 2003, 125, 4619.
[16] V. Seneviratne, R. Frech, J. E. Furneaux, M. Khan, in preparation.
[17] G. M. Sheldrick, T. R. Schneider, Method. Enzymol., 1997, 277, 319.
[18] A. C. Larson, R. B. Von Dreele, GSAS, General Structure Analysis System (Los Alamos National Laboratory rep. no. LA-UR-86-748, Los Alamos, 1987).
[19] Y. G. Andreev, P. G. Bruce, J. Phys. Cond. Matter, 2001, 13, 8245.

Powder Diffraction Studies of Nickel Open Framework Materials

Nathalie Guillou and Carine Livage

Institut Lavoisier, UMR CNRS C8637, Université de Versailles St-Quentin-en-Yvelines, 45 Avenue des Etats-Unis, F-78035 Versailles (France)
e-mail: guillou@chimie.uvsq.fr

Introduction

The preparation of open frameworks based on transition metals is actually one of the most important aims of research due to their practical application as catalysts, hosts in intercalation compounds and their potential electronic properties. The use of an organic moiety which can be part of the framework, as carboxylate ions, combined with hydrothermal conditions, can considerably enlarge the range of possible structural architectures. As illustrated by recent results concerning cobalt succinates [1] and manganese glutarate [2], the dimensionality of the metal oxide network, and therefore the stability of the compounds are increased by a higher degree of flexibility of the organic. With nickel, the chemistry is even more generous with novel M-O-M connectivities in which polyhedra can share faces, edges and /or corners [3]. Therefore, we focused our attention on nickel edifices built up from dicarboxylates. Due to the difficulty to grow single crystals of nickel hybrids, powder diffraction is most of the time essential for our studies. We report here three of our more significant results concerning *ab initio* structural determinations: two succinates from high resolution synchrotron data [4,5], and one glutarate from conventional X-ray source [6].

Experimental Section

All reactions were carried out in Teflon containers under autogenous pressures with reagents purchased from Aldrich Chemicals and used as supplied. In a typical reaction, a mixture of nickel (II) chloride hexahydrate, dicarboxylic acid, potassium hydroxide and H_2O (or H_2O/ethanol) was stirred until homogeneous and then heated at 180°C for two days. After cooling, pale green powders were obtained, washed with distilled water and dried at room temperature [4-6].
Samples of the two succinates were sealed in glass capillaries and high-resolution synchrotron powder data were collected on the powder diffractometer on the Swiss-Norwegian Beamline (SNBL) at the European Synchrotron Radiation Facility (ESRF) in Grenoble. Measurements were made with a Si (111) analyzer crystal to select a monochromatic wavelength of 0.7999 Å. Patterns were scanned with step length of 0.0035° (2θ) and were divided in two 2θ regions (1-15° and 15-45°), with times per step of 1 and 3s respectively, to improve the counting statistics at higher 2θ angles. The data were normalized by using the monitor counts.
The X-ray powder diffraction data of the nickel glutarate were collected on a Siemens D5000

diffractometer by using Bragg-Brentano geometry and $CuK_{\alpha 1,2}$ radiation (λ = 1.5418 Å). It was scanned over an angular range 5-90° (2θ) with a step length of 0.02° (2θ). To improve the counting statistics at high angles, the pattern was divided in two 2θ regions (1-35.98° and 36-90°), with times per step of 32 and 64 s, respectively.

X-Ray Diffraction Analysis

Indexing: In all cases, the extraction of the peak positions for indexing was performed by means of the WinPLOTR program [7] and pattern indexing was carried out with the computer program DICVOL91 [8] from the first twenty lines, with an absolute error on peak positions of 0.008°(2θ) for synchrotron data and of 0.03 °(2θ) for conventional diffractometer ones. The adequacy of unit cells and space groups was then confirmed by structureless whole pattern profile refinements by the Le Bail method [9] integrated in the FullProf program [10].

Structural investigations

$Ni_7[(C_4H_4O_4)_4(OH)_6(H_2O)_3]\cdot 7H_2O$ **(1)** and $Ni_7[(C_4H_4O_4)\ (OH)_2(H_2O)_2].1.6H_2O$ **(2)**
In both cases, SHELXTL [11] was used for Direct methods calculations. A list of 2921 integrated intensities [1253 for **(2)**] was extracted in the angular range 1-44°(2θ). 252 phases [233 for **(2)**] were observed for |E| values greater than 1.2 and refined using 4213 and 10764 unique triplets for **(1)** and **(2)**, respectively. By increasing the number of Direct methods attempts to 256, the most probable E-map [with a SHELXS combined figure of merit of 0.176 and of 0.195 for **(1)** and **(2)**, respectively] revealed, in both cases, the location of all independent nickel atoms, with 17 surrounding oxygens and few carbons for **(1)**, and with 13 surrounding oxygens for **(2)**. These corresponding atomic coordinates were used as the starting model in the Rietveld refinement, which converged approximately to R_B = 0.30 and R_F = 0.20 for **(1)**, and to R_B = 0.28 and R_F = 0.17 for **(2)** , confirming the validity of initial hypotheses. Successive difference Fourier maps alternated with profile refinements in the Rietveld method allowed completion of the inorganic framework. At this stage, the use of soft distance and angular constraints, to stabilise the oxide framework, gave gradually clearer difference electron density maps and allowed to complete the organic moieties and the location of the free water molecules.

$Ni_{20}[(C_5H_6O_4)_{20}(H_2O)_8]\cdot 40H_2O$ **(3)**
Structure solution was initialized with the EXPO package [12], integrating EXTRA [13], for extracting integrated intensities, and SIR97 [14] for Direct methods structure solution. A list of 101 reflections was extracted in the angular range 7-70° (2θ). The two nickel atoms with their environments, and a few carbons, were found unambiguously from the E-map with the highest figure of merit. This partial structure was then used as fragment to complete the structural model. The corresponding atomic coordinates were used as starting model for Rietveld refinement. Successive Fourier difference calculations were then performed with SHELXL [11] to finalize the structural model.

Details of the final Rietveld refinements carried out with FullProf [10] integrated in WinPLOTR [7] are summarized in Table 1. The final fits obtained between calculated and observed patterns are shown in Figure 1.

Table 1: *Crystallographic data for the three compounds*

Compound	1	2	3
Crystal system	Monoclinic	Rhombohedral	Cubic
Space group	$P2_1/c$	$R\text{-}3c$	$P4_3\,3\,2$
a (Å)	7.8597(1)	21.0372(1)	16.5812(7)
b (Å)	18.8154(3)		
c (Å)	23.4377(4)	45.7975(3)	
β (°)	92.0288(9)		
V (Å^3)	3463.9(2)	17552.9(3)	4558.8(6)
Figures of Merit	M_{20} = 34	M_{20} = 25	M_{20} = 39
	F_{20} = 210 (0.0026, 36)	F_{20} = 99 (0.0020, 102)	F_{20} = 75 (0.0095, 28)
2 θ range (°)	2.5-40	2-45	5-90
No. reflections	2266	1786	416
No. atoms	55	32	16
No. struct. parameters	170	96	42
R_P, R_{WP}	0.049, 0.062	0.053, 0.062	0.069, 0.095
R_B, R_F	0.063, 0.066	0.046, 0.037	0.033, 0.030

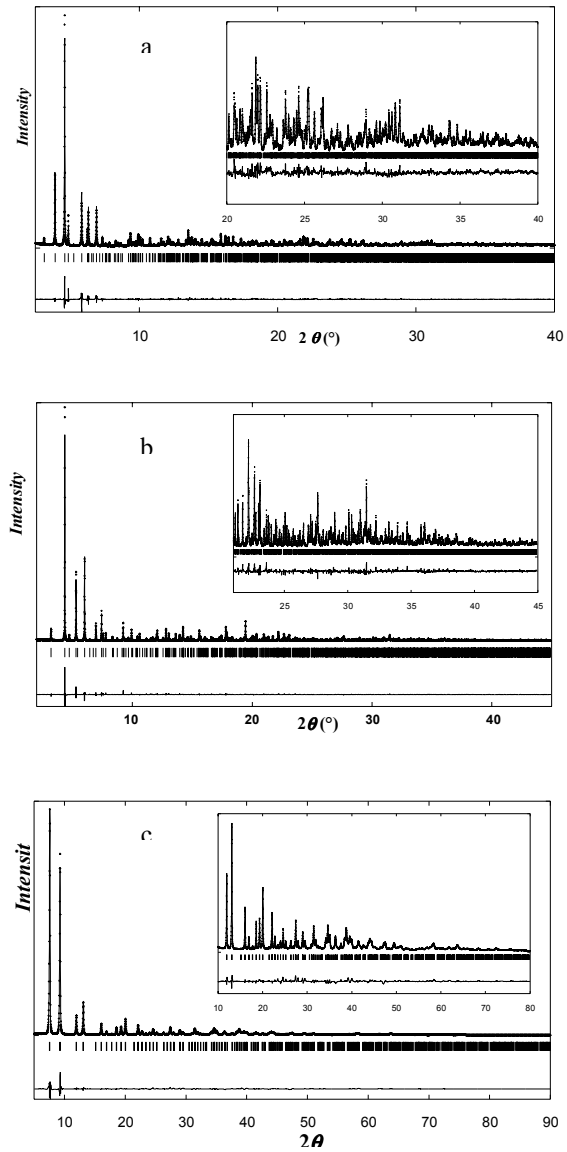

Figure 1*: Final Rietveld plots of* ***(1)*** *(a),* ***(2)*** *(b) and* ***(3)*** *(c). Zooms at high angles are shown as inset.*

Description of the Structures and Discussion

The structure of **(1)** [5], can be described from hybrid organic-inorganic layers in the *bc* plane, constructed from nickel oxide corrugated chains running along the *b* axis connected *via* succinate ions along the *c* axis (Fig. 2). All carboxylates of the four independent succinates are deprotonated. Half of the organic molecules (dark grey) decorate the chains, and then the others (light grey) covalently connect them along the *c* axis. Nickel atoms occupy seven independent crystallographic sites with an octahedral coordination of oxygen atoms arising from four succinate ions, two μ_4, two μ_3, and three μ_2 oxygens, and two terminal water molecules. Inorganic chains are built up from hexameric units connected *via* a seventh octahedron, which shares two edges in *trans* position with two neighbouring hexamers (Fig. 2). The hexameric unit is constructed from a dimer of face sharing octahedra grafted onto a tetramer formed by two dimers of edge sharing octahedra connected by corners *via* hydroxyl ions. The two face sharing nickels are connected to the tetramer, *via* edges with the two neighbouring nickel octahedra, and *via* corners with the two opposite ones. Considering bond valence calculations [15], we attributed the μ_4-O to OH groups and the μ_2-O sites were considered as statistically occupied by one water molecule and two OH groups. The three dimensional arrangement is ensured by strong hydrogen bonds, directly between two adjacent layers. A pseudo-three-dimensional hybrid framework is thus formed with channels containing seven free water molecules. Thermodiffractometry showed a reversible dehydration without damage of the oxide framework until c.a. 300°C. That confers to the material sorption properties with a specific area of 135(4) m^2g^{-1} [5].

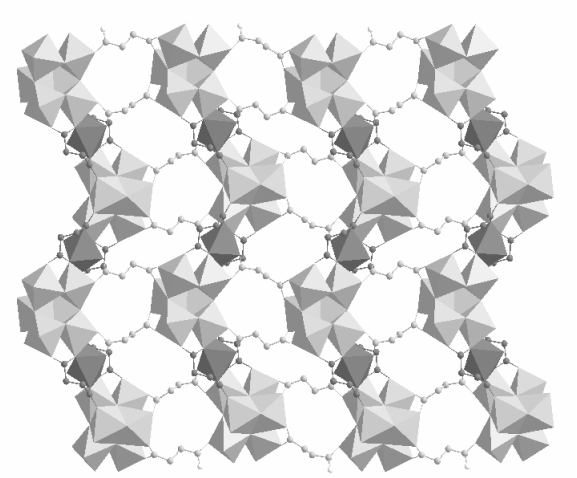

Figure 2: *Projection of the structure of* ***(1)*** *along the a axis where hexanickel units (light grey) are each connected to two bridging Ni octahedra (dark grey). Decorating succinate ions are represented in dark grey and bridging ones in light grey.*

(2) was the first metal carboxylate which presents a three dimensional oxide network [4]. Its structure can be described from layers of edge sharing octahedra in the *ab* plane, constructed from circular 12-rings surrounded by six truncated triangular 15-rings (Fig. 3). Their connectivity is insured along *c* via "isolated" corner sharing octahedra, to build up a remarkable honeycomb nickel oxide framework. The oxide framework is decorated by three independent, deprotonated succinate anions. Two of them (dark grey) have multidendate carboxylate groups which each coordinate to three nickel atoms, in a μ_2 and a terminal fashion. The third one (light grey) presents one carboxylate with the connectivity described above and a second carboxylate with a μ_2 oxygen and a non bonded one.

(3) presents an amazing chiral three-dimensional network of edge sharing nickel octahedra, generated by two independent nickel atoms located on the threefold and on the twofold axes. Each Ni1 octahedron shares three edges with three Ni2 octahedra, when each Ni2 octahedron shares two of its *trans* edges with two neighboring Ni1 polyhedra.

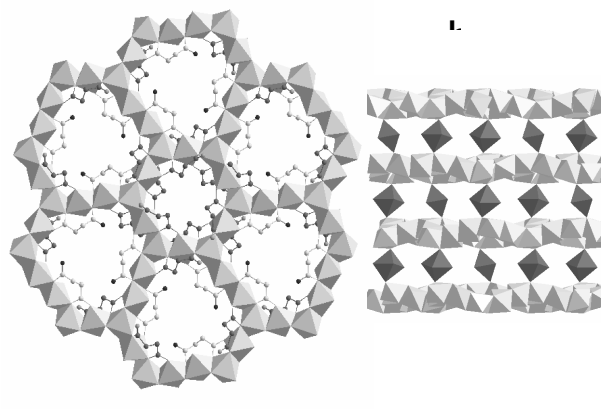

Figure 3: *(a) View of a single Nickel oxide layer in* ***(2)****; (b) View of the connection of the layers via isolated corner sharing octahedra (dark grey).*

This complicated oxide network can be simply described from helixes running along the *a* axis, where Ni1 and Ni2 polyhedra alternate (Fig. 4a). Each helix is connected to four out-of-phase parallel neighboring ones through a third Ni2 octahedron, for generating corrugated twenty membered rings. That also induces the formation of perpendicular helices (Fig. 4b). The oxide framework is decorated by two independent deprotonated glutarate anions (Fig. 4c). The first one (dark grey) located on the twofold axis has two multidendate carboxylate groups which are each coordinated to three nickel atoms. The second one (light grey) presents two carboxylates with a μ2 oxygen and a non bonded one. This glutarate ion is located on a threefold axis, with statistic occupancy of 2/3. Bridging water molecules complete octahedral nickels environments. The twenty membered rings intersect each other to generate very large crossing tunnels in the [111] direction. They contain disordered water molecules which could easily be removed. That leads to a specific area of 346(10) m^2g^{-1}.

In summary, three nickel carboxylates were synthesized by hydrothermal techniques. The novelty of these structures illustrates the flexibility of nickel oxide networks and confirms the versatility of nickel inorganic condensation under hydrothermal conditions. The structure determination of **(1)** (55 atoms and 165 atomic coordinates), by Direct methods strategy and Fourier difference maps, from synchrotron powder diffraction data, reaches the limits of "traditional" *ab initio* methods. Above this limit and for larger cells, a new way of collecting [16] or direct space strategies in the case of organic materials [17], must be used, as was shown recently. Concerning **(2)**, the critical step for determining the structure was to find the true symmetry. Indeed, a such gigantic unit cell [V = 17552.9 (3) $Å^3$] combined to a rhombohedral system tends to increase the number of possible reflections (102) compared to that of observed ones (20), which decreases figures of merit. At the mean time, single crystals of this phase could be obtained by Forster and Cheetham *via* a new synthetic approach [4], and confirmed the rhombohedral symmetry. Nevertheless, an *ab initio* structural investigation from synchrotron data, already collected, was undertaken.

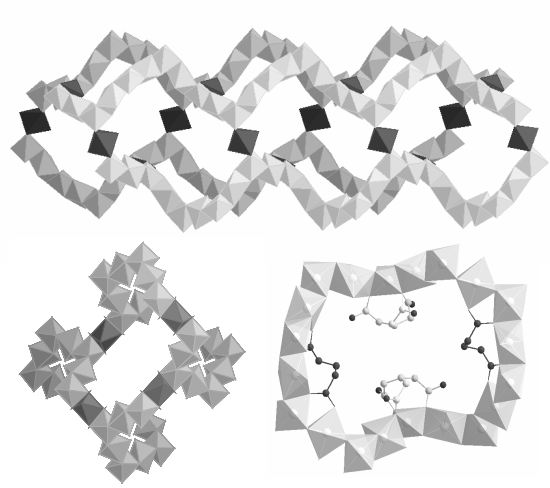

Figure 4: *(top) View of four helices with alternating Ni1 and Ni2 (light grey) connected by Ni2 octahedra (dark grey); (bottom left) view of these four helices in the perpendicular direction;(bottom right) Polyhedral view of a corrugated twenty membered ring with the two independent glutarate ions. The dark grey one is disordered with statistic occupancy of 2/3.*

Most of the oxide framework (only one oxygen atom was missing) was found from Direct methods strategy, which demonstrates, once again, the power of powder diffraction. The structure determination of **(3)** was less difficult than the two first ones but it represents a nice example of what it could be done with conventional diffractometer data. Indeed, the exact overlap of non equivalent reflections, due to cubic symmetry, increases the difficulty to extract the relative intensities, and then to start the *ab initio* structural determination. Moreover, the problem of disorder between framework water molecules and dicarboxylate oxygens was not crucial. Last but not the least, the nickel glutarate is the first carboxylate which presents a chiral structure with a three dimensional network of very large crossing channels, it is a pure ferromagnet at 4 K, and it becomes porous after removing the water of hydration [6].

Acknowledgments

We thank the ESRF for allowing us access to their synchrotron facility. The Authors gratefully acknowledge the assistance of Wouter van Beek during synchrotron data collection, and Prof. Gérard Férey for helpful discussions.

References

[1] C. Livage, C. Egger, G. Férey, Chem. Mater., 2001, 13, 410.
[2] R. Vaidhyanathan, S. Natarajan, C.N.R. Rao, J. Chem. Soc. Dalton Trans., 2003, 172, 1459.
[3] N. Guillou, Q. Gao, P. M. Forster, J.-S Chang, M. Noguès, S.-E. Park, G. Férey, A.K. Cheetham, Angew. Chem. Int. Ed., 2001, 40(15), 2831.

[4] P.M. Forster, A.K. Cheetham, Angew. Chem. Int. Ed., 2002, 41, 457.
[5] N. Guillou, C. Livage, W. van Beek, M. Noguès, G. Férey, Angew. Chem. Int. Ed., 2003, 42, 457.
[6] N. Guillou, C. Livage, M. Drillon, G. Férey, Angew. Chem. Int. Ed., 2003, 42, 5314.
[7] T. Roisnel, J. Rodriguez-Carvajal, Mater. Sci. Forum Vols., 2001, 378-381, p 118.
[8] A. Boultif, D. Louër, *J. Appl. Crystallogr.*, 1991, 24, 987.
[9] A. Le Bail, H. Duroy, J.F. Fourquet, *Mater. Res. Bull.,* 1988, 23, 447.
[10] J. Rodriguez-Carvajal, in "Collected Abstract of Powder Diffraction Meeting", Toulouse, 1990, p 127.
[11] G. M. Sheldrick, SHELXS97 and SHELXL97, University of Göttigen, 1997, Germany.
[12] A. Altomare, M. C. Burla, M. Camalli, B. Carozzini, G. L. Cascarano, C. Giacovazzo, A. Guagliardi, A. G. G. Moliterni, G. Polidori, R. Rizzi, *J. Appl. Crystallogr.* 1999, 32, 339.
[13] A. Altomare, M. C. Burla, G. Cascarano, C. Giacovazzo, A. Guagliardi, A. G. G. Moliterni, G. Polidori, *J. Appl. Crystallogr.* **1995**, *28*, 842-846
[14] A. Altomare, M. C. Burla, M. Camalli, G. L. Cascarano, C. Giacovazzo, A. Guagliardi, A. G. G. Moliterni, G. Polidori, R. Spagna, *J. Appl. Crystallogr.* **1999**, *32*, 115-119
[15] N. Brese and M. O'Keeffe, Acta Crystallogr. B47 (1991), 192.
[16] T. Wessels, C. Baerlocher, L.B. McCusker and E.J. Creyghton, J. Am. Chem. Soc. 121 (1999), 6242.
[17] K. D. M. Harris, M. Tremayne and B. M. Kariuki, Angew. Chem. Int. Ed., 40 (2001), 1626; E. Tedesco, G. W. Turner, K. D. M. Harris, R. L. Johnston, B. M. Kariuki, Angew. Chem. Int. Ed 39, (2000), 4488.

Short-range Order of Glassy Polymers by Neutron Diffraction with Polarization Analysis and MD-simulations

J. Colmenero[1,2,3*], A. Arbe[2], F. Alvarez[1,2]
[1]Departamento de Física de Materiales, Universidad del País Vasco (UPV/EHU), Apartado 1072 20080 San Sebastián (Spain)
[2]Unidad de Física de Materiales (CSIC-UPV/EHU), Apartado 1072, 20080 San Sebastián, Spain
[3]Donostia International Physics Center, Paseo Manuel de Lardizabal 4, 20018 San Sebastián (Spain)
wapcolej@sc.ehu.es

Introduction

Although nowadays it is generally accepted that the conformation of polymer chains in the bulk follows the random coil model proposed by Flory [1], the short-range order of polymer melts and glassy polymers is still poorly understood. The effects of short-range order become apparent in a diffraction experiment at Q-values (Q: wave number) higher than about 0.5 $Å^{-1}$. A typical diffraction pattern obtained, for example, by neutron diffraction from a fully deuterated polymer shows marked diffraction maxima at Q-values between 1 and 2 $Å^{-1}$ which, in principle, correspond to inter-chain correlations and weaker maxima at higher values, corresponding to intra-chain correlations [2]. However, almost nothing is known about the relationship between these maxima and the particular chemical structure of the monomer or the microstructure of the chain. For instance, some polymers as 1,4–polybutadiene or poly(vinyl chloride) show only one "inter-molecular" peak while others display a peak with a shoulder or even two clearly distinguished peaks as, e.g., 1,2–polybutadiene or polyisoprene [3]. It is noteworthy that the presence of such shoulders or second peaks in the intermolecular range of Q is not always correlated with the existence of a bulky side group in the monomer, as it could be expected from simple arguments.

For an amorphous system the structural information is contained in the so-called radial distribution function g(r) or in its Fourier transform counterpart: the static structure factor S(Q). In the case of amorphous polymers composed by carbons and hydrogens, S(Q) can be measured by neutron diffraction using a fully deuterated sample, i.e., a sample where all hydrogens are replaced by deuterons. As the neutron scattering lengths of carbon and deuteron are very similar, both atoms are almost indistinguishable for neutrons. However, in the case of complicated molecular systems as polymers, the average structural information contained in either g(r) or S(Q) does not allow to easily unveil the short range order details. It is therefore of utmost importance in these cases to obtain additional information on the particular correlations arising from groups of selected atoms. This knowledge can be achieved by the study of partial static structure factors or partial radial distribution functions. For instance, in the case of polymers only composed by carbon and hydrogen atoms, the X-ray diffraction intensity mainly highlights the carbon–carbon correlations due to the values of the X-ray scattering factors of carbon and hydrogen. Experimentally, other different partial structure factors can be accessed by means of the isotopic substitution techniques combined with neutron diffraction with polarization analysis. In the case of polymers, the isotopic labeling is based on the very different neutron scattering lengths of hydrogen and deuteron atoms. Moreover, it seems that substitution of hydrogen by deuteron atoms hardly affects the structural properties of amorphous polymers in general. Thus, by taking advantage of these features, one can profit of selective deuteration labeling techniques in order to obtain the different partial contributions to the

total static structure factor arising from differently deuterated samples. On the other hand, neutron diffraction measurements with polarization analysis allow separating the coherent and incoherent contributions to the scattering and provide coherent cross sections at an absolute scale. This kind of measurements can be carried out by means of the so-called diffuse scattering spectrometers as, for instance, the D7 instrument at the Institute Laue-Langevin (ILL) in Grenoble (France) or the DNS instrument at the Forschungszentrum (FZ-IFF) in Jülich (Germany). However, we have to point out that, though these techniques access experimentally the partial static structure factors in absolute scales, the interpretation of the results in terms of the atomic correlations is usually extremely difficult.

On the other hand, modern computer simulation techniques seem to be one of the most promising tools for unraveling the local structure and the dynamics of polymer melts. First of all, computer simulation enables precise insight into the atomic structure and dynamics. Second, one can artificially modify in an easy way the scattering lengths of partial groups of atoms in the simulation, thus enhancing particular correlations in the calculated structure factors. However, to do this, fully atomistic and well-equilibrated samples are necessary, i.e., first of all the simulated cells have to be validated by extensive scattering experiments. After this comparison, the simulation conditions can also be improved. Thereby, it seems that a combination of computer simulation and neutron diffraction experiments with polarization analysis on partially deuterated samples, is so far the best route to provide new insight into the problem of the short-range order in polymers. To our knowledge, a coordinated effort in this line has only been carried out in a few cases [3-6] up to date. In this work, after giving basic information about the neutron diffraction technique with polarization analysis and the simulation procedure as well, we will show some examples of the application of this procedure taken from the recent literature.

Neutron diffraction with polarization analysis

In a usual neutron diffraction experiment one always measures the total scattered intensity, which is a sum of the coherent and the incoherent contributions. Polarization analysis can separate experimentally the coherent and incoherent components and thus a purely coherent diffraction pattern for further analysis is obtained. Additionally, this method provides a reliable intensity calibration using the incoherent scattering of the sample as an internal standard. In this way the measured structure factors can be directly compared with model calculations or with results from simulations without any arbitrary adjusting procedures.

The experiments described in this paper have been carried out by the D7 and DNS instruments mentioned above. Detailed technical information about these instruments can be found in the so-called "ILL-Yellow Book" (www.ill.fr) and in the book "Neutron Scattering Experiments at the Research Reactor in Jülich" (www.neutronscattering.de). Although these two instruments have a time-of-flight option, which allows analyzing the energy of the scattered neutrons, this option is not considered for diffraction measurements. The typical Q-range covered by this kind of instruments extends from about 0.3 up to 4 $Å^{-1}$. This is just the range where the short-range order of glassy polymers and polymer melts manifest in a diffraction pattern.

If one of these instruments is operated with the spin analysis option, the scattering intensity is measured in two different modes. In the non-flip mode only neutrons which maintain their spin direction in the scattering process are registered by the detector system, whereas in the spin-flip mode the neutrons reverse their spin direction before hitting the sample, so that only neutron scattered with spin-flip are detected. Polarizer and analyzers consist of an arrangement of the so-called "supermirrors" in a permanent magnetic field. Details are described in the two technical references above mentioned.

In the absence of magnetic neutron scattering, the non-flip (NF) and spin-flip (SP) intensities are determined by the coherent (coh) and incoherent (inc) intensities: $I_{NF} = I_{coh} + I_{inc}/3$; and $I_{SF} = 2I_{inc}/3$. From these expressions, the differential coherent scattering cross-section can be calculated in absolute units by

$$\frac{d\sigma_{coh}}{d\Omega}(Q) = \frac{2}{3}\frac{d\sigma_{inc}}{d\Omega}\frac{I_{NF} - \frac{1}{2}I_{SF}}{I_{SF}} \qquad (1)$$

Because all instrument and sample dependent quantities (amount of sample in the beam, primary beam intensity, detector efficiencies etc.) cancel out in the derivation of this formula, only the knowledge of the (tabulated) incoherent cross-section $d\sigma_{inc}/d\Omega$ is necessary. In this way the uncertainty connected with the usual "vanadium calibration" can be avoided. However, under realistic conditions several corrections have to be applied to the value obtained by the straightforward expression (1), being multiple scattering the most important. Their effects are shown in Fig. 1 for a representative example. Multiple scattering is a rather complicated problem for neutron scattering with polarisation analysis because consecutive flipping of the neutron spin might restore its original direction leading to an "apparent coherent scattering". Different approaches have been used in the literature to correct the measurements for these effects [3-5]. An analytical method has been recently developed to cope with this situation [7].

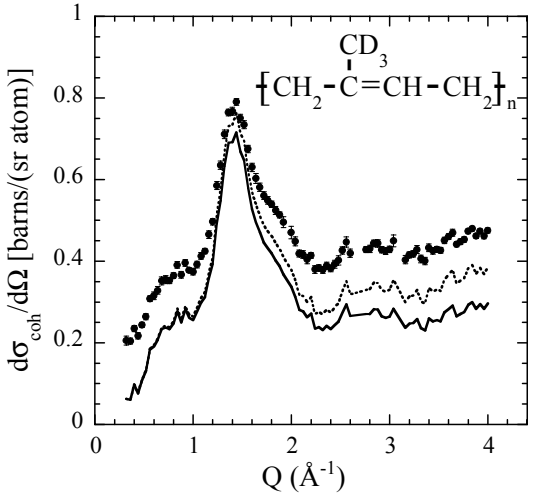

Figure 1. *Differential coherent neutron scattering cross-section from D7 for polyisoprene with deuterated methyl groups (PId3) sample at 100 K. The full symbols with error bars show the raw data obtained using equation (1) only with a background correction. The dotted line represents data after multiple scattering correction. The continuous curve shows the final data treatment stage after the inelasticity correction.*

As an example, Fig. 2 shows typical results obtained by neutron diffraction with polarization analysis in the case of a fully deuterated sample and a fully protonated as well. In the case of the fully deuterated sample, the scattering is dominated by the coherent component and thereby the results obtained are similar to those obtained in a standard diffraction experiment where the total scattering is measured. In contrast, in the case of the fully protonated sample, the incoherent component dominates the scattering. However, as Fig. 2(b) shows, the polarization analysis allows measuring the coherent contribution even in this less favourable case. These measurements were carried out at a temperature of 100 K.

Simulation method

In a classical molecular dynamics (MD) simulation, the coordinates of the different atoms of the simulation cell are recorded as a function of the simulation time (usually this time extends until a few nanoseconds). Starting from these atomic coordinates the coherent differential cross-section, which is measured by neutron diffraction with polarization analysis, can be calculated.

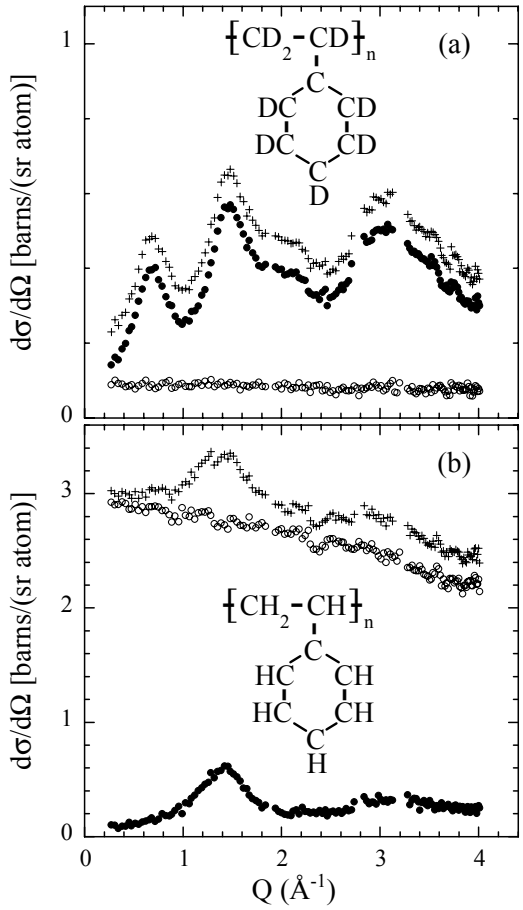

Figure 2. *Differential neutron scattering cross-sections obtained from D7 measurements for polystyrene (PS) at 100 K. The full circles correspond to coherent scattering, the empty circles to incoherent scattering and the crosses to the total scattering. (a) Fully deuterated sample PSd8. (b) Fully protonated sample PSh8.*

For an isotropic sample and taking the orientational averaging, this is defined as [8]:

$$I_{coh}(Q) = \frac{d\sigma_{coh}}{d\Omega} = \frac{1}{N}\sum_{i,j=1}^{N}\langle b_i\rangle\langle b_j\rangle\frac{sin(Qr_{ij})}{Qr_{ij}}$$

where the $\langle b_i\rangle$ stand for the nuclear scattering lengths for neutrons ($\langle b_H\rangle$ = - 0.3741×10^{-14} m; $\langle b_C\rangle$ = 0.6648×10^{-14} m; $\langle b_D\rangle$ = 0.6674×10^{-14} m) and N is the total number of atoms (the cross sections like σ_{coh} are given in units of [barn/atom], and $I_{coh}(Q)$ is in units of [barn/(sr atom)], 1 barn = 10^{-28} m^2). In this kind of calculations, expression (2) is averaged for a large number of snapshots throughout the atomic trajectories. Since the scattering lengths of carbon and deuteron atoms are very similar, these two atoms are almost indistinguishable for neutrons. In this context, for the case of the fully deuterated samples the coherent intensity measured - or calculated - results to be just proportional to the static structure factor S(Q). In other samples, the coherent intensity given by expression (2) is just what is known as partial static structure factor.

It is noteworthy that the incoherent differential cross-section – which is also measured in a neutron diffraction experiment with polarization analysis – is in fact a Q-independent incoherent term defined as

$$I_{inc} = \frac{d\sigma_{inc}}{d\Omega} = \frac{1}{N}\sum_{i=1}^{N}(\langle b_i^2 \rangle - \langle b_i \rangle^2) = \frac{\sigma_{inc}}{4\pi} \quad (2)$$

However, in a real experiment, and due to the so-called inelasticity effects – a part of the scattering is inelastic but there is not energy discrimination at the detector – the measured I_{inc} usually shows a tendency to decrease with Q (see Fig. 2). Since I_{inc} is also involved in expression (1), inelasticity corrections have to be considered for the measured $I_{coh}(Q)$ even at rather low temperatures.

The MD-simulations described in this paper are fully atomistic simulations carried out within the Insight (Insight II 4.0.0 P version) environment and by means of the Discover-3 module from Molecular Simulations Inc. (now Accelrys) with the Polymer Consortium Force Field (PCFF) [9]. The model systems were built by means of the well known Amorphous Cell protocol, which was proposed for the first time by Theodorou and Suter [10]. A typical simulated cell consists in a cubic cell containing one polymer chain of about 100 monomer units. Periodic boundary conditions were assumed in order to model the bulk system. After standard minimization procedures (Polak-Ribiere conjugate gradients method) and equilibration runs, the simulations were carried out in the NVT ensemble and usually extend until 10 ns. More technical details can be found in references [3,11,12].

Representative results

In this section we present two representative recent examples of the synergy between neutron diffraction with polarization analysis and MD-simulations for unraveling structural questions related with the short-range order of glassy polymers and polymer melts.

Atomic correlations in polyisoprene and the evolution with temperature of the structure factor S(Q)

Polyisoprene (PI) is a well-known glass-forming polymer of chemical formula $[-CH_2-CH=C(CH_3)-CH_2-]_n$ and glass transition temperature of about 200 K. Figure 3 shows the coherent intensity measured by neutron diffraction with polarization analysis on a fully deuterated and monodisperse sample of PI, which was prepared by anionic polymerization. These measurements were carried out at a temperature of 100 K. The experimental coherent intensity (equivalent to S(Q) in the case of a fully deuterated sample) shows two first overlapping peaks of about the same intensity in the so-called "intermolecular Q-range". These peaks are centered at Q ~ 1.4 Å^{-1} and Q ~ 1.9 Å^{-1} respectively. A third peak also of about the same intensity appears at a higher value of Q of about 3 Å^{-1}. This peak seems to be a universal feature of all amorphous polymers and, since it does not shift with temperature, it has been usually associated to intra-chain correlations (covalent bonds). Figure 3 also shows the coherent intensity calculated from the atomic trajectories of a MD-simulation of PI carried out at the same temperature. As can be seen, the agreement between experimental and simulated data is rather good taking into account the difficulties of simulating polymers at low temperatures well below their glass transition. It is noteworthy that the same kind of agreement between experimental and simulated data has also been found in the case of a fully protonated PI sample and two different partially deuterated samples (see ref. [3] for details). Based on these results we can conclude that the simulated cell is a good representation of the local structure of real PI. Therefore, we can now profit from the simulation capabilities and calculate the different contributions to S(Q) corresponding to the different atomic correlations in the sample. We will thus focus on the fully deuterated sample (see Fig. 3). Although we have distinguished four different kinds of atoms in the cell (main chain carbons; methyl group carbons; main chain deuterons; methyl group deuterons) for simplicity here we only show carbon-carbon (CC), deuteron-deuteron (DD) and carbon-deuteron (CD) contributions. Looking at the figure, it is evident that the peak centered at the lower Q-value is almost exclusively due to CC-correlations. However, the second peak in this Q-range cannot easily be attributed to any particular atomic correlation, being a combination of CC, DD and CD contributions. Furthermore, also the peak at about 3 Å^{-1} seems to arise from a combination of contributions from the different atomic correlations. The atomic correlations giving raise to this peak correspond to short distances and have to be of intra-chain nature. We point out that this peak does not shift with temperature neither in the experimental data nor in the simulations results.

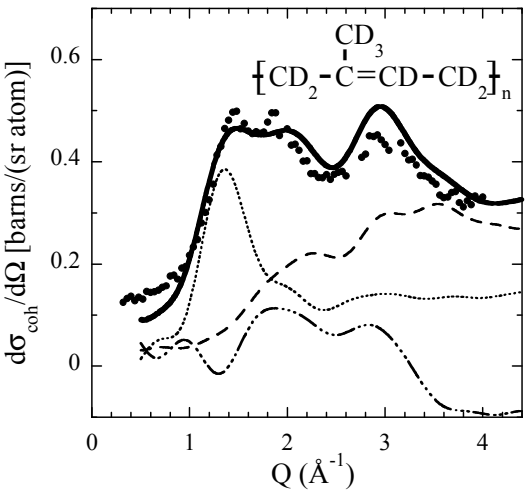

Figure 3. *Differential coherent neutron scattering cross-section for PId8 obtained from D7 measurements at 100 K (full points) in comparison with that obtained from the simulation results (continuous line). The contributions to the coherent scattering originating from the different atomic correlations and properly weighted by the corresponding neutron scattering lengths are also shown: carbon-carbon correlations (dotted line), deuteron-deuteron correlations (dashed line) and carbon-deuteron correlations (dashed-dotted line).*

Now, after discussing the origin of the main peaks of S(Q), we can focus on their temperature evolution. In principle, the expected behavior for an inter-molecular peak in an amorphous polymer is a decrease of the intensity and a shift to lower Q-values with increasing temperature. The results obtained from both neutron diffraction and MD-simulations in the case of PI are shown in Fig. 4. In this case the experimental results correspond to standard neutron diffraction (D20 instrument at the ILL, Grenoble, France) without polarization analysis, i.e., what it is measured is just the total scattering (coherent plus incoherent). However, since we are dealing with a fully deuterated sample, the total scattering is dominated by the coherent contribution as it has been above commented (see Fig. 2(a) as a representative example). Figure 4 shows that the results obtained in PI are very different from those expected. The main feature is the increase of the intensity of the first peak of S(Q), which already starts at low temperatures below the glass transition of PI. According to our previous discussion, at 100 K this first peak of S(Q) basically originates from the contribution to the scattering from the carbon-carbon and in particular from carbon chain-carbon chain correlations. Therefore, at first glance, we would expect that the increase of the intensity with temperature relates to these correlations. Moreover, this peculiar temperature dependence would indicate, at least apparently, an enhancement of the order within structure at high temperature. Figure 5 shows that the interpretation is in fact very different. This figure displays the temperature evolution of the CC-, DD-, and CD-contributions to S(Q) calculated from MD-simulations carried out at different temperatures. We can immediately see that the "anomalous" temperature dependence of the first peak of S(Q) is not due to the temperature dependence of the underlying CC-correlations, which reflect the inter-chain packing and show the expected behaviour. Rather, it is the complex temperature evolution of DD- and CD-contributions that finally leads to an increase of intensity of the first peak of S(Q). Hence, the "anomalous" temperature dependence of this peak is not indicative of increasing inter-molecular order with increasing temperature.

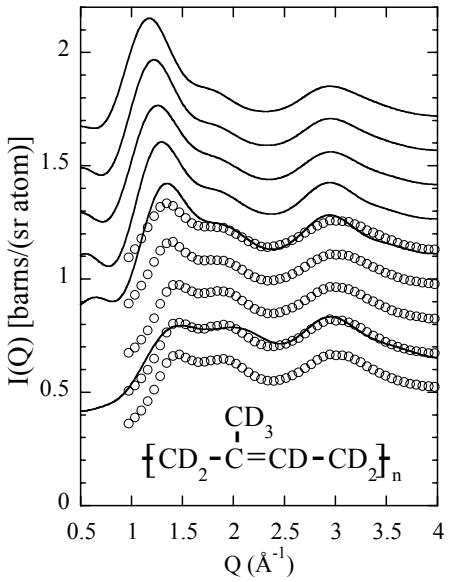

Figure 4. *Temperature evolution of the total differential scattering cross section I(Q) obtained from D20 measurements for a fully deuterated polyisoprene sample (PId8) (circles) and calculated from the simulations (solid lines). The scale of I(Q) indicated in the figure corresponds to the experimental curve at 2 K. The curves corresponding to other temperatures have been shifted vertically 0.15 units each for clarity.*

The origin of the "polymerization peak" of the structure factor of polystyrene

As it has been presented in Fig. 2, the coherent intensity measured by neutron diffraction with polarization analysis on a fully deuterated sample of atactic polystyrene (PS) reveals a peak at Q ~ 1.4 Å^{-1}, which has been associated with the ubiquitous "amorphous halo" observed in polymer melts, polymer glasses and rubbers. In addition, another peak is present at an unusual low Q-value of about 0.7 Å^{-1}. This, in principle, anomalous peak also appears in the X-ray scattering pattern of atactic PS and it was first reported in 1936 [13]. Although PS has been extensively investigated in the past by X-ray diffraction, the microscopic origin of the low Q peak of S(Q) – which was called "polymerization peak" – is still poorly understood. Figure 2(b) shows that this peak almost disappears in the coherent scattering pattern measured by neutron diffraction with polarization analysis on a fully protonated sample of PS, but it is highlighted when this kind of measurements are carried out on a partially deuterated sample (PSd3, see Fig. 6). This figure also shows data calculated from fully atomistic MD-simulations carried out on a PS cell [6]. The agreement between experimental and simulated data is quite good, taking into account that the temperature of the measurements (320 K) is rather different than that of the simulations (523 K).

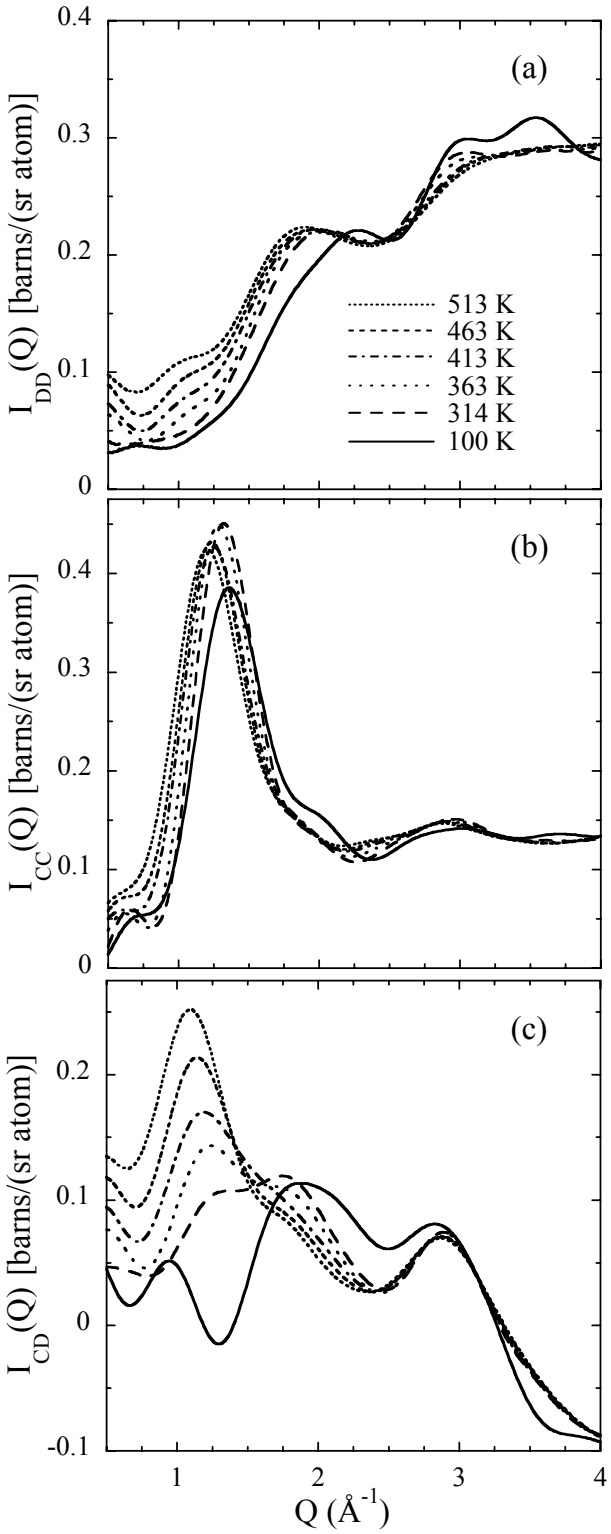

Figure. 5. *Temperature evolution of the contributions to the coherent scattering originating from the different atomic correlations in the case of PId8 sample. (a) Deuteron-deuteron correlations. (b) Carbon-carbon correlations. (c) Carbon-deuteron correlations. In all cases the different curves correspond to the different temperatures indicated in (a).*

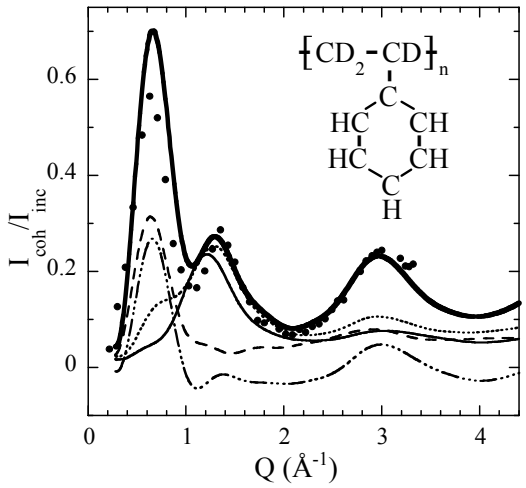

Figure 6. *Ratio between the differential coherent and incoherent neutron scattering cross-sections for PSd3 obtained from DNS measurements at 320 K (full points) in comparison with that obtained from the simulation results at 523 K (continuous thick line). The contributions originating from the different atomic correlations and properly weighted by the corresponding neutron scattering lengths are also shown: total carbon-carbon correlations (dotted line), hydrogen-hydrogen correlations (dashed line) and carbon-hydrogen correlations (dashed-dotted line). In these two last cases, hydrogen can be either deuteron or proton. The continuous thin line shows the carbon phenyl-carbon phenyl contribution.*

As in the case of the PI above discussed, starting from the simulation data the different contributions to the scattering shown in Fig. 6 can be calculated. To do this, different atoms were considered separately: main-chain carbons, main-chain deuterons, phenyl carbons and phenyl hydrogens. Therefore, ten different contributions were calculated. For simplicity, in Fig. 6 only the contributions related to the total CC-, H(D)H(D)- and CH(D)-correlations, as well as those arising from carbon phenyl-carbon phenyl correlations, are shown. As can be seen, the second peak centered at 1.4 $Å^{-1}$ is mainly due to CC-correlations and, in particular, to the carbon phenyl–carbon phenyl correlations. Therefore, this peak is mainly controlled by the relative position of phenyl rings in the sample and - against the habitually assumed ideas - it cannot be the true amorphous peak of atactic PS. On the other hand, concerning the so-called "polymerization peak", all atomic pair correlations seem to contribute to this peak. A detailed analysis of such correlations however indicates that the major contributions are mostly those involving main chain atoms. In this way this peak reflects inter-chain packing and thereby it can be considered the true "amorphous peak". In conclusion, we can see that the so-called "polymerization peak" seems to be rather normal and can be easily explained in terms of atomic pair correlations without invoking any kind of intermediate range order.

References

[1] P. J. Flory, Principles of Polymer Chemistry, Cornell University Press, London, 1953.
[2] B. Frick, D. Richter, CL. Ritter, Europhys. Lett., 1989, 9, 557.
[3] F. Alvarez, J. Colmenero, R. Zorn, L. Willner, D. Richter, Macromolecules, 2003, 36, 238.
[4] H. Furuya, M. Mondello, Hyung-Jin Yang, Ryong-Joon Roe, R. W. Erwin, C. C. Han, S. D. Smith, Macromolecules, 1994, 27, 5674.
[5] J. Eilhard, A. Zirkel, W. Tschöp, O. Hahn, K. Kremer, O. Schärpf, D. Richter, U. Buchenau, J. Chem. Phys., 1999, 110, 1819.
[6] I. Iradi, F. Alvarez, J. Colmenero, A. Arbe, Physica B (in press).
[7] R. Zorn, Nucl. Instr. Methods A, 2002, 479, 568.
[8] See, for example: G. L. Squires, Introduction of the Theory of Thermal Neutron Scattering, Dover, New York, USA, 1996.
[9] H. J. Sun, Comput. Chem., 1994,15, 752; H. Sun, S. J. Mumby, J. R. Maple, A. T. Hagler, J. Am. Chem. Soc., 1994, 116, 2978; H. Sun, Macromolecules, 1995, 28, 701; 1994, 26, 5924; H. Sun, S. J. Mumby, J. R. Maple, A. T. Hagler, J. Phys. Chem., 1995, 99, 5873; 1998, 102, 7338.
[10] D. N. Theodorou, U. W. Suter, Macromolecules, 1985, 18, 1467; 1986, 19, 139; 1986, 19, 379.
[11] F. Alvarez, A. Arbe, J. Colmenero, Chemical Physics, 2000, 261, 47.
[12] J. Colmenero, F. Alvarez, A. Arbe, Phys. Rev. E, 2002, 65, 041804.
[13] J. R. Katz, Trans. Faraday Soc., 1936, 32, 77.

SAXPD Studies of Phospholipid Membranes

Georg Pabst

Institute of Biophysics and X-ray Structure Research, Austrian Academy of Sciences
Schmiedlstraße 6, A-8042 Graz, Austria
Georg.Pabst@oeaw.ac.at

Introduction

Membranes composed of various phospholipid species serve since a long time as model systems for biological membranes. In nature, they provide the structural matrix into which functional units such as proteins are imbedded. There is, however, more to phospholipids than providing just a simple structural matrix. Today it is well recognized that the lipid composition of membranes has a tremendous effect on the way a biological membrane works and interacts with membrane active agents. Consequently, we need to explore besides single lipid component membranes also model systems composed of lipid mixtures mimicking different biological membranes.

Out of the large repertoire of available experimental techniques, x-ray diffraction emerges as the prominent tool to give information on the overall structural, but also mechanical properties of the model membrane system. Here, we are fortunate that lipids often self-assemble in the presence of an aqueous medium into onion-like multilamellar vesicles (MLVs), thus giving rise to diffraction peaks. Depending on temperature, pressure, composition, etc., these lipid/water systems display a variety of liquid crystalline structures, out of which the so-called L_α phase (corresponds to smectic A) is considered to be the biologically most relevant one. The scattered x-ray intensity originates from randomly oriented scattering domains, thus giving rise to Debye-Scherrer diffraction rings. This is why we call it powder diffraction although there is actually a lot of water inside the system.

The data analysis is, however, different from standard powder diffraction problems, as I will point out below: It is well known, that fluctuations govern the physical properties of smectic crystalline phases. As a consequence the positional order of smectics is only quasi-long range. The fluctuations are most pronounced in the L_α phase and as a consequence typically only 2 to 3 quasi-Bragg reflections are observed (Fig. 1).

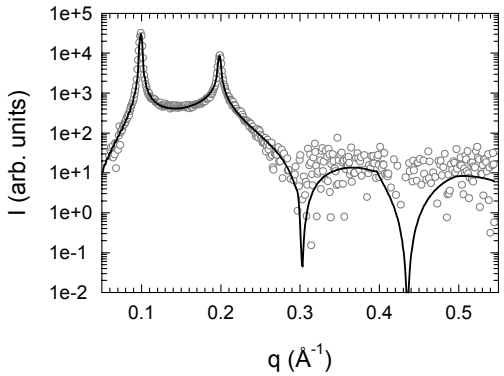

Figure 1: *Small-angle x-ray powder diffraction (SAXPD) pattern of fully hydrated dimyristoyl phosphatidylcholine in the L_α phase at 30°C exhibits only two quasi-Bragg reflections. The solid line gives the fit of the global model to the data showing good agreement to quasi-Bragg and diffuse scattering over 4 orders of magnitude in intensity.*

The situation often becomes even worse, when lipid mixtures are studied. Then the diffraction patterns frequently exhibit only one weak diffraction peak [1]. The strategy is therefore clear: In order to derive

electron density profiles, we need to devise a model which considers, both the quasi-Bragg peak intensity and the diffuse scattering, respectively (Fig. 1). In 2000, we have developed such a full q-range model [2], which we have recently extended to low resolution and lamellar gel phase data [1]. In the following, I will briefly outline the basic ideas of the model and give two prominent examples of its application.

The Model

The scattered intensity of a MLV dispersion as a function of the scattering vector q is given by [1, 2]:

$$I(q) = \frac{|F(q)|^2 S(q)}{q^2} + N_u \frac{|F(q)|^2}{q^2}, \qquad (1)$$

where $F(q)$ is the form factor due to the Fourier transform of the electron density profile and $S(q)$ the structure factor, which describes the crystal lattice in reciprocal space. The second term in Eq. (1) accounts for additional diffuse scattering caused by uncorrelated membranes and its contribution to the total scattered intensity is scaled by N_u. To model the form factor, we build an electron density profile by using a series of Gaussians (Fig. 2). This is the simplest realistic model available.

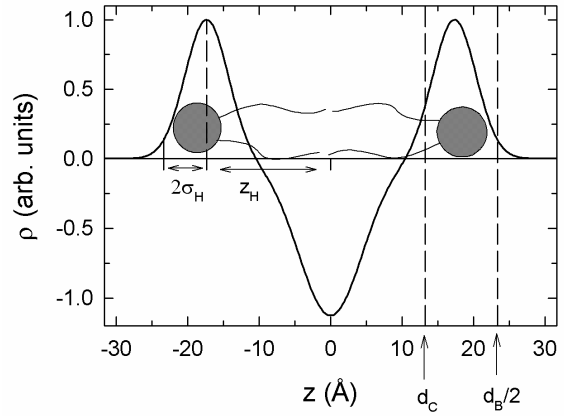

Figure 2: *Model of the electron density profile of a lipid bilayer. The electron dense headgroups are represented by a Gaussians of positive amplitude at ± z_H and of width σ_H. The electron sparse region of the methyl through is modelled by a Gaussian of negative amplitude at the bilayer centre. The membrane thickness is defined as $d_B = 2 (z_H + 2 \sigma_H)$. The thickness of the hydrocarbon chain region, $d_C = d_B/2 - d_H$ depends on the steric headgroup size (e.g. $d_H = 10$ Å for phosphatidylcholines).*

The structure factor accounts for static and dynamic defects of the crystalline lattice (Fig. 3). Dynamic disorder given by fluctuations in particular affects the shape of the quasi-Bragg peaks. As such fluctuations of stiff layers with randomly varying interlayer separations cause a Lorentzian decay of the Bragg peak intensity (paracrystalline theory [3]). Contrary, long-wavelength bilayer undulations are the source of a power-law decay of the reflection intensities (Caillé theory [4]). Importantly, the decay constant η is proportional to the bilayer bending rigidity K_c and the interbilayer interaction modulus, B. Thus, a detailed shape analysis of the quasi-Bragg reflections also opens the window to mechanical parameters as I will discuss in an example below. For further details on the global model and how to obtain additional structural parameters such as the lateral area, or the number of water molecules per lipids refer to [1] and [2].

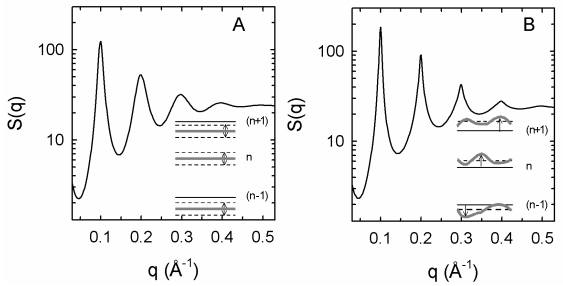

Figure 3: *Structure factors due to the paracrystalline theory (A) and the Caillé theory (B). Both S(q)'s show a decrease of intensity and an increase of width for higher scattering vectors. Note the different peak shapes in (A) and (B). The insets sketch the different disorders involved.*

3. Some Application Examples

3.1. Pretransitional Swelling of Phosphatidylcholines

Some phosphatidylcholines, e.g. dimyristoyl phosphatidylcholine (DMPC), show in the vicinity of the fluid to gel phase transition a non-linear increase of the lamellar repeat distance (Fig. 4).

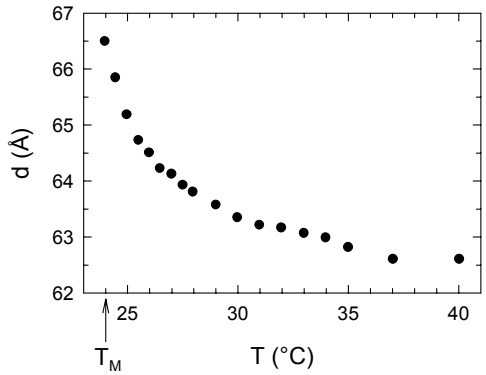

Figure 4: *Pretransitional Swelling of DMPC in the vicinity of the main phase transition temperature T_M. The cause of this "anomalous" behaviour has been matter of controversy for several years. Is it caused by an increase of the water layer, or is it rather the membrane thickness; or both? One of the major reasons for this debate was the insufficient number of diffraction peaks observable (Fig. 1), precluding traditional data analysis techniques to give sufficient insight on the structural parameters. The issue of pretransitional swelling was therefore a well suited case for the application of our global data analysis model [5].*

The results for the temperature behaviour of the structural parameters are shown in Fig. 5. The increase of d_B is quasi-linear over whole studied temperature range with a small non-linear component of about 0.5 Å in the very vicinity of T_M (Fig. 5A). The membrane thickening can be attributed to the continuous freezing-out of the hydrocarbon chains. In contrary, the water layer thickness first decreases as the temperature is lowered, levels off at about 15°C above T_M and then exhibits a sudden increase just before undergoes the phase transition (Fig. 5B). The expansion of d_W in the vicinity of T_M is about 1.5 Å. The pretransitional swelling of d is therefore dominated by the expansion of the water layer.

What is the cause for the d_W expansion? In order to answer this question, we have determined the fluctuation parameter η, which governs the power law decay of the quasi-Bragg peaks. The bending fluctuations continuously decrease, as the transition temperature is approached (Fig. 5C). However, just before the system undergoes the transition, η exhibits a sudden increase. This causes in turn a steric repulsion of adjacent bilayers and thus leads to the increase of d_W.

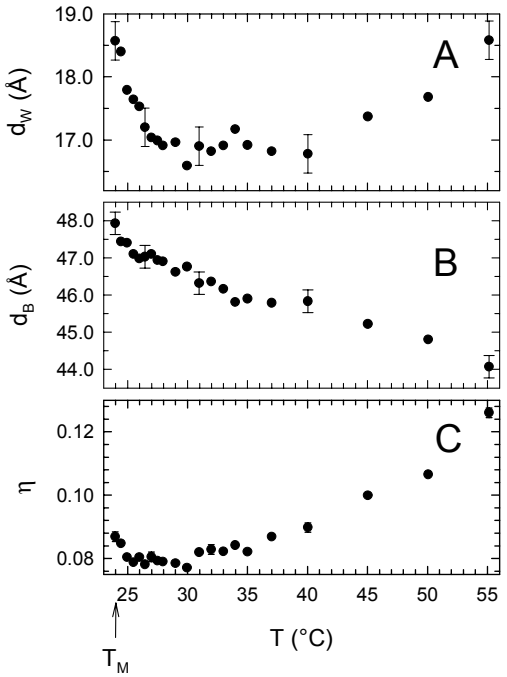

Figure 5: *Temperature dependence of the water layer thickness (A), membrane thickness (B) and fluctuation parameter (C) for fully hydrated DMPC near the main phase transition temperature (T_M = 24°C).*

Bending fluctuations depend, besides temperature, on the bilayer bending rigidity K_c and the interbilayer interaction modulus B. In order to elucidate the temperature dependence of these mechanical parameters, we have subsequently estimated B from osmotic pressure experiments. By this technique the membrane separation is continuously reduced and B is given by $(-\delta P/\delta d)_T$ for osmotic pressures $P \rightarrow 0$. It is then straightforward to calculate K_c using the previously determined η and B values. With this procedure, we were able to demonstrate that the bending fluctuation increase due to a sudden drop of the bending rigidity in the vicinity of T_M [5].

3.2. Thermal Unbinding of Lipid Multibilayers

In the second application example I present data from a lipid mixture of palmitoly-oleoyl-phosphatidlyethanolamie (POPE) and palmitoyl-oleoyl-phosphatidylglycerin (POPG). This composition is characteristic for bacterial cytoplasmic membranes. The system displays in a certain range of lipid composition and ionic strength a thermal unbinding transition [6] (Fig. 6). This transition has been predicted by theory almost twenty years ago [7], however, experimental evidences have been so far been scarce.

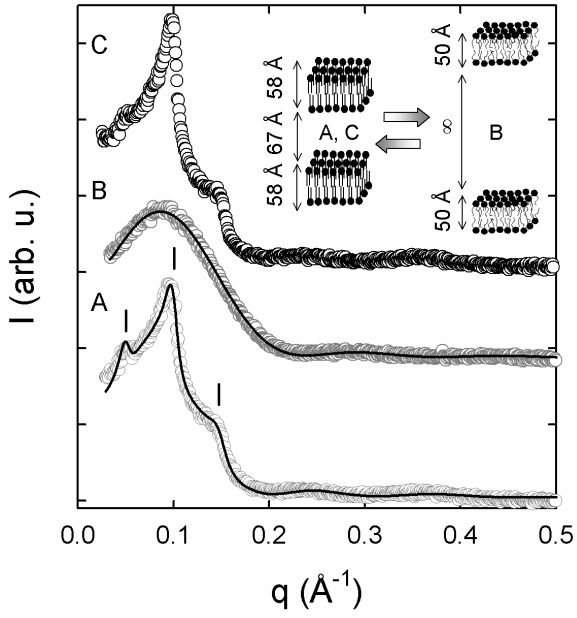

Figure 6: *Discontinuous unbinding of a POPE/POPG 87:13 mol/mol mixture in 20 mM Na-phosphate buffer containing 130 mM NaCl upon heating through the main phase transition. Diffraction patterns (A) exhibits 3 quasi-Bragg reflection and corresponds to a bound system in the gel phase at 20°C. The system looses all correlations and exhibits pure diffuse scattering in the L_α phase at 30°C (B). The absence of positional correlations means that the bilayers are in an unbound state. The system returns to its bound state upon cooling back to 20°C (C). Solid lines show the global fits to the scattering data. The inset gives a schematic of the findings with the structural parameters determined from the fit.*

The unbinding transition is driven by an increase of steric repulsion due to bending fluctuations, which finally overcome the attractive van der Waals forces and lead to a complete unbinding of the multibilayer stacks. In present scenario the unbinding transition goes in hand with the gel to fluid phase transition,

where the bending rigidity is reduced by about one order of magnitude. The unbinding transition is fully reversible and returns to its bound state when it is brought back to the gel phase (Fig. 6C).

By applying the global data analysis technique we were able to determine the structural parameters within the bound and the unbound state [6]. The diffuse scattering of the latter case can be modelled by simply setting the first term of Eq. (1) equal to zero. Using additional information from wide-angle diffraction of the hydrocarbon chains we have subsequently determined the interaction potentials showing that the system is only weakly bound at low temperatures. Thus, the decrease of bending rigidity upon transforming into the L_α phase is sufficient to unbind the whole system. From this detailed analysis we were further able to exclude any other change in interbilayer interaction as being the cause for the unbinding of the multibilayers. For details see ref. [6].

Conclusion

I have given a brief introduction into a global analysis technique of SAXPD patterns from phospholipid membranes. From the steadily growing number of applications [8], I have chosen two experimental examples to demonstrate that the method provides a powerful tool in order to obtain detailed insights both on the structure and interaction, respectively of fully hydrated model membrane systems. Generally, it should be noted, however, that its application is in principle not restricted to phospholipid based model membranes. Surfactant or liquid crystalline system display similar features and may be analysed analogous.

Acknowledgments

I am deeply grateful to Michael Rappolt, Beatriz Pozo Navas, Peter Laggner, Karl Lohner, Velajudhan A. Raghunathan and John Katsaras for active collaboration, many fruitful discussions and continuous support.

References

[1] G. Pabst, R. Koschuch, B. Pozo-Navas, M. Rappolt, K. Lohner, and P. Laggner, J. Appl. Cryst., 2003, 36, 1378.

[2] G. Pabst, M. Rappolt, H. Amenitsch, and P. Laggner, Phys. Rev. E, 2000, 62, 4000.

[3] R. Hosemann and S.N. Bagchi, Direct Analysis of Diffraction by Matter, 1962, Amsterdam: North-Holland; A. Guiner, X-ray Diffraction, 1963, San Francisco: Freeman; P. Laggner, Topics in Current Chemistry, 1988, 145, 173.

[4] A. Caillé, C. R. Acad. Sci. Paris (Sér. B), 1972, 274, 891; R. Zhang, R.M. Suter, and J.F. Nagle, Phys. Rev. E, 1994, 50, 5047.

[5] G. Pabst, V.A. Raghunathan, J. Katsaras, and M. Rappolt, Langmuir, 2003, 19, 1716.

[6] B. Pozo-Navas, V.A. Raghunathan, J. Katsaras, M. Rappolt, K. Lohner, and G. Pabst, Phys. Rev. Lett., 2003, 91,028101.

[7] R. Lipowsky, and S. Leibler, Phys. Rev. Lett., 1986, 56, 2541.

[8] Besides refs. [1], [2], [5], and [6] presently published applications of the global data analysis technique from this group are: G. Pabst, M. Rappolt, H. Amenitsch, S. Bernstorff, and P. Laggner, Langmuir, 2000, 16, 8994; I. Winter, G. Pabst, M. Rappolt, and K. Lohner, Chem. Phys. Lipids, 112, 137; M. Rappolt, M. Fernández Vidal, M. Kriechbaum, M. Steinhart, H. Amenitsch, S. Bernstorff, and P. Laggner, Eur. Biophys. J, 2003, 31, 575.

X'Pert Software with XML: Leading the way forward in data sharing

X'Pert Software for XRD data

A complete family of analytical software
Whether you're in research, development or production control, there are PANalytical X'Pert Software packages to support your XRD data collection and analysis.
The complete range, which centers on the X'Pert Data Collector, is based on the XRDML data platform.

A universal standard for structured data
PANalytical is the first company in the XRD community to bring you an open format based on the universal XML standard: XRDML. It ensures that your data remain accessible, transparent and secure and it guarantees total reproducibility. Information on instrument type, settings, test conditions and experimental parameters is included. Moreover, XML files are human readable.
To get on the way forward in data sharing, visit:

www.xrdml.com

PANalytical
Lelyweg 1
7602 EA Almelo
The Netherlands
Tel.: +31 546 534 444
Fax.: +31 546 534 598
E-mail: info@panalytical.com

www.panalytical.com

XRD

Winning by Sharing

PANalytical

STOE STADI P

Powder diffractometer

- Pure $K\alpha_1$ radiation using Fe, Co, Cu or Mo radiation
- High resolution yielding well-defined peak profiles
- Transmission / Debye-Scherrer or Bragg-Brentano mode
- Analysis of air-, moisture-sensitive and micro samples
- Enclosing control and evaluation software package WinX^{POW}
- Various high- and low-temperature systems and sample changers
- Scintillation counter, position sensitive and imaging plate detectors
- High throughput and combinatorial analysis

STOE & Cie GmbH P.O.Box 101302 D-64213 Darmstadt
Phone: (+49) 6151 / 98870 Fax: (+49) 6151 / 988788
E-mail: stoe@stoe.com Homepage: http://www.stoe.com

Crystal Structure Visualization

Diamond is an application for the exploration and drawing of crystal structures. With its high data capacity, its wide range of functions beginning with the generation of molecules reaching up to the construction of rather complicated inorganic structural frameworks, *Diamond* is the tool for molecular and solid state chemists as well as for surface and material scientists.

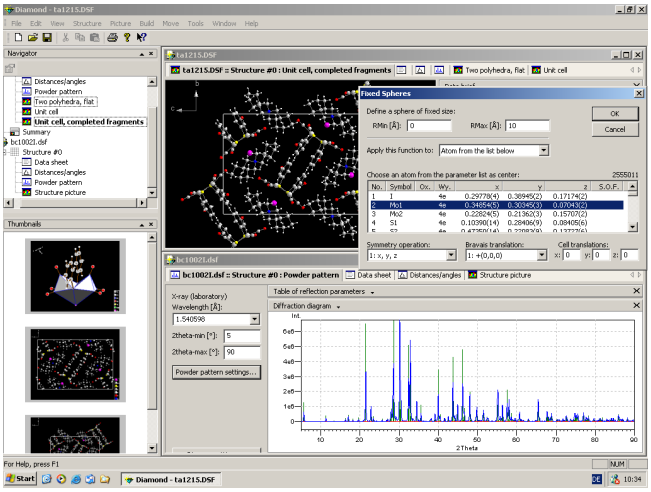

Phase Identification from Powder

Match! is an easy-to-use software for phase identification from X-ray powder diffraction data. Using an elaborate algorithm, it compares the user's diffraction pattern to the patterns stored in the ICDD PDF database in order to identify the phases which are present in the user's sample. Single as well as multiple phases can be identified based on both peak data and raw (profile) data (if present).
***Match!* will become available in 3rd quarter 2003.**

Structure Solution from Powder

Endeavour uses an innovative concept: a combined global optimization of the difference between the calculated and measured diffraction pattern and of the potential energy of the system.
Since *Endeavour* is based upon the experienced Diamond visualization technology, the user can watch the crystal structure evolving from a completely random arrangement of atoms to the final model during the structure solution process.

Free-of-charge demonstration versions are available for download from our webpage.

CRYSTAL IMPACT GbR
Postfach 1251
D-53002 Bonn
Germany

Tel.: +49 (228) 981 36 43
Fax: +49 (228) 981 36 44
E-mail: info@crystalimpact.com
http://www.crystalimpact.com

CRYSTAL IMPACT

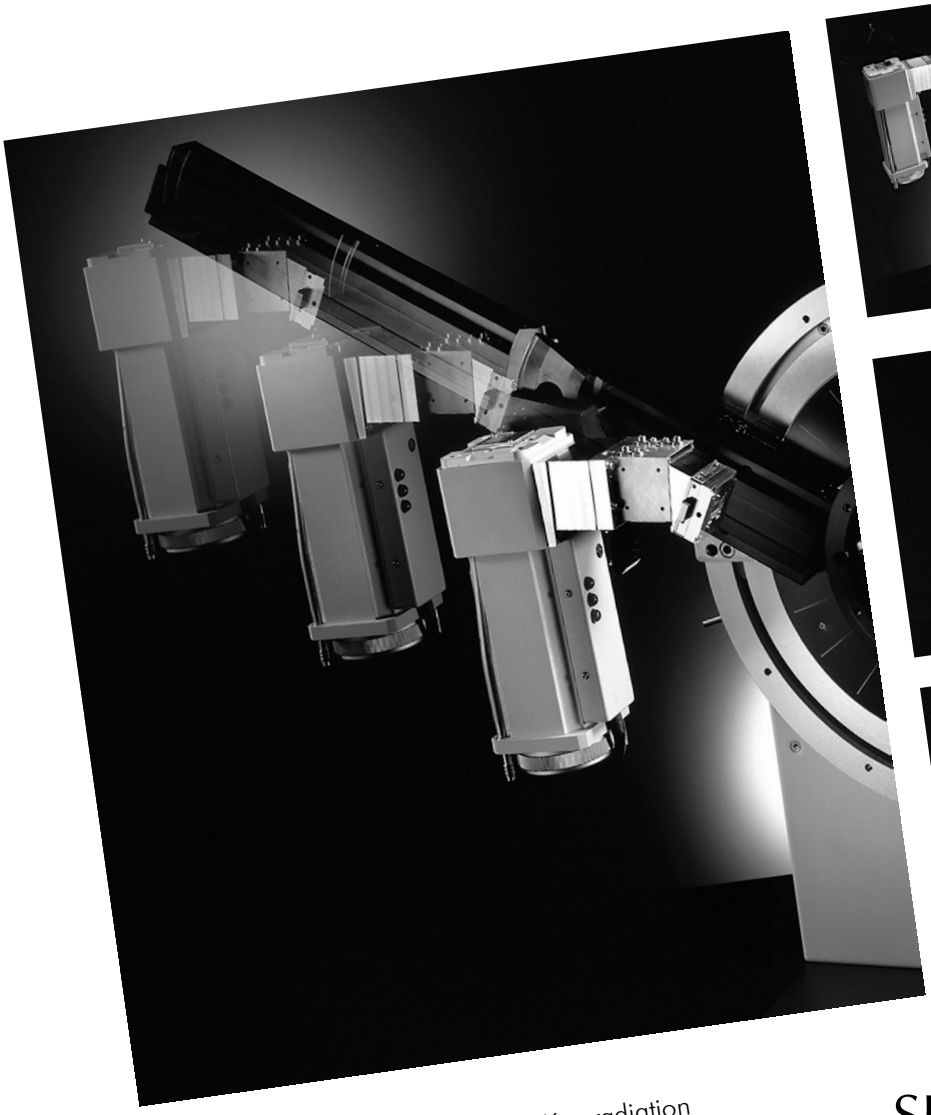

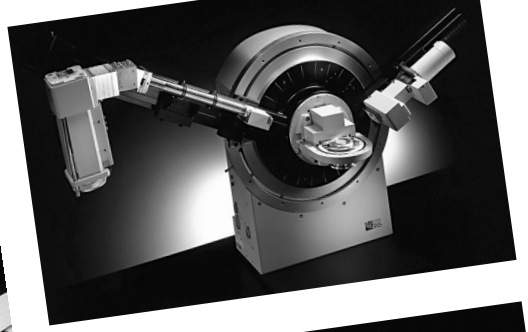

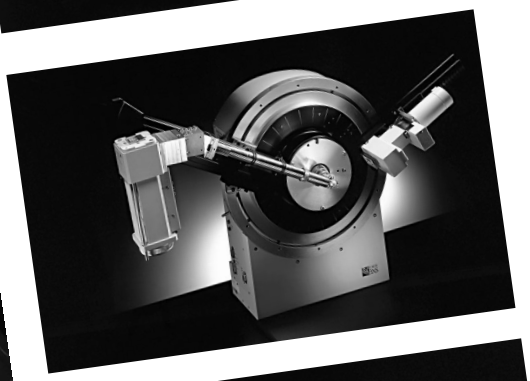

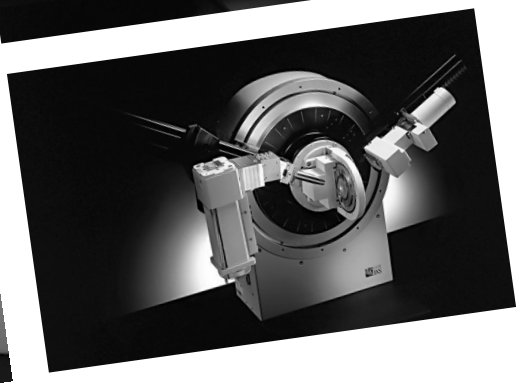

- Unambiguous results using pure $K\alpha_1$ radiation
- Large sample variety: powders, bulk samples, capillary samples, air-sensitive samples, samples with preferred orientation, small amounts of sample, low absorbing samples, foils, fibers, liquids …
- 6 predefined geometries:
  - Bragg-Brentano reflection
  - Bragg-Brentano capillary transmission
  - Bragg-Brentano foil transmission
  - High flux micro reflection
  - High flux capillary transmission
  - High flux foil transmission
- Virtually unlimited versatility
- Compact design for long-time stability
- Compatible with all D8 goniometers
- Compatible with all D8 attachments: sample stages, secondary optics and detectors

SUPERIOR FLUX, RESOLUTION, AND VERSATILITY…

… Vαrio1 FOR D8 ADVANCE AND D8 DISCOVER

find out what's inside

Germany:
Tel. (+49) 721/595-2888
Fax (+49) 721/595-4587

USA:
Tel. (+1) 608/276-3000
Fax (+1) 608/276-3006

http://www.bruker-axs.com
E-mail: info@bruker-axs.com

BRUKER ADVANCED X-RAY SOLUTIONS

BRUKER axs

JUNE 2003 EDITION OUT NOW!

If you're working in the developing world and have limited or no access to the Internet, then the free Xtal Nexus CD-ROM is here to help.

Packed with a host of crystallographic software packages and resources, these virtual Internet CD-ROMs have been produced with the permission of software and website custodians. The organizer of the Nexus project, the IUCr Committee on Electronic Publishing, Dissemination and Storage of Information, invites academics and students using single-crystal, powder diffraction and other crystallographic analysis methods in developing countries that are isolated from the Internet to register their interest. The CD-ROMs are free of charge and available while stocks last.

The CD-ROM is sponsored by the IUCr, the EPSRC-funded Collaborative Computational Project No. 14 (CCP14) for Single Crystal and Powder Diffraction, and the Neutron Program for Materials Research of the National Research Council of Canada.

Contents

Multiple software packages and suites relevant to single-crystal, powder diffraction, crystallographic structure validation and crystallographic teaching, including

- single-crystal structure solution and refinement suites for PC
- crystallographic structure visualization programs
- powder diffraction pattern visualization, peak profiling and indexing software
- powder diffraction structure solution
- classic and modern crystallographic program source code
- Rietveld refinement packages
- structure validation and checking software
- powder pattern simulation and journal-quality structure plotting and photorealistic rendering programs
- educational websites dealing with crystallographic teaching
- webpage-based tutorials on how to use many of the programs within the CD-ROM
- part of the IUCr website including IUCr Commissions.

Send your request for a free Xtal Nexus CD-ROM (preferably via e-mail or by conventional mail) to

Lachlan M. D. Cranswick
NPMR, NRC
Building 459, Station 18
Chalk River Laboratories, Chalk River
Ontario, Canada, K0J 1J0

E-mail: lachlan.cranswick@nrc.gc.ca
Tel: +1 (613) 584-8811 ext. 3719
Fax: +1 (613) 584-4040
WWW: http://neutron.nrc.ca/

The CD-ROMs, and regular updates, will be sent by airmail.

Computer Corner

Updates on Freely Available Crystallographic and Powder Diffraction Software

(Suggestions, corrections, comments and articles on new or updated software are appreciated; especially if you know of new program features, program updates and announcements that should be mentioned here).

Lachlan M. D. Cranswick
Neutron Program for Materials Research (NPMR),
National Research Council (NRC),
Building 459, Station 18, Chalk River Laboratories,
Chalk River, Ontario, Canada, K0J 1J0
Tel: (613) 584-8811; Fax: (613) 584-4040
E-mail: Lachlan.Cranswick@nrc.gc.ca
WWW: http://neutron.nrc.gc.ca/

New Fullprof installer for Windows with Winplotr, EdPCR GUI Graphical control

(by Juan Rodriguez-Carvajal, Javier Gonzalez-Platas and Thierry Roisnel)

The latest Fullprof comes with a complete installer that loads the entire suite of Fullprof related programs.

This includes Winplotr, which itself includes a CIF and Shelx INS importer, as well as links to the GFourier program. The latest Winplotr can also not only read Fullprof Rietveld files, but also Rietan, Jana and Debvin files.

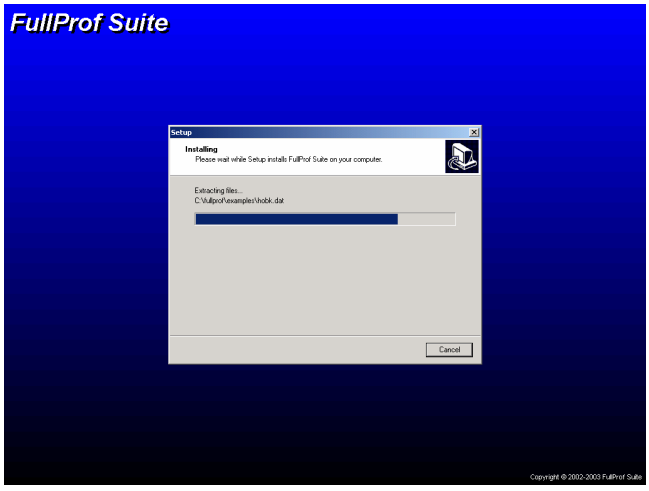

Figure 1: Installation of the Fullprof suite for MS-Windows via its new setup program.

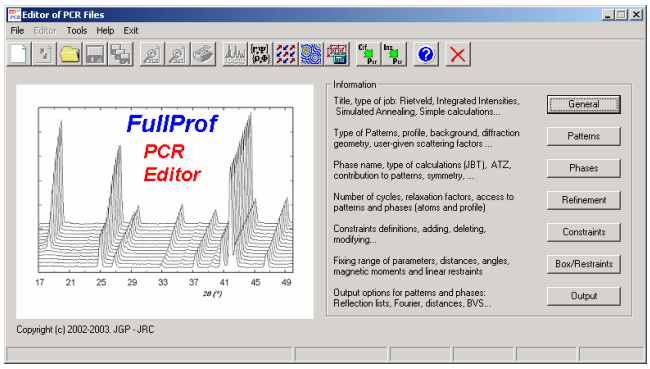

Figure 2: Image of the starting screen for the Fullprof PCR Editor

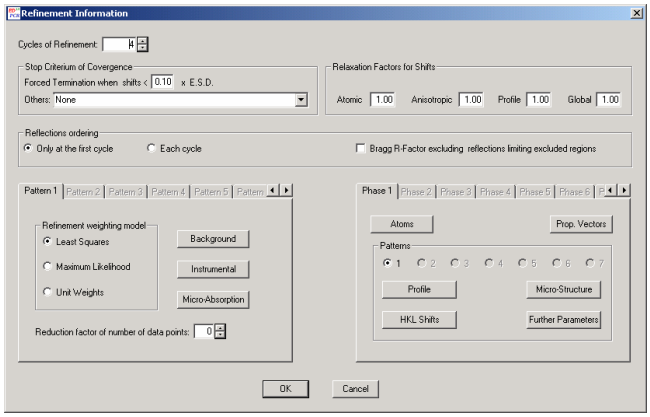

Figure 3: The initial refinement information screen in EdPcr

Updated EXPGUI interface for GSAS with new graphical instrument parameter file editor

(by B.Toby)

The latest EXPGUI software by Brian Toby has a number of updates including a new Instrument Parameter file editor. Rather than a tedious editing of a cryptic ASCII file to change parameters, this can now be done via a Graphical User Interface, including the options of importing a profile from a GSAS EXP file, minimizing the risk of typographic errors from manually typing in the data.

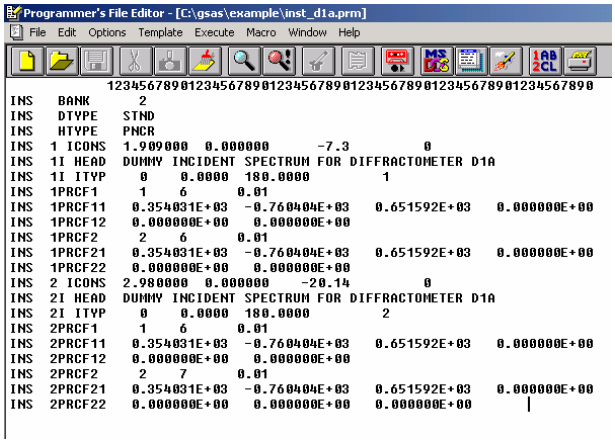

Figure 4: Editing a GSAS instrument parameter(PRM) file the traditional way, with an ASCII text editor.

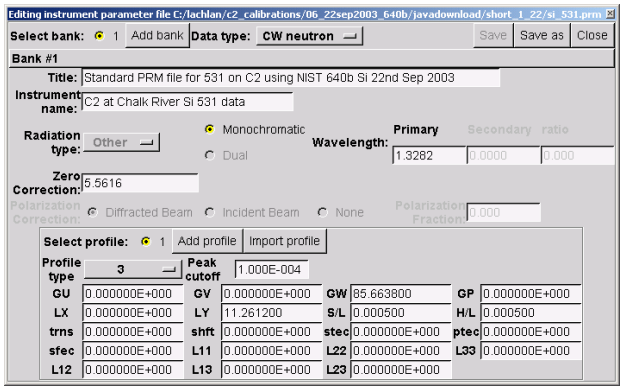

Figure 5: Editing a GSAS instrument parameter(PRM) file using the EXPGUI Instrument Parameter File editor (INSTEDIT). With this, it is easy to create or modify a GSAS instrument parameter file.

The Every Shifting Internet: changing download sites for many Rietveld and crystallographic packages.

It is claimed in a demotivational poster from http://www.despair.com/ titled "Change" that "When the winds of change blow hard enough, the most trivial of things can turn into deadly projectiles". While not really in that ballpark, changing network and management policies can mean that computer services can change, resulting in orphaned crystallographic software having to seek new homes. Relatively recent examples of this are the GSAS, Fullprof and XND Rietveld packages.

Using Google at http://www.google.com/ or another search engine can be an effective way of refinding the software. Though be wary that search engines may not refind the homepage of the software, but a page that links to the homepage. So some minor detective work and perseverance may be required. The CCP14 website at http://www.ccp14.ac.uk/ normally mirrors most of this type of software.

Rietveld Software Updates (as of mid December 2003):

Hugo Rietveld website:
http://home.wxs.nl/~rietv025/
BGMN (12th Nov 2003)
http://www.bgmn.de/
DBWS (22nd February 2000)
http://www.physics.gatech.edu/downloads/young/download_dbws.html
Debvin (25th May 2001)
ftp://ftp.cc.uniud.it/DEBVIN/
GSAS (13th June 2003)
http://www.ccp14.ac.uk/ccp/ccp14/ftp-mirror/gsas/public/gsas/
EXPGUI (5th December 2003)
http://www.ncnr.nist.gov/programs/crystallography/
Jana (23rd October 2003)
http://www-xray.fzu.cz/jana/jana.html
LHPM-Rietica (27th November 2001)
ftp://ftp.ansto.gov.au/pub/physics/neutron/rietveld/Rietica_LHPM95/
MAUD for Java (GPL'd) (3rd December 2003)
http://www.ing.unitn.it/~luttero/maud/
Prodd (19th August 2002)
http://www.ccp14.ac.uk/ccp/web-mirrors/prodd/~jpw22/
Profil (24th May 2001)
ftp://img.cryst.bbk.ac.uk/pdpl/
Rietan 2000 (GPL'd) (20th November 2003)
http://homepage.mac.com/fujioizumi/rietan/angle_dispersive/angle_dispersive.html
Winplotr/Fullprof (15th October 2003) (if Fullprof FTP site is unavailable, use the CCP14 Mirrors)
http://www-llb.cea.fr/winplotr/winplotr.htm
ftp://charybde.saclay.cea.fr/pub/divers/fullprof.2k/ (if Fullprof FTP site is unavailable, use the CCP14 Mirrors)
Winmprof (21st June 2001)
http://lpec.univ-lemans.fr/WinMProf/
XND (1st October 2003)
http://www-cristallo.polycnrs-gre.fr/xnd/xnd.html
ftp://ftp.grenoble.cnrs.fr/xnd/ (if XND FTP site is unavailable, use the CCP14 Mirrors)

All the above Rietveld programs are also available via the CCP14 based mirrors in UK, USA, Australia and Canada (http://www.ccp14.ac.uk/mirror/).

Summary lists of some software available via the EPSRC funded CCP14 website:

"What do you want to do?" (lists of software by single crystal and powder methods)
http://www.ccp14.ac.uk/mirror/want_to_do.html

Anharmonic Thermal Refinement Software
http://www.ccp14.ac.uk/solution/anharmonic/
Data Conversion for Powder Diffraction
http://www.ccp14.ac.uk/solution/powderdataconv/
Image Plate Software
http://www.ccp14.ac.uk/solution/image-plate/
Incommensurate Structure Software
http://www.ccp14.ac.uk/solution/incomm.htm
Indexing Software for Powders
http://www.ccp14.ac.uk/solution/indexing/
LeBail Method for Intensity Extraction
http://www.ccp14.ac.uk/solution/lebail/
Pawley Method for Intensity Extraction
http://www.ccp14.ac.uk/solution/pawley/
PDF, High Q Powder diffraction Analysis Software
http://www.ccp14.ac.uk/solution/high_q_pdf/
Peak Find/Profiling Software for Powder Diffraction
http://www.ccp14.ac.uk/solution/peakprofiling/
Pole Figure and Texture Analysis Software
http://www.ccp14.ac.uk/solution/pole_figure/
Powder Diffraction Data Visualisation

http://www.ccp14.ac.uk/solution/powder_data_visual/
Rietveld Software
http://www.ccp14.ac.uk/solution/rietveld_software
Search-Match Phase Identification Software
http://www.ccp14.ac.uk/solution/search-match.htm
Single Crystal Structure Solution Software relevant to Chemical Crystallography
http://www.ccp14.ac.uk/solution/xtalsolution/
Single Crystal Structure Refinement Software relevant to Chemical Crystallography
http://www.ccp14.ac.uk/solution/xtalrefine/
Single Crystal Suites linking to multiple programs relevant to Chemical Crystallography
http://www.ccp14.ac.uk/solution/xtalsuites/
Spacegroup and Symmetry operator determination software and source code
http://www.ccp14.ac.uk/recomm/sym_operators_to_spacegroups.html
http://www.ccp14.ac.uk/recomm/spacegroups_to_sym_operators.html
Spacegroup and Structure Transformation Software
http://www.ccp14.ac.uk/solution/transform/
Structure Conversion and Transformation
http://www.ccp14.ac.uk/solution/structconv/
Structure Drawing and Visualisation
http://www.ccp14.ac.uk/solution/structuredrawing/
Unit Cell Refinement of Powder Diffraction Data
http://www.ccp14.ac.uk/solution/unitcellrefine/

PPP - Powder Pattern Prediction

Armel Le Bail
Université du Maine, Laboratoire des Fluorures, CNRS UMR 6010, Avenue O. Messiaen, 72085 Le Mans, Cedex 9, France.
E-mail: alb@cristal.org ;
WWW: http://sdpd.univ-lemans.fr/

Powder patterns are predictable by a direct consequence of crystal structure predictability. The ICDD PDF-2 contains already a few hundreds of theoretical powder patterns coming from special ICSD data (having the THE comment - for theoretical) used for building their calculated powder patterns. For instance there are 24 theoretical SiO2 powder patterns in PDF-2, calculated from the atomic coordinates coming from ref [1] and deposited in ICSD. As a user I would prefer to know if the data from a database are experimental or not. But I surely would be interested in saving time by identifying my new compound as having been predicted already.

"Are crystal structures predictable?" was the title of a 1994 publication [2]. Ten years after, considerable progress have been made in structure prediction, enumeration, simulation, polymorph-generation, etc, either by using force-field, energy-minimization, distance-least-squares, valence-rule, simulated-annealing, design, packing-considerations, etc. The most active field seems to be in "protein structure prediction" nowadays, a Google search with these three words returns 220000 pages while "inorganic structure prediction" returns 28000, most of the latter pointing at a few commercial software. Thousands of structures have been predicted already, unfortunately they cannot be retrieved very simply and searched. Moreover, there are very few chances that ICDD/ICSD/CSD /CRYSTMET would accept the massive deposition of purely theoretical powder patterns or crystal data. My opinion is that the small and medium predicted crystal structures need for a special database (let the proteins apart). Software for phase identification by search-match in a powder pattern database give the choice for selecting some data subsets: mineral, organic (etc) and so, why not a theoretical subset ?

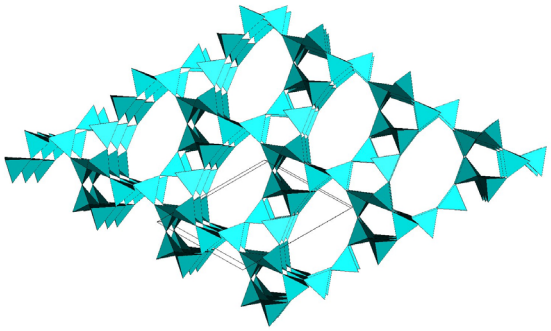

Figure 1: Will that predicted structure (PCOD1050015) be really observed some day?

Being mostly interested in inorganic compounds, I considered that making a database of predicted compounds would be better than waiting indefinitely for it. First of all, a database must be fed. I decided to become myself a predictor, starting by the most simple approach, using geometrical restraints applied to some series of well defined polyhedra-based compounds (tetrahedra, octahedra...). This concept is of course absolutely not new. Zeolite researchers have documented more than 1000 hypothetical structures by using classical physical model building [3] during the past 60 years. Simulated annealing is a rapid generator of hypothetical 4-connected framework structures and others. More than 5000 hypothetical zeolite structures were reported in ref. [4]. Many recent works in inorganic structure prediction have produced huge quantities of hypothetical compounds (using commercial packages as CERIUS, etc), there is no room here for citing them all. However, no systematic categorization was attempted so that, if interested, people would have to rebuild these hypothetical structures by themselves.

A preliminary version of the predicting sofware is available, named GRINSP (Geometrically Restrained INorganic Structure Prediction) [5]. The main purpose of GRINSP is to generate hypothetical structures which will be documented in a searchable database : PCOD (Predicted Crystallography Open Database), a subset of the COD [6]. If you are a structure predictor and want

to deposit your predicted structures in PCOD, that is already possible (CIF files only).

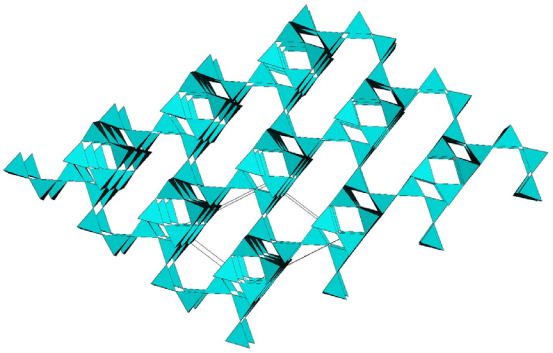

Figure 2: Another improbable zeolite : PCOD1050017.

GRINSP does not work by applying simulated annealing to a starting random configuration. Version 0.9 works schematically as follows, by using the Monte Carlo method : manual selection of the constraints on cell parameters and of restrained interatomic distances; random selection of the cell parameters inside of the predefined range; random positioning of a first T atom of the TX2 compound; random positioning of the next T atoms in respect of the distance restraints with the previous ones; if a model fulfills all criteria, place the X atoms at T-T midpoints, refine the atomic positions and cell parameters; continue to try to predict structures in that way till a certain number of independent runs are made; find if the predicted structures are new or were already described (using the CS fingerprint - Coordination Sequence).

In the GRINSP algorithm, the number of T atoms in a randomly selected cell is not predetermined, it is predicted as well. Only distances are considered (not angles - though considering a range for the second T-T distances is like giving angles). Currently, there are many limitations in that preliminary beta version. The choice of the space group is limited to P1. So that, GRINSP 0.9 is only efficient for a maximum number of 10-20 T atoms in a triclinic cell (which you may force to be cubic-like or hexagonal-like or etc). It will be able to predict only the very small zeolites (ABW, EDI, BIK...) or the compact SiO2 phases (quartz, etc) and also a lot of hitherto unknown phases (see the PCOD [6]). Further work is thus needed for improving the GRINSP efficiency: introduction of all space groups and management of special positions (considering only the unique T atoms); introduction of other polyhedra types (octahedra in a first time), predicting structures combining them; increase speed by not recalculating always everything (distances); Increase the box size for the CS (coordination sequence) calculations (729 cells is not always enough); reduce the output to the non-redundant predicted structures; etc ! GRINSP is distributed under the GNU Public License - so, you may decide to make improvements by yourself, provided the modified source code is made available under the same licence.

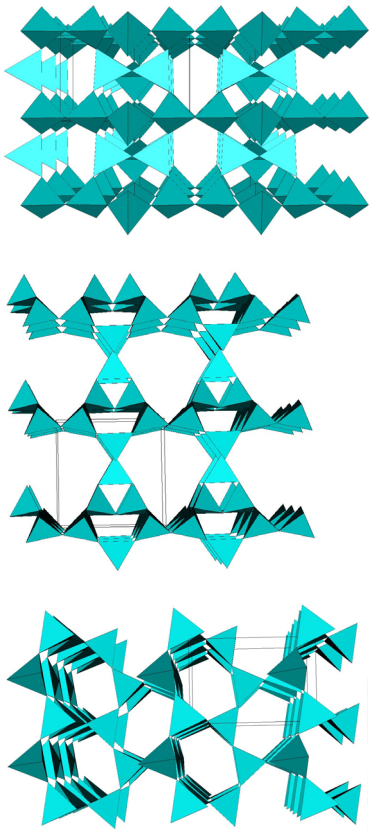

Figure 3: Three orthogonal views of PCOD1020007.

It can be anticipated that predicted/enumerated crystal structures may soon (during the next decades) exceed in number the really determined ones. It is probable that the "one stucture - one publication" which is almost the rule for the real crystal data will never be applied to the virtual ones. Therefore, it is logical to offer room for storage of these predicted or enumerated crystal structures. As a beginning, PCOD [6] contains an enumeration of 150 SiO2 polymorphs built up by using GRINSP. Predicting software should propose in first place in their lists the really observed compounds. This is the case of GRINSP which always places quartz, tridymite, cristobalite, EDI, ABW, BIK, JBW, SOD, YUG, etc, at the first places of the smallest predicted cells, with parameters close to the real ones. The next step for PCOD, if high standards are attained in the quality of the predicted models, is to produce a set of predicted powder patterns usable by search-match software. Thanks to the PCOD, phase identification would be extended to the hitherto unknown compounds, saving time in difficult structure determinations. But that dream is far from being realized yet, in spite of thousands of predicted crystal structures listed in the past 20 years (including thousands of zeolites).

Only cell parameters in the range 4.9-13 Å were considered in the preliminary predictions. Other known zeolites "predicted" in this range are triclinic or monoclinic BIK, SOD and YUG.

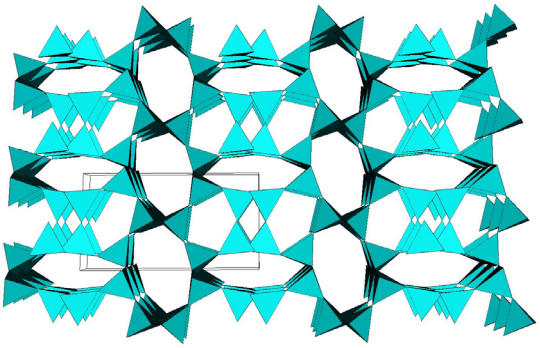

Figure 4: The predicted and very improbable PCOD1050025.

Table I: Comparison of some GRINSP-predicted cell parameters with dense SiO2 polymorphs or zeolites, idealized or observed ones

Predicted / Observed

	a	b	c	$R_{(DLS)}$
Quartz	4.965	4.965	5.375	0.0009
	4.912	4.912	5.404	
Tridymite	5.073	5.073	8.400	0.0045
	5.052	5.052	8.270	
Cristobalite	5.024	5.024	6.796	0.0018
	4.969	4.969	6.926	
ABW	9.331	5.175	8.873	0.0068
	9.9	5.3	8.8	
EDI	6.919	6.919	6.407	0.0047
	6.926	6.926	6.410	
JBW	5.209	7.543	7.983	0.0066
	5.3	7.5	8.2	

Even if many chimeric compounds will be added into PCOD, we can expect some treasures too. Either chimeric or to-be-observed-some-day, some structures as predicted by GRINSP are at least nice and decorative (see the figures). And one can expect that the real compounds (quartz, cristobalite, etc), retrieved and simulated by GRINSP as well, would be identified by a search-match from theoretical powder patterns built up from the data listed in the Table I. So that powder pattern prediction is really the next step. When PCOD will have a non-negligible number of entries, a file of ds and Is will be built up automatically from the crystal data (CIF files) and proposed for compilation to the search-match software. Why not to expect even some day that predictions will be as accurate as structures really determined and refined. That day, a database of real structures will have much less interest. About redundancy, and prediction of variants of topologically identical phases, should they all be inserted into the PCOD? I would say yes, since databases of real compounds are also plenty of such variants.

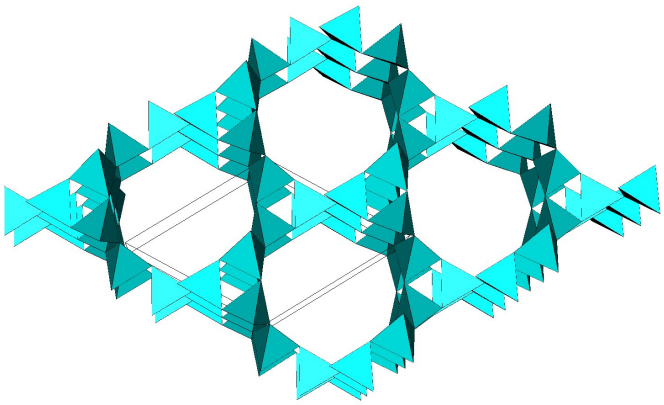

Figure 5: PCOD1030007 with large ring aperture, another chimeric zeolite.

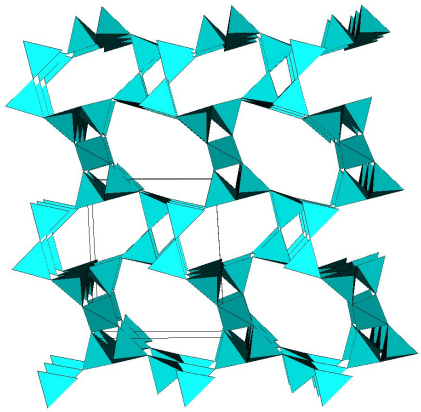

Figure 6: PCOD1060041, improbable triclinic simulation, or not?

So, do not only mention and show nice pictures of your huge quantities of predicted crystal structures in your manuscripts, also deposit their atomic coordinates at PCOD, as CIF files. Thanks!

References:

[1] M.B. jr Boisen, G.V. Gibbs, M.S.T. Bukowinski, Phys. & Chem. of Minerals (Germany) 21 (1994) 269-284.

[2] A. Gavezzotti, Acc. Chem. Res. 27 (1994) 309-314.

[3] J.V. Smith, Chem. Rev. 88 (1988) 149-182.

[4] M.W. Deem and J.M. Newsam, J. Am. Chem. Soc. 114 (1992) 7189-7198.

[5] A. Le Bail (2003), Program GRINSP : http://sdpd.univ-lemans.fr/grinsp/

[6] COD (Crystallography Open Database) : http://www.crystallography.net/

Balls & Sticks (Easy-to-Use Structure Visualization Program) for Windows

Sung J. Kang and Tadashi C. Ozawa[1]
1. Chigasaki Academy of Science & Technology, 1-10-17 Matasunami, Chigasaki, Kanagawa 253-0022, Japan
E-mail: tcozawa@jcom.home.ne.jp
WWW: http://www.toycrate.org/

Balls & Sticks was originally developed for material scientists who routinely need to visualize crystal structures in order to discover or optimize physical properties of crystalline materials from structural point of view.

There are many structure visualization programs designed for use by crystallographers, and those tend to include many sophisticated features requiring in-depth knowledge of crystallography to use. Often some of those sophisticated features are not necessary for non-crystallographers, such as materials scientists, and a simpler program is more desired. We have intended to design Balls & Stick as an "easy-to-use" structure visualization program so that researchers with minimal knowledge of crystallography can easily master its use. Particularly, we hoped that even undergraduate students could master the use of the program quickly, and they could spend more of their time analyzing structure of their interests rather than spending significant amount of time figuring out how to use the software. For this purpose, the number of functions in the program has been kept small, and development of the program was concentrated on "ease of use" GUI. Balls & Sticks is available only for Microsoft Windows operating system, so far.

Balls & Sticks fully utilizes Windows' GUI, and the program's GUI design is made close to other popular Windows applications so that users can quickly get used to the operation of Balls & Sticks. For example, many of the shortcut keys ("Ctrl+N" for editing a new structure and "Ctrl+O" for opening a file) are assigned in the same way as most of the Window's GUI applications. Also, property editing (size, color, lighting, etc.) of all the objects, such as atom, bond, polyhedra, unit cell outline and background color, can be done by right-clicking those object to invoke property-editing dialog boxes (Fig 1). In addition, animations of structures can easily be created by compiling snap shots of several static configurations of structure (Fig 2). Some of the sample animations can be found in the gallery area at Balls & Sticks' web site.

The development of Balls & Sticks is still continuing, and several new features have recently been added. Deleting and recovering specific elements has been improved, and also, crystal axes can now be labeled as either a-b-c or x-y-z. In addition, bond-thickness-exaggeration (Fig 3) and fog / depth-cueing (Fig 4) functions have been added to visualization model options, and these functions can be accessed by pressing [Ex] button on the floating toolbar. All these updates are made to allow more flexible visualization of crystal structures while maintaining "ease of use" of the software.

Currently, "easy to use" powder X-ray diffraction pattern simulator is being developed, and it will be inter-linked with Balls & Sticks so that the same structural data can be shared between them to generate diffraction pattern and structure figure, respectively. Some of the features in Balls & Sticks have been added due to the requests of users and we still consider adding more of useful features depending on user demands.

Balls & Sticks is freely available at http://www.toycrate.org/ or its CCP14 mirrors via http://www.ccp14.ac.uk/ .

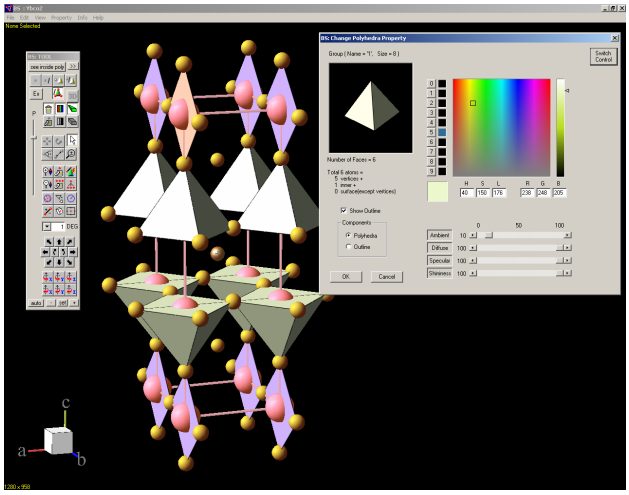

Figure 1: Polyhedra property editing dialog box which can be invoked by right-clicking on a polyhedra of interest.

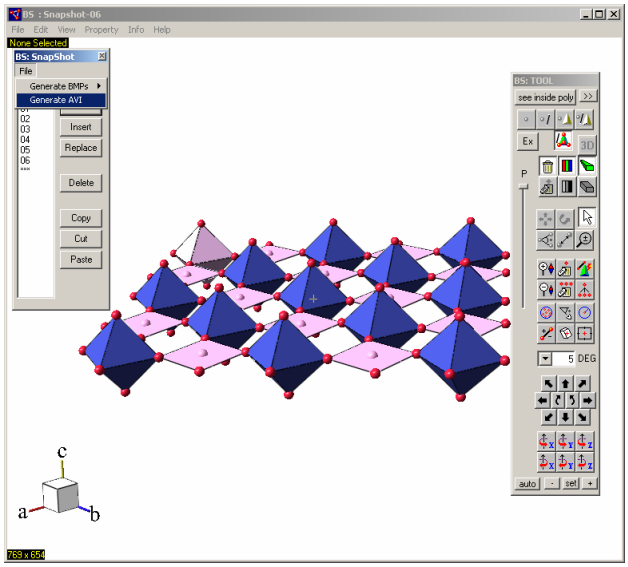

Figure 2: Snap shot dialog box and AVI (animation file) generation menu.

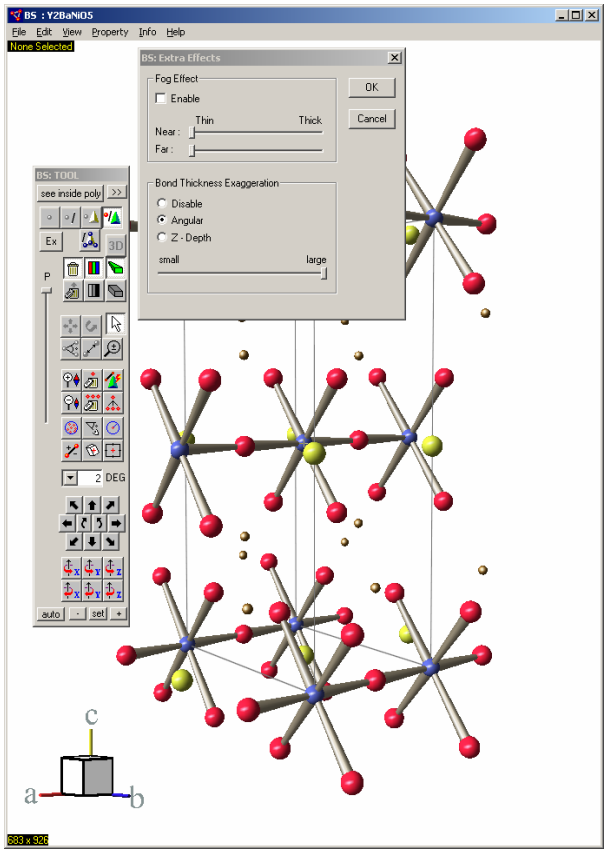

Figure 3: Bond-thickness-exaggeration controls and generated structure.

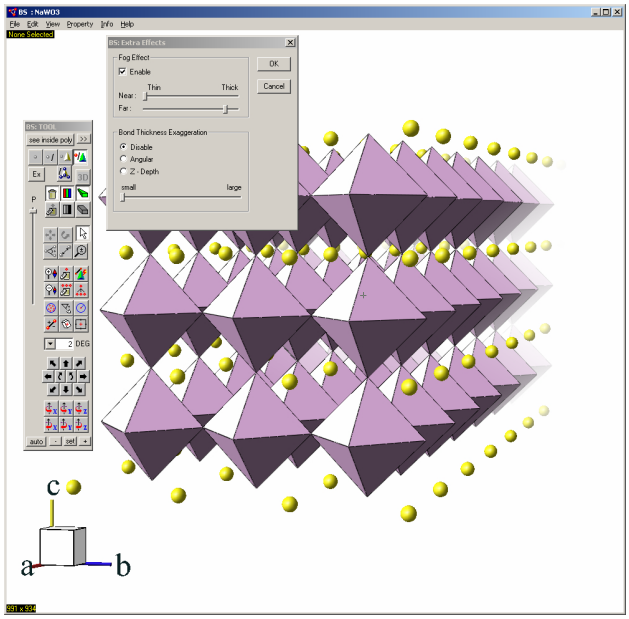

Figure 4: Fog controls and depth cued structure image.

ICSD-for-WWW, a crystallographic database on the WWW Server now available for PCs including Windows, Macintosh, Linux & Unix.

Alan Hewat[1] and Peter Hewat[2]
1. Diffraction Group Leader, Institut Laue-Langevin (ILL), B.P. 156X Grenoble Cedex 9, FRANCE.
Tel: (33) 476.20.72.13; Fax: (33) 476.20.76.48 E-mail: hewat@ill.fr WWW: http://www.ill.fr/dif/
2. Institut National de Recherche en Informatique et en Automatique (INRIA) ZIRST - 655 Avenue de l'Europe, 38330 Montbonnot Saint Martin, France.
Tel: (33) 6.2381.6283; WWW: http://hewat.free.fr/
E-mail: Peter.Hewat@inrialpes.fr

Introduction

Since 1997 ILL Grenoble has provided a WWW interface to the ICSD (Inorganic Crystal Structure Database), a product of the FIZ Karlsruhe, a non-profit laboratory of the ILL's German Associate. You need only to click on http://icsdweb.fiz-karlsruhe.de/ to use this database, but in this article we will describe how you can install the software to run on your own machine if you want to be independent. The software will run on personal computers including Windows and Macintosh OS-X machines as well as on Linux and Unix servers such as SGI, HP, Sun and IBM-AIX. Although you may download the software, you may not modify it, and we cannot provide individual support if you do not have a licence from FIZ.

You will only be able to download a demo database of 3380 inorganic structures, but the full ICSD database, which must be licensed from FIZ, now contains over 73,500 entries. The rate of adding new entries has greatly accelerated with the growth of electronic publishing, since journals can now submit the contents of their new issue directly to the database. ICSD is not simply a collection of CIF coordinate files, but contains many other data fields containing information about the conditions of measurement, the results of various tests for possible errors in the structure, links to electronic versions of the original papers and much more. All entries are checked and re-checked, not only for trivial syntactic errors, but more importantly for reasonable symmetry, bond lengths, coordination, temperature factors etc.

Installing ICSD-for-WWW in 4 steps

The ICSD-for-WWW interface has been re-written entirely in the new web-based PHP language, which is based on PERL but integrated with the usual HTML and Javascript. It is not necessary to understand these technical details, only that this means that the exact same interface code can be installed on almost any operating system. The ICSD database itself has been transferred to a modern SQL query language format, but of course all the queries are handled by the WWW interface, which is familiar even to non-specialists.

Indeed one objective is to make crystallographic results available to the non-crystallographer.
Installation will be described for a Windows-XP machine, but is very similar for other systems, for which instructions are given on http://icsd.ill.fr/icsd/install/. (Please read them before attempting installation!)
1 Install an Apache+PHP+MySQL WWW server. For Windows, a complete package (jaws) is available that installs like many other Windows application. Apache is a free webserver, PHP refers to the PHP interpreter, and MySQL to the SQL database engine.
2 Download the ICSD-PHP software to your Apache html directory.
3 Download the ICSD demo database, to your MySQL data directory.
You should now be able to use ICSD-for-WWW to search for structures, but if you then want to draw the structure or the diffraction pattern, calculate bond-lengths etc., you will need to complete the 4th step.
4 Download the ICSD support applications, which are machine dependent, to your cgi-bin directory.
Using ICSD-for-WWW
Connect to http://icsdweb.fiz-karlsruhe.de/ (or to http://localhost/icsd/ if you have installed the server software on your own machine). If the server does not recognise that your computer is licensed to access the full database, you will be invited to type a username/password or else to click on "Demo". You will then be invited to fill in one or more "query boxes". The titles to the query boxes contain examples of the query required, and drop down beneath the query form when clicked. To learn to use the interface the user can simply click on these titles, click on an example query, and immediately see the result of that query. If necessary, additional queries can be added and the search repeated.

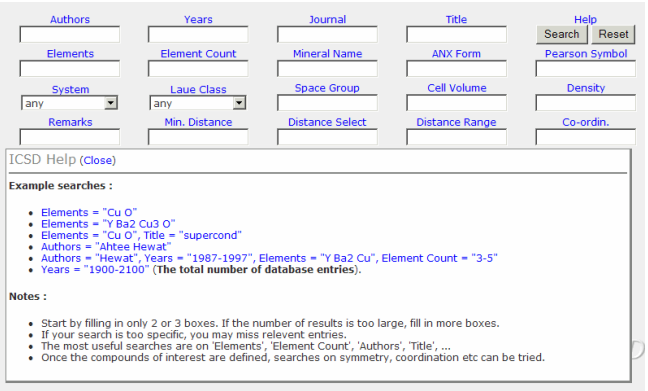

The user can then order the selected entries according to year, author name, formula, space group or mineral name, select those that appear of interest, and list those References. Direct links to PDF files of the original publication are provided in some cases, notably for IUCr journals. These references can also be exported to the EndNote personal reference database, which will automatically format them appropriate for citing a particular journal. The Details button can be used to compare several entries, the Bonds button calculates bond-lengths and angles, while the Pattern button produces postscript or PDF plots with [hkl] labels. Finally, the Structure button produces interactive 3D structure drawings in VRML or PDB/Chime format. Entries can be compared by super-imposing diffraction patterns or structure drawings.
For example, in the full database we found 22 entries for copper oxide containing Cu^{2+}. (Try a different example if you only have the demo database). Most copper oxide entries are simply CuO of course, but ICSD also found the interesting compound Cu_4O_3 by O'Keefe and Bovin (1978), where the formula indicates that the average copper valence is 1.5 !

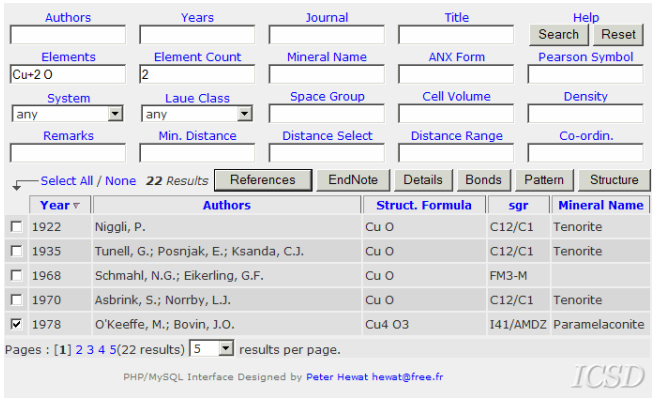

Clicking the Details button confirms that indeed Paramelaconite appears to be a mixed valence compound containing Cu^{1+} on site (8c) and Cu^{2+} on (8d).

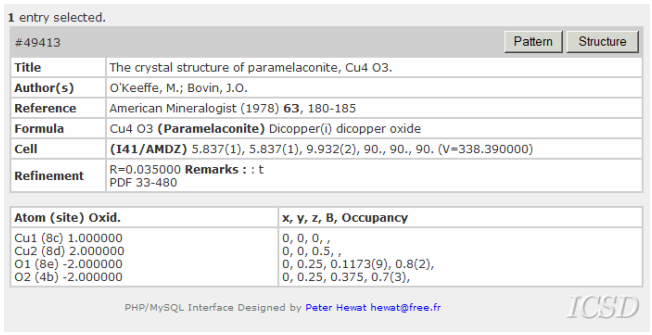

To investigate further, we click on the Structure button. The drawing of the crystal structure is completely automatic – we do not need to specify which atoms are bonded (although we can if we wish using the Bonded Atoms box). We have various other options to draw the structure, but generally we need only click on the Display button to obtain a 3D VRML drawing of Paramelaconite produced using xtal-3d.

1 entry selected.

Edit the CCSL data, select the **Atoms** and **Bonds** model, and click on **Display**. Choose 2 or more structures to compare them. You may need help with the **3D display** or with special **drawing options** . Most **problems** are due to the **Space Group** representation.
Please check the symmetry operations in the print-out !! (button below).

```
N *Paramelaconite-Cu4 O3-[I41/AMDZ] O'Keeffe, M.; Bovin, J.O.(1978)
C 5.837000 5.837000 9.932000 90.000000 90.000000 90.000000
S GRUP I 41/A M D
A Cu1      0.000000  0.000000  0.000000  0.000000 0.000000
A Cu2      0.000000  0.000000  0.500000  0.000000 0.000000
A O1       0.000000  0.250000  0.117300  0.800000 0.000000
A O2       0.000000  0.250000  0.375000  0.700000 0.000000
T Cu1  4   0.006600  0.009300  0.002100 -0.002300 0.000000 0.000000
```

PDB/Chime | VRML2 | Cell | At.Names | Transparent | Black B/G
Perspective | Axes | Shaded | Title | Wireframe | Gzip file
Blink time 1.0 | Atoms Small Spheres | Bonds Polys+Cylins
Reference Plane | Multiple Cells: x: 1 y: 1 z: 1
0.0, 0.0, 0.0
0.0, 0.0, 0.0
0.0, 0.0, 0.0
Bonded atoms | Min Bond: 0.75 | Max Bond: 2.75
Defaults | Display

Re-display | Save VRML structure | Print CCSL output | Valence-Sum
VRML drawing with **xtal-3d** by **Marcus Hewat.**

ICSD shows us that there are indeed two very differently coordinated copper atoms (green) – one at the centre of a square of 4 oxygen atoms (red) and the other with only 2 oxygen neighbours. If we were to select the option to label the atoms we would see that Cu1 had two oxygen neighbours and Cu2 four.

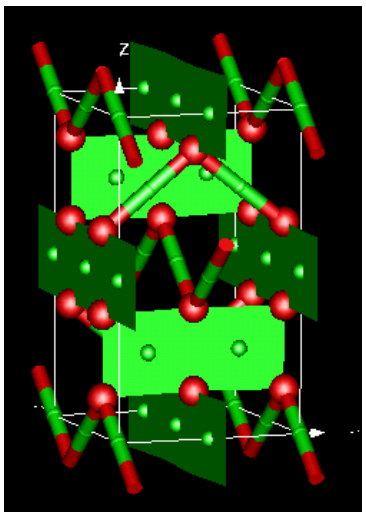

But we can do better ! If we click the Valence-Sum button, ICSD displays the Brown-Shannon valence sum for the various Cu-O bonds. We see that the valence sum for Cu1 is indeed 1, while for Cu2 it is 1.51, somewhat less than 2.0. It is not unusual that the valence sum is not a simple integer for all atoms, since coordination is usually a compromise between the relative sizes of the different types of atoms and some bonds are strained. Xtal-3d, which did this calculation, had to automatically decide whether to use the bond-valence parameters Ro and B for Cu^{1+} or for Cu^{2+}; it did this by simply trying both and then finding that Cu2 was closer to Cu^{2+}.

```
****************** Valence Sums for File=AGre41.ccl ********************

Bond-valence sum for Cu1 is 1.00 assuming Ro=1.610 B=0.370 for Cu1+ to O -2
Bond-valence sum for Cu2 is 1.51 assuming Ro=1.679 B=0.370 for Cu2+ to O -2
```

Instead of using xtal-3d, we can generate PDB/Chime format, which displays as a simple space-filling model.

In either case we must install the appropriate plug-ins to display on Windows or other computers.

This simple example shows that any scientist, not necessarily a crystallographer, should be able to use ICSD to find compounds containing copper in mixed-valence states, and to understand the structure of these compounds with a few clicks of the mouse-button. ICSD is designed not only for crystallographers! If we have chosen the example of copper, it is because such mixed valence compounds are found as high temperature superconductors, as colossal magneto-resistive magnetites and as many other new materials with very interesting properties. The structures of these materials are often difficult to understand by many non-crystallographers working with them.
But returning to the crystallographers, we can also use ICSD to calculate the bond-lengths (with bond-angles and standard errors if required). Clicking on the Bonds button brings up a similar form containing the cell dimensions, space group and atom coordinates. Incidentally, the format used for both structure drawing and bond-length calculations is that of the Cambridge Crystallographic Subroutine Library, which is used for these calculations. These forms can of course be edited to see the effect on the structure of adding or removing specific atoms, or displacing them. The list of Cu-O bonds again shows that Cu1 has only two oxygens at 1.87Å, while Cu2 has two at 1.97Å and another two at 1.92Å.

Bond Lengths and Angles

Edit the CCSL data, specify the bonds to calculate, and click on **Bondla**. Choose 2 or more structures to compare them. Most **problems** are due to the **Space Group** representation.
Please check the symmetry operations in the print-out !! (button below).

```
N *Paramelaconite-Cu4 O3-[I41/AMDZ] O'Keeffe, M.; Bovin, J.O.(1978)
C 5.837000 5.837000 9.932000 90.000000 90.000000 90.000000
S GRUP I 41/A M D
A Cu1     0.000000 0.000000 0.000000 0.000000 0.000000
A Cu2     0.000000 0.000000 0.500000 0.000000 0.000000
A O1      0.000000 0.250000 0.117300 0.800000 0.000000
A O2      0.000000 0.250000 0.375000 0.700000 0.000000
```

Enter the **max**imum and **min**imum bond lengths and a pair of ions eg **Cu-O** (blank means all ion pairs) and click the **Bondla** button to calculate bond lengths (with angles if required).

Bonds from 0.0 **to** 2.75 **Å between atoms** **with** angles -> Bonds

PHP/MySQL Interface Designed by Peter Hewat hewat@free.fr ICSD

Paramelaconite-Cu4 O3-[I41/AMDZ] O'Keeffe, M.; Bovin, J.O.

	Atom1	Atom2	Atom3	Value	Error
Bond	Cu1	O1		1.8673	
Bond	Cu1	O1		1.8673	
Bond	Cu2	O1		1.9663	
Bond	Cu2	O1		1.9663	
Bond	Cu2	O2		1.9159	
Bond	Cu2	O2		1.9159	
Bond	O1	O2		2.5595	

Finally, for the crystallographer, and especially for the Rietveld refinement, the ICSD can calculate the powder diffraction pattern for both X-rays and neutrons, or even compare powder patterns for different structures, labelling the [hkl] peaks if required.

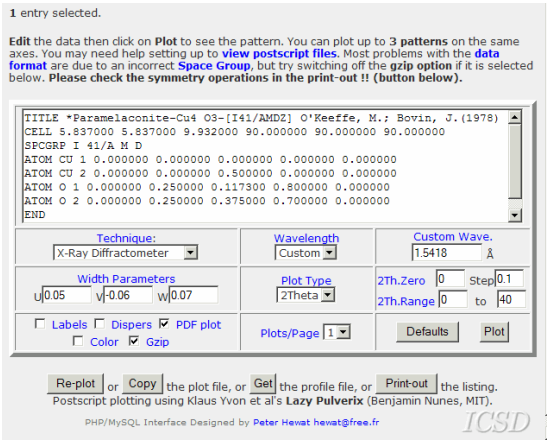

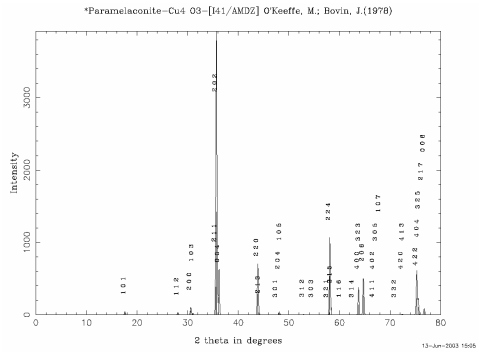

Now we have found out a lot about Cu_4O_3 from ICSD itself, but if we are still interested we will certainly want to read the original paper.

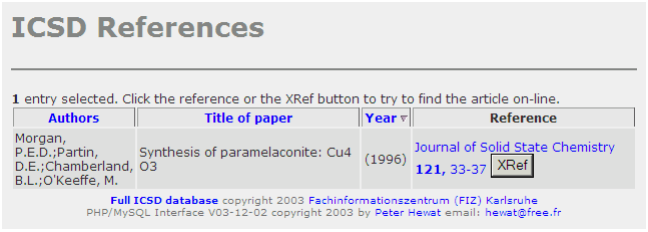

If we click on References we obtain links that will allow us to obtain the full text of this paper; the Journal of Solid State Chemistry 121, 33-37 link goes directly to this paper, but if a direct link is not available, we can instead try the Xref button. This will automatically fill in a form with the article details that can be submitted to the CrossRef organisation, which maintains a database of all electronic publications.

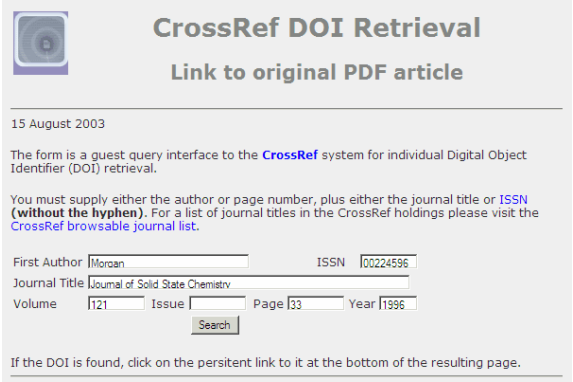

In either case, we will quickly bring up a WWW page from the Journal of Solid State Chemistry, allowing us to read the abstract, and if we have a subscription, download the complete paper in PDF form.

Not all journals yet provide electronic copies of old publications, but this will very soon be common. The IUCr has lead the way in this, and already has electronic versions of all papers going back to 1948 ! These can all be accessed directly from the ICSD-for-WWW interface. Indeed, future papers submitted to Acta Cryst journals will be automatically screened before publication by ICSD-for-WWW to find earlier work to alert the referees !

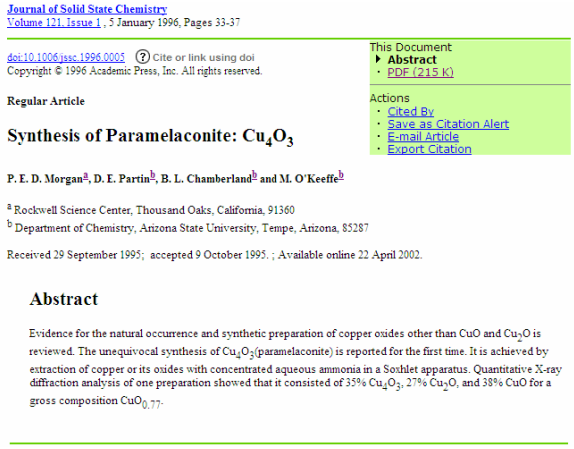

Technically everything is now in place to make it much easier for crystallographers to check on earlier research before undertaking new measurements, and to compare their own results to those of others. But access to journals and databases still requires paying for subscriptions. This has become a passionate topic for debate, as Frank Gannon, Executive Director of EMBO put it "Logically, scientists respond to the calls to 'free the literature' or advertisements proclaiming the 'freedom of expression' with feelings that some of them last felt in the 1960s." Nature has published an extensive debate about electronic access to journals and databases that you can read on Nature Debates - Future e-access to the primary literature

The bottom line is that some-one must pay for the work involved in publishing journals and databases, even when this is done by non-profit organisations like FIZ and IUCr. One solution is to obtain a government grant, as in the UK, to provide free nation-wide access to essential databases like ICSD-for-WWW from a central server. Another is to ask authors to pay for publishing their own work, a very small percentage of the cost of the research itself. In that case the published work would be made freely available on the WWW.

For the present, there is no one solution that fits all. Rather than criticise non-profit organisations that are trying to make it easier for more scientists to obtain more information, crystallographers might instead encourage their colleagues to support existing databases. Potential supporters of ICSD-for-WWW should contact FIZ-Karlsruhe on http://www.fiz-informationsdienste.de/en/DB/icsd/

VMRIA - A DELPHI-based visual object-oriented program for Rietveld Refinement, Powder Indexing and analysis of neutron diffraction data.

Victor B. Zlokazov
JINR FLNP Dubna, 141980 Russia.
E-mail: zlokazov@nf.jinr.ru ;
WWW http://www.ccp14.ac.uk/ccp/web-mirrors/vmria

The purpose of the VMRIA Rietveld and powder diffraction software is two fold:

1. to accumulate experience in dealing with modern programming techniques – such as visual object-oriented programming as implemented within DELPHI;
2. optimization of mathematical methods for solving the main problems of analysing of neutron diffraction data.

Compared with Visual C++ Delphi has obvious advantages: the same possibilities combined with the incomparably greater comfort offered to the user of high level programming language; and compilers running under both Windows and Linux. Fortran is no longer popular among younger generations of scientists; therefore, the problem of transition to other programming styles is topical. VMRIA is an attempt to implement the most successful algorithms of the Fortran programs for the analysis of diffraction data within the Delphi programming style. It is a console with a set of self-explaining keys; which means calling certain procedures and working with them via graphical dialog, using automatic syntactical control and on-line help. It is a portable code written entirely by DELPHI involving a typical Windows user-friendly application running in a multi-task environment; and combining all the benefits of graphical / numerical representation of in- and output data and dialog / batch modes of processing this data.

The procedures carried out by VMRIA are as follows:

1. Different sorts of data visual representation and transformation to other formats.

2. Shape-independent peak analysis - search of peaks and their fitting.

3. Shape-independent multi-spectrum and multi-phase Rietveld analysis. (in particular, for RTOF-spectra, for which the program is specially adjusted);

4. Powder matching.

5. Automatic three-dimensional Fourier synthesis.

6. Multi-phase powder Indexing.

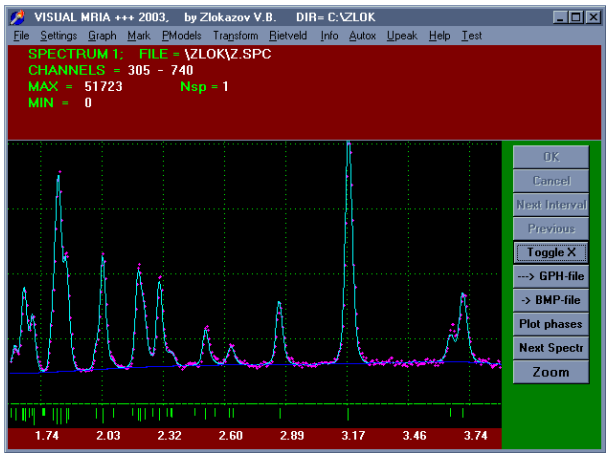

Figure 1: Results of Rietveld analysis of the IUCr test spectrum of ZrO2 + 2% of Hf (replacing Zr)

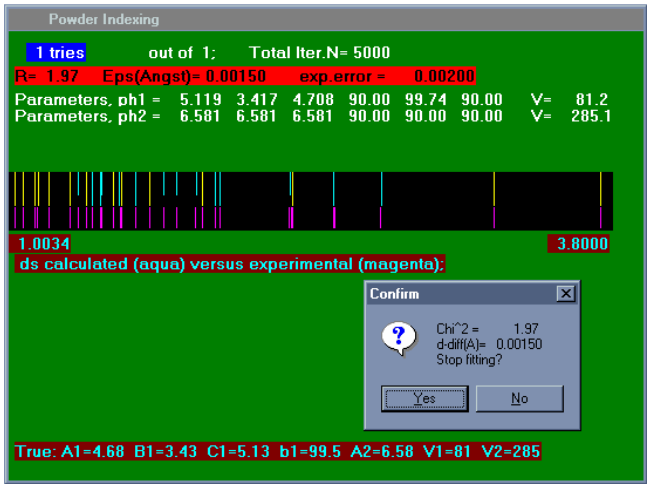

Figure 2: Results of 2 phase powder indexing of a mixture of Copper oxide (monoclinic) and Rubidium Chloride (cubic) d-spacings

The batch-like feature mode is implemented by (optional) use of an ini-file. This provides for the input of the most routine data needed and the execution of the most routine preparatory operations. The dialog is recommended for the explorative part of the data analysis.

THE MOST IMPORTANT CLASSES.

The data and procedures of VMRIA are implemented as Delphi classes. Class methods are codes implementing different class algorithms. Object is a union of properties (data), methods and events linked to them. Under events in the classes interrupts and program prompts for user actions are meant such as specifying the necessary data and reacting on error diagnostics or result analysis. The main data is implemented as class TSpectrum. This class is ready to be transformed to dealing with such data formats as HDF or NeXus. The methods of this class are different procedures for the simple spectrum processing. An important descendant of the class TSpectrum is the

class TpeakModel - for building the peak model - either as analytical (given by formula), having a more or less regular form, or as based on a graph with however cumbersome shape, into which parameters A,C,W are introduced according to:

p(A,C,W,x) = A m((x - C)/W).

Another descendant of the class TSpectrum is the class TpeakSearch - for the automatic peak search in the spectrum and dividing the spectrum into intervals containing single peaks or unresolved multiplets. The algorithm is based on a previous high- and low-frequency filtering of the spectrum; on sequential identifying of single peaks and subtracting them from the spectrum. Peak identification is based on syntactical recognition of a peak by such indications as min-max properties and amplitude-independent function characteristic - quasi-curvature:

q(f(x),x) = f''(x)/sqrt(1 + f'(x)^2),

followed by the statistical analysis of the possible peak amplitude, area and shape criterion.

A special case is the class TParameter - the most important class for the performing the regularized Gauss-Newton least-square fitting. Its properties: array of structures, each of which is 8 quantities: parameter number, parameter value (first, initial, then fitted one), parameter lower and upper bounds, two coefficients of an (optional) linear dependence between the parameters, fitted parameter error, comment; array of control data for the fitting; array of the fit quality characteristics; arithmetic functions for the fitting; regularization function (for Bayesian estimation).

Its methods: a Gauss-Newton matrix descent with projection of parameters onto linear restrictions in square or modulus metrics with optional use of adaptive weights (for robustness) and Bayesian (Tichonov's) regularization as separate procedure or in combination with statistical (Monte-Carlo) trial sequence.

Analysis

The algorithms of the analysis are implemented by the class methods. The mathematics of the used methods for the extraction of the physical information from the spectra is described in ref.[1-5].

References

1. Zlokazov V.B., Chernyshev V.V. J.Appl.Crystallogr. (1992) 25,447-451.
2. Zlokazov V.B. Comp. Physics Communic., 1995, v.85, p.415-422.
3. Zlokazov V.B. J. Appl. Crystallogr., (1997).30, p.996-1001.
4. Zlokazov V.B. Nucl. Instr. & Meth.,1977,v.143,No 1,p.151-156.
5. Zlokazov V.B. Comp. Physics Communic., 1978,v.13,No 5/6,p.389-398.

Update on Ab Initio Structure Determination using FOX

Vincent Favre-Nicolin[(a)] & Radovan Černý[(b)]
(a) CEA/DRFMC/SP2M/NRS, 17, rue des Martyrs 38054 Grenoble Cedex 9; (b) Laboratoire de Crystallographie, Université de Genève, Switzerland
E-mail: vincefn@users.sourceforge.net or Vincent.Favre-Nicolin@cea.fr

Introduction

FOX, 'Free Objects for Xtallography' [1] is a free, open-source program for windows and Linux written for the ab initio structure determination from powder diffraction. It performs direct-space structure determination, allowing a modular description of the structure as a combination of atoms, polyhedra and molecules. It was initially successful for solving inorganic structures, thanks to (i) its ability to detect and correct dynamically for special positions and the sharing of atoms between polyhedra, without requiring any a priori knowledge on atoms overlap, and (ii) the possible use of multiple patterns (neutron + X-Ray). The aim of this short article is to show how it has evolved since the first versions, with a highlight on solving organic structures.

Algorithm news

FOX was designed with a modular algorithm, i.e. with the ability to combine different criteria (several powder patterns, anti-bump repulsion). From the initial use of Rwp factors as “cost functions”, FOX has now moved to using χ^2 for all diffraction data, keeping the ability to combine these with restraints and anti-bump costs. This is a more rigorous approach to the structure solution process, as the χ^2 criterion used corresponds to the evaluation of the log(Likelihood) of the structure. This new formalism should allow Fox to take into account more restraints, and also to implement a Maximum Likelihood description of the structure (e.g. take into account missing or disordered parts of the structure in calculated intensities, ...). Some of these have already been introduced in Fox, although they are hidden from the end user (unless you compile Fox yourself, which is easy -hint, hint !).

Improving structure solution for organic compounds using a flexible description

A major change in the description of Molecules was introduced in Fox v1.6: the simplest way to describe a molecule conformation is to deduce all atoms starting from one end of the molecule, the parameters being a set of dihedral angles. This has the advantage of describing the molecule with a number of parameters exactly equal to the number of Degrees Of Freedom (DOF), and thus this 'z-matrix' approach has been the main approach used in direct-space structure determination. However this approach has numerous

shortcomings, e.g. (i) the displacement of one atom at the beginning of the molecule will imply the displacement of all the atoms after that one (you cannot move atoms in the middle of the molecule independently from other parts of the structure), (ii) the order of the atoms in the description will greatly influence the flexibility of the molecule and the ability to find the correct conformation, and (iii) this format makes it difficult (if not impossible) to describe flexible cycles.

For this reason, in version 1.5 was introduced a new format (the old z-matrix format can be converted through a menu): molecules are described using a list of atoms defined by their (x,y,z) orthonormal coordinates, and linked together by a set of restraints on bond lengths, bond angles and dihedral angles. In order to reduce the number of parameters from the 3N atomic coordinates, Fox analyses the restraints to determine the free torsion angles, and then creates a set of allowed conformation changes. The huge advantage of this description is that by using individual atom coordinates, any structural change on all or part of the structure can be trivially implemented:
- rotation around free torsion angles
- exchange of groups
- mirror (flipping)
- rotation of atom groups inside the molecules
-...

Combined with a use of a quaternion to parametrize the orientation of the molecule (avoiding 'gimbal lock' when χ=0 or 180°), this added flexibility has vastly improved the speed of convergence for organic structures: for the Cimetidine structure (used as a benchmark, with 8 free torsion angles), the number of trials required to solve the structure has gone down from near 4 million to about 1.2 million, corresponding to about 7 minutes on a 1.4 GHz computer.

When this new modelling was introduced, Fox allowed by default a lot of flexibility for the atoms, so that the intermediate conformations could be somewhat wrong with respect to the user-chosen restraints. This was purposely introduced, as tests have shown that this added 'flexibility' improved the convergence towards the structure solution, by 'smoothing' the sharp-edged hypersurface the model has to explore before finding the correct global minimum. This confused a number of users, especially for large structures, where the undesired flexibility was the most visible. This is amended in the new version (1.6, December 2003) of Fox, which now uses by default less flexibility, and allows several models:

- flexible with automatically assigned free torsion angles (recommended for most structures)
- rigid body (with the separate option to fixing the orientation)
- user-chosen free torsion angles

Displaying 3D GSAS Fourier Maps and exporting the 3D view to POVRay [Fig. 1]

Besides the main objective of solving structures, Fox can also display structures in 3D using OpenGL. This can be useful in conjunction with GSAS and EXPGUI, as Brian Toby added to EXPGUI the export of the structure in the Fox xml format. With Michael Polyakov, he also added the import and 3D display of GSAS Fourier maps in Fox. It is now possible to display several contour levels for a given map, and several maps (i.e. F_{obs} and F_{obs}-F_{calc}) can be shown together as well.

Finally, the Fox 3D view can be exported as a POV-Ray (http://www.povray.org) file, to produce ray-traced quality images of the structures, with Fourier maps.

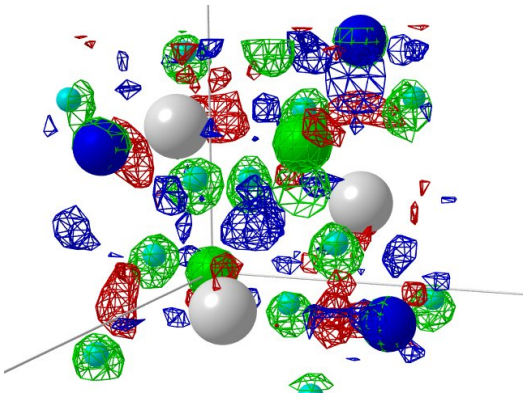

Figure 1: Garnet structure shown with Fourier maps imported from GSAS. Maps are F_{obs} (green), F_{obs}-F_{calc} in blue (at +2σ) and red (at -2σ). The image was produced using POV-Ray (http://www.povray.org), as version 1.6 of Fox introduces the export of the 3D view to POV-Ray.

Highlight on recent structures solved using FOX

Fox continues to be successful in solving new inorganic (hydrides, oxides, intermetallic) structures, such as the MgIr structure ([2], fig.2): this Frank-Kasper type intermetallic compound was solved from synchrotron powder data in the orthorhombic cell (V = 5025 Å^3) and spacegroup Cmca using modelling with free atoms (13 Ir and 12 Mg atoms). The model was confirmed later with single crystal data.

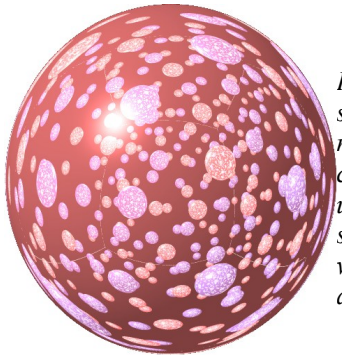

Figure 2: The MgIr structure, as seen in reflexion from one central Ir atom (drawn using POVRay). The structure was solved with 25 independent atoms.

There is also a growing number of organic structures solved using Fox: the two following examples show that 50 independent non-H atoms is definitely not a limit any more for Structure Determination in direct space using a Single Powder Pattern :

- The first ([3], fig.3) is the structure of the form II of PhenoBarbital ($C_{12}H_{12}O_3N_2$, or 5-ethyl-5-phenylbarbituric acid, a commercial drug). The unit cell is triclinic with P-1 spacegroup, with 3 molecules in the asymmetric unit cell, each with 4 free torsion angles[1], making a total of 30 DOF (Degrees Of Freedom) and 51 non-hydrogen atoms.

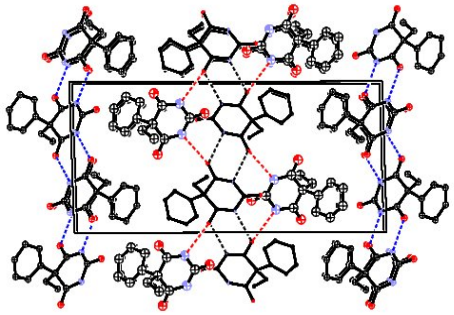

Figure 3: View of the unit cell of PhenoBarbital ($C_{12}H_{12}O_3N_2$). There are 3 independent molecules, with a total of 30 DOF.

- The second ([4], fig. 4) is the structure of β'-PSP (1,3-di-n-hexadecanoyl-2-n-octadecanoylglycerol), $C_{53}H_{102}O_6$, which was solved with FOX by increasing gradually the degrees of freedom [bond distances and angles around the glycerol moiety followed by all (56) non-H torsion angles]. This took about two months of calculation time. The structure will be submitted together with the β-polymorph to Chem. Phys. Chem. by Dirk J.A. De Ridder*, Kees Goubitz, Mihaela M. Pop, René A.J. Driessen, René Peschar and Henk Schenk.

Future developments, users feedback.

Although the main author (V. Favre-Nicolin) now works on the diffraction of nanostructures (quantum dots,...), the development of Fox is still going on. The handling of organic molecules will continue to improve with the use of the OpenBabel library (http://openbabel.sourceforge.net) to import molecule structures from a large number of formats. Another awaited development is the incorporation of (efficient) derivative calculations into Fox, which would open the way to profile fitting, least-squares, structure factor extraction, Fourier calculations, other direct-space algorithms, etc... New restraints may also be added to solve structures which are more complex or without quality data, e.g. intermolecular restraints, energy minimization, etc... Finally, the switch to a Maximum-Likelihood evaluation of structural models should allow taking into account missing or disordered parts of the structure, but how exactly this will be available to the end user is still debated. For all of these features, please bear in mind that Fox is an open-source project and that anyone can contribute to it; many calculations are already present to ease the implementation of new features (e.g. interatomic distances for energy calculations, etc..)

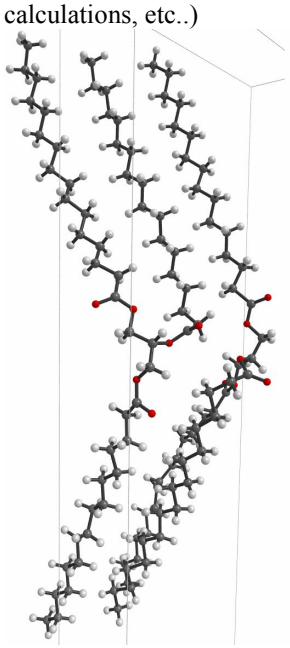

Figure 4: the structure of β'-PSP (1,3-di-n-hexadecanoyl-2-n-octadecanoylglycerol), $C_{53}H_{102}O_6$, also solved with Fox. The complexity of the structure required a progressive increase of the degrees of freedom (first near the glycerol moiety, up to the 56 non-H torsion angles !) to solve it.

It is also important to remember that Fox development is user-driven. So if you have a tough structure which you believe would benefit from a new feature, sending an email to the author with some data for testing is highly encouraged! Also, users should subscribe to the Fox mailing list (http://lists.sourceforge.net/lists/listinfo/objcryst-foxx), which is used to announce new versions of Fox (10-15 emails per year). This allows to test new versions of Fox before general release, which is extremely important for the windows version of Fox, as Fox is essentially tested by the author under Linux – the stability of the windows version of Fox depends largely on users' feedback.

References

[1] V.Favre-Nicolin and R. Černý, J. Appl. Cryst. 35, 734, http://objcryst.sourceforge.net/Fox/
[2] R. Černý, G. Renaudin, V. Favre-Nicolin, Viktor Hlukhyy and Rainer Pöttgen, in preparation
[3] Cyril Platteau, Jacques Lefebvre, Stéphanie Hemon &Carsten Baehtz, in preparation for J. Appl. Cryst.
[3] Dirk J.A. De Ridder*, Kees Goubitz, Mihaela M. Pop, René A.J. Driessen, René Peschar and Henk Schenk, in preparation for Chem. Phys. Chem.

[1]The two dihedral angles defining the relative orientation of the phenyl, ethyl and barbital groups around the tetragonal atom were unfixed, as the exact geometry was not known. The other two free torsions define the rotations of the phenyl and ethyl group.

Unindexed Powder Pattern of the Week (UPPW)

Armel Le Bail
Université du Maine, Laboratoire des Fluorures, CNRS UMR 6010, Avenue O. Messiaen, 72085 Le Mans, Cedex 9, France.
E-mail: alb@cristal.org ;
WWW: http://sdpd.univ-lemans.fr/

During the last five years, an important effort was made in order to propose new powder pattern indexing software (see the review by Robin Shirley in the IUCr Computing Commission Newsletter No.2 [1]). Confrontation of computing programs in a Round Robin is one good way to provide informations to the potential users : should they acquire one or several of them, and which ones? Are some software more efficient in some cases? Finally in which conditions will they fail? Trying to provide useful answers to these questions is not easy. For organizing a Round Robin you need for data, and you need as well to convince people to participate (the best is to obtain the participation of the software developers themselves). Some say that the only possible data should be the best ones (from third generation synchtrotron sources). But standard crystallographers know that no sample is directly submitted to a synchrotron beam, it should deserve such an instrument. Realizing that a sample deserves synchrotron radiation is only made after a struggling conventional powder X-ray diffraction study. Anyway, a powder pattern will have to be indexed only if the compound is not identified as being already known. The best way for phase identification from powder diffraction data is to apply a search-match software which should have access to the most complete collection of data distributed into the various ICDD products (PDF-2, PDF-4 organics, etc [2]).

Paradoxically, one can identify a compound from an ICDD unindexed powder pattern. It may look strange that ICDD accepts, and even sometimes pays (Grant-in-Aid) for adding unindexed powder patterns in the database, but this occurs only if justified : "Any unindexed patterns require special justification to be accepted in the PDF. In particular, strong evidence of phase purity would be essential". Is it still always justified nowadays that some recent data in the PDF stay unindexed? Is it really that they are not undexable or is it because the operators were not confident in their indexing results? It was worth trying to index some recent uncomplete ICDD data by the most recent software, as well as by the old good major ones, and to see what happens. Indeed, this exercise was frequently practiced by P.-E. Werner, author of TREOR, see for instance his chapter in the SDPDD book [3]. Thus, selected uncomplete ICDD powder patterns were proposed, one per week, in a permanent Round Robin entitled UPPW (Unindexed Powder Pattern of the Week) [4]. There is enough data for several years !

Participants have one week for sending their solution(s). There is already a collection of these problems/solutions available which can be consulted by people wanting to have informations about the current performances of indexing computer programs. Well, how to be sure that the correct solutions were proposed? Most of the time a consensus is observed through convergent proposals, with figures of merit not that bad, indicating that a small supplementary effort from the ICDD providers would have transformed most of these UPPWs into indexed powder patterns (see figures 1 and 2). The main complaint from the participants was that they would need the raw data in order to estimate the quality and error bars. Moreover, some indexing program like EFLECH/INDEX by Joerg Bergman, winner of the indexing part of a previous SDPD Round Robin [5], require the full trace and not only the peak positions and intensities.

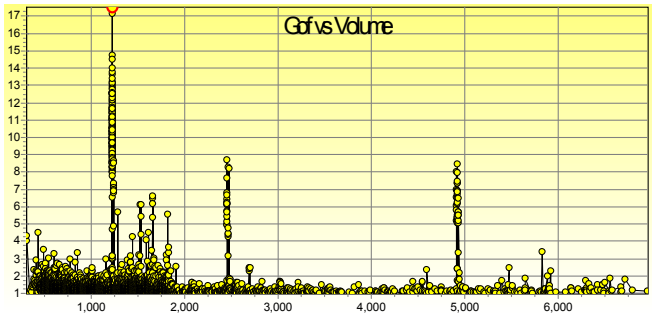

Figure 1: Using TOPAS for UPPW-1: goodness of fit versus the cell volume giving an overview of the cell proposals.

In fact, indexing a powder pattern is insufficient. Once believed to be indexed, a penultimate tests is to apply whole profile fitting with cell constraint (either the so-called Pawley or Le Bail methods) which would provide more arguments (Rp, Rwp factors, complete visual estimation, space group proposal) supporting the solution (or not) than the usual figures of merit. The ultimate test is by no less than to solve and refine the structure, which should be the unique proof of the cell veracity. This cannot be done from unindexed ICDD data, unless obtaining the raw data from the authors (it was possible in one case untill now, for UPPW-5, probably the most difficult case distributed already), or if a new pattern is recorded. Peter Stephens (X3B1 line [6]) proposed synchrotron beam time for that. If the structures of the UPPW compounds interest you, it is easy to obtain some samples which were provided by chemical company, for many of them. Moreover, if you need help in indexing your data, you are encouraged to submit your raw pattern (email address : uppw@cristal.org) which could become one of the next UPPWs, indexed by the experts in the field.

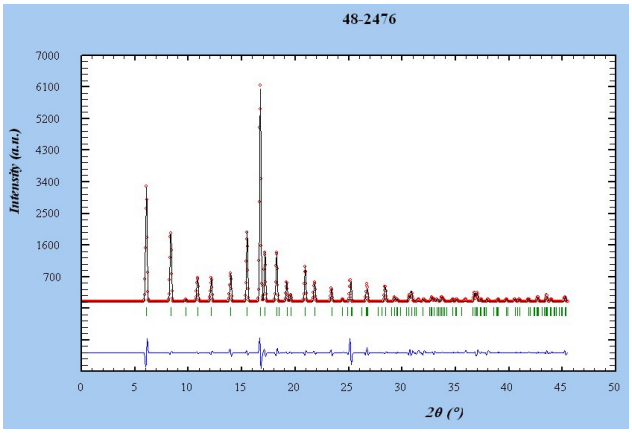

Figure 2: UPPW-2: fit on a pseudo-powder pattern by McMaille.

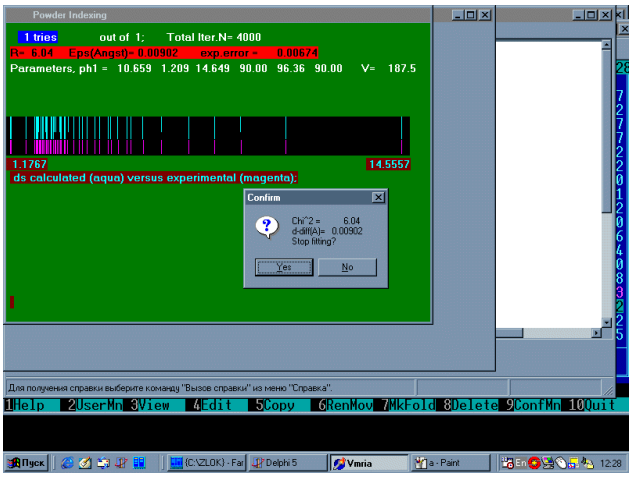

Figure 3: Indexing UPPW-2 by AUTOX showing that no line involving the Miller indice k is necessary at all.

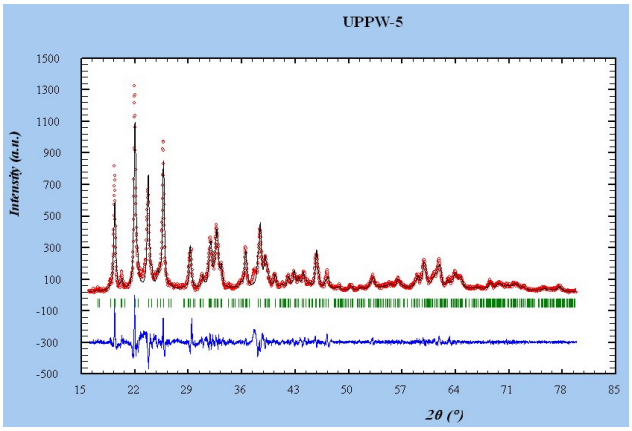

Figure 4: Cell-constrained whole profile fitting by FULLPROF, on the raw data, selecting one of the most probable cells obtained for the quite difficult UPPW-5.

A review paper about modern indexing should be written soon from these UPPWs results, gathering opinions from the authors of the most recent indexing computer programs (to be published in Z. Kristallogr.).

References

[1] R. Shirley, http://www.iucr.org/iucr-top/comm/ccom/newsletters/ - Overview of powder-indexing program algorithms (history and strengths and weaknesses), IUCr Computing Commission Newsletter 2 (2003) 48-54.
[2] ICDD - http://www.icdd.com/
[3] Structure Determination from Powder Diffraction Data, W.I.F. David, K. Shankland, L.B. McCusker, and Ch Baerlocher, Eds, IUCr Monographs on Crystallography, Vol 13, Oxford Science Publications, 2002.
[4] UPPW - Unindexed Powder Pattern of the Week - http://sdpd.univ-lemans.fr/uppw/
[5] SDPD Round Robin 2002 - http://www.cristal.org/sdpdrr2/
[6] Powder diffraction beamline X3B1 at the NSLS, BNL - http://powder.physics.sunysb.edu/

DRAWxtl, a Program for Crystal Structure Display

Larry W. Finger[(a)] & Martin Kroeker[(b)]
(a) Geophysical Laboratory (retired), USA; (b) University Freiburg, Germany
E-mail: Larry.Finger@lwfinger.net and martin@ruby.chemie.uni-freiburg.de
WWW: http://www.lwfinger.net/

The computer program DRAWxtl is designed to display a crystal structure on ordinary computers with minimal user input and maximal flexibility. It reads the basic description of a crystal structure, including unit-cell parameters, space group, atomic coordinates and thermal parameters, combines them with parameters that define the view, and outputs a geometry object that contains polyhedra, planes, lone-pair cones, spheres or ellipsoids, bonds, and the unit-cell boundary lines. With the recently released version (V4.0), the program now renders the structure object immediately using a series of OpenGL calls using the glut-programming interface. As before, scene descriptions for the popular Persistence of Vision (POV) ray-tracing program, or Virtual Reality Modeling Language (VRML) are written. The POV scene file can be used 'as is' to produce high-quality hard-copy diagrams, but it can also be edited to make use of the more sophisticated features of POV such as transparency, backgrounds and/or light effects. The VRML version is suitable for use with WWW browsers such as Netscape or Internet Explorer, and can be used to make displays suitable for interactive examination by users.

DRAWxtl can make ball-and-stick, polyhedral, or mixed diagrams, with atoms represented as spheres or thermal ellipsoids. For the latter type, anisotropic coefficients can be input as U_{ij}, B_{ij}, or β_{ij}, depending upon what is available. Polyhedral diagrams can be made with polyhedra of any desired shape, not just tetrahedra or octahedra. For the type of drawings commonly used with frameworks such as zeolites, it is also possible to make the 'polyhedron' of tetrahedral ions about the center of the cages.

The program can read structural input from files with the CIF, CSD (the Cambridge Structure Database), GSAS, SCHAKAL, and SHELX formats, as well as its own native format. As a result, crystallographic data do not need to be retyped or reformatted.

The program also outputs a table of bond distances from each of the atoms in the asymmetric unit to all other atoms. All symmetry operators are used in this calculation, with distances shorter than a specified limit (defaults to 3.5 Å) written to the listing file. This output can be used to check that input parameters are valid. For anisotropic atoms, the eigenvalues (RMS amplitudes) and eigenvectors for the ellipsoids are computed and listed.

This program is written in highly portable C and will run on a wide variety of machines including 386- and later PC's, Macintoshes, high-end workstations, and VMS systems. The only requirements are a floating-point coprocessor and a C compiler. The developers use Microsoft Visual C 6.0 (LWF) and gcc (MK and LWF). For the Windows operating system, we distribute executables. Only source code is available for other platforms.

Sample Drawings

To demonstrate the ease of producing high-quality diagrams, the familiar buckyball molecule will be used as an example. In the figure below, the POV picture on the right is produced from the input sequence on the left. The initial lines describe the unit-cell, the space group and the atoms of the asymmetric unit of the crystal structure. The 'box' command turns off the plotting of the unit cell, which is on by default. The 'pack' command selects the range of fractional coordinates to be plotted in the diagram, and the 'origin' command selects the fractional coordinates of the center of the output diagram. The 'sphere' and 'bond' commands determine the elements to be drawn, and 'phong' sets the nature of the reflection spots on the spheres. The 'view' command sets the orientation of the displayed object. The input lines for this example have been ordered by function for illustrative purposes – the data may be input in any order.

Sample drawing produced by DRAWxtl.

Sample Input:

```
title Buckyball
cell 14.16 14.16 14.16
spgp F m 3
atom c 1 0.04908 0.00000 0.24510
atom c 2 0.10028 0.08284 0.21346
atom c 3 0.18313 0.05120 0.16226
box 0.0 Black
pack -0.25 0.25 -0.25 0.25 -0.25 0.25
origin 0 0 0
sphere c 0.4 Red
bond c c 0.1 1.2 1.5 Gray30
phong 1.0 30.0
view -18 0 0
end
```

POV Diagram produced

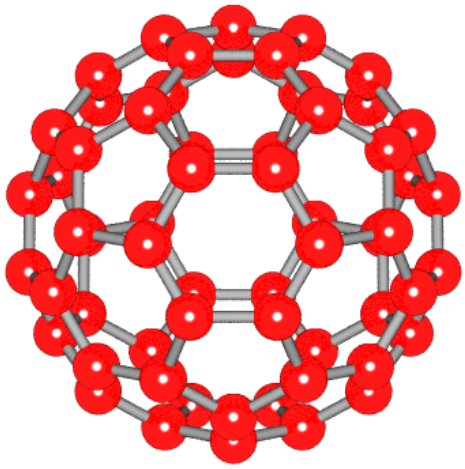

In addition to the ball-and-stick model shown above, the program may be used to produce polyhedral models of varying complexity. One of the simplest cases is that of rutile or stishovite as shown below. This tetragonal structure consists of columns of edge-shared octahedra parallel to the c axis (toward the viewer), with these columns corner linked to one another.

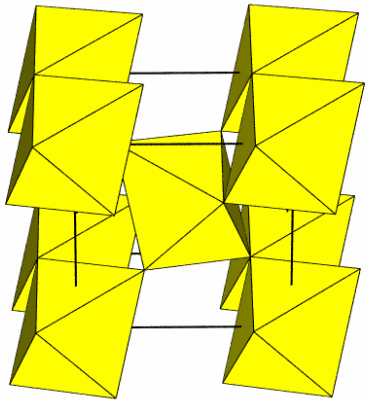

Polyhedra may be combined with ball-and- stick features to produce diagrams of greater complexity. In $AlSiO_3OH$, the phase shown below, yellow (lighter) octahedra represent Al, Si octahedra are in maroon (darker), and hydrogen atoms are represented by spheres with O-H bonds. This structure is stable at high pressure and was solved and refined from a high-resolution powder pattern collected at the ESRF (Schmidt et al., American Mineralogist 83, 881, 1998). This study is the first in which the position of hydrogen could be located from a difference Fourier map and subsequently refined from an x-ray powder diffraction profile.

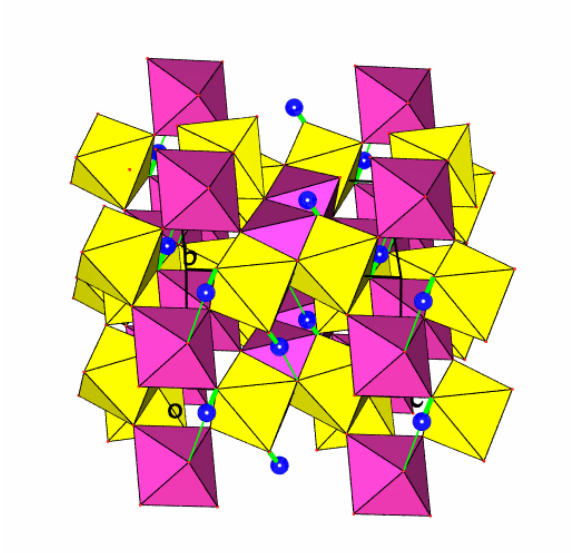

The diagram of faujasite, shown below, is an example of the zeolite-framework diagram. In this sample, each of the vertices represents a tetrahedrally coordinated cation. The only special requirement to produce such a diagram is to enter a dummy atom in the center of each void. As can be seen, the program can represent extremely complex polyhedra.

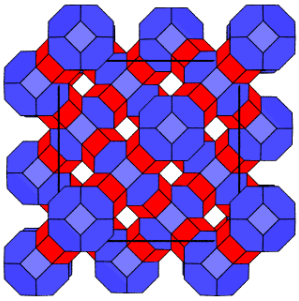

One of the new features in the latest version is the ability to generate conical sections capped with a hemisphere to represent lone-pair electrons as shown below in an isolated pseudo-tetrahedron from Cs_3SbO_3. Either one or two pairs, as appropriate, are generated with the length of the cone specified by the user.

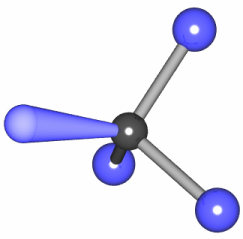

An additional type of diagram that can be produced by DRAWxtl consists of thermal ellipsoids with optional cutout of one octant as shown for the AsF_6 molecule below from the Shelx test suite. In diagrams such as these, the ellipses along the principal axes are drawn, and the cylinders representing bonds are clipped at the ellipsoid surfaces. The user controls what fraction of the probability density function is contained within the surface. This example is drawn with the default value of 50%.

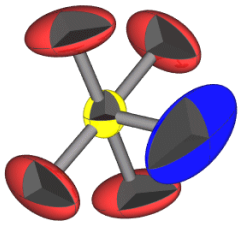

When this program was originally written, it would have been very difficult to develop a graphical-user interface (GUI) that would run on several operating systems. As one of the developers normally uses Linux, and the other Windows, it was essential that the program be portable; therefore, it has always been a command-line code. Of course, many modern users are more comfortable with a GUI. To satisfy them, we have developed shell programs that contain widgets to provide the "point-and-click" interface by internally calling the command-line code without the user having to enter the commands. For Windows, a shell written in C is shown to the left of this paragraph. We have also prepared a similar shell written in the Tcl/Tk language that will run on Linux or Windows. Now that OS X, the latest Macintosh operating system can spawn external programs, it seems highly likely that we will be able to support that platform with a shell. In addition, a number of graphical toolkits have been coded for the express purpose of making it easier to develop platform independent GUIs. We are currently investigating which of these would be the most useful if we were to convert DRAWxtl into a full GUI program.

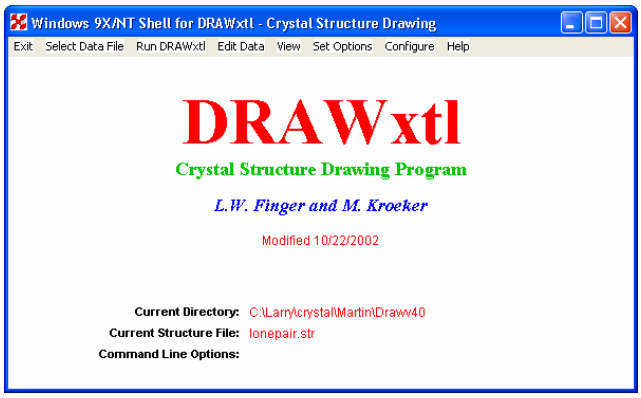

Obtaining the Program

The source code, executable programs for Windows (9X, Me, XP, NT, and 2000), sample data sets, and the manual are available from:
http://www.lwfinger.net/drawxtl/ and CCP14 mirrors.

DRAWxtl is open-source software, and is free to anyone. We hold copyright on the code, and like any other piece of intellectual property, we ask that you respect our rights. You may distribute the program to any other individual, but only in the form you received it from us. You may make any changes you like, but only the original version may be distributed. We have enough trouble fixing our own bugs, without worrying about problems introduced by someone else.

CMPR - a platform-independent graphical tool for powder diffraction

Brian H. Toby
NIST Center for Neutron Research, National Institute of Standards & Technology
E-mail: Brian.Toby@nist.gov
WWW: http://www.ncnr.nist.gov/xtal/

In response to a request for a short article on CMPR, a computer program for miscellaneous powder diffraction manipulations, I have written an overview of what the program does. To start, however, I'll try to anticipate the most commonly asked questions.

What does CMPR do?
The goals of CMPR are to read, write and plot powder diffraction data in a variety of formats; to graphically display diffractograms and stick plots; to provide rescaling; to generate & display reflection positions, showing systematic extinctions; to perform peak-fitting; to interface to other software, such as auto-indexing and smoothing software; to search & display entries from the JCPDS-ICDD database. CMPR is designed to be easily extensible, so that people (not just me) can add new features to the program.

What is new in CMPR?
1. CMPR has been combined with the LOGIC powder diffraction database search program for access to the ICDD database.
2. A self-installing executable now makes installation on Windows very simple.
3. CMPR now runs on the Mac OS X platform; OS X executables are now on the Web.

Can I use CMPR on my computer?
Yes, if it runs one of the following operating systems: Windows (-95,-NT,-98,-2000,-ME or -XP), Linux, Mac OS X, most versions of UNIX, probably VMS (http://www.rsmas.miami.edu/vms-tcl.html). Anything else (OS/2, Atari...) -- you are probably out of luck.

How do I get it; what does it cost?
It is free and the source code is in the public domain. See http://www.ncnr.nist.gov/xtal/software/cmpr/ for documentation and information on downloading.

OK, with that out of the way, what does it do? In the following paragraphs, I'll go through the major functions of the program. When CMPR starts, two windows open, as seen below. One window is the graphical user interface (GUI) and the other is for plotting diffraction data. One can select between "panels" of the GUI by clicking on the "notebook tabs" directly below the menu bar.

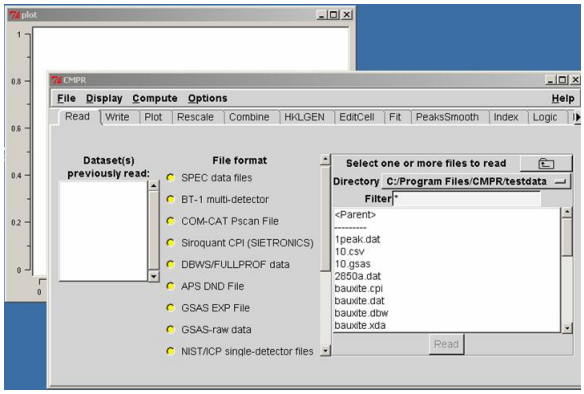

The example above shows the Read panel, where diffraction data can be imported. Note that there are many supported formats. In fact, when CMPR starts, it finds and loads the routines needed to read the files, so it is very easy to add more formats - no compilers needed. While I do not plan on writing any more import routines myself, instructions for writing these routines yourself are provided. If GSAS and CMPR are installed together, CMPR can use the GSAS TCLDUMP program to read observed and computed diffractograms (and more) from GSAS experiment files.
In the Write panel, CMPR can write data files. Not many formats are supported, but again, you can add more yourself. In the Plot panel, you which files are displayed and how they are displayed. CMPR can export plots to the Grace (XMGRACE) program, which produces publication-quality output. Grace runs nicely in UNIX and OS X; Windows uses will likely prefer to use the .csv output option and "build" the plot yourself.
The LOGIC panel provides an interface to my program for accessing the International Centre for Diffraction Data [JCPDS] database. One can search for entries based chemical constraints, on the presence or absence of peaks in regions of a pattern, etc. Entries can be displayed or can be imported for plotting, as shown below. Many other fine programs are available for accessing the JCPDS database in Windows, but few, if any, programs are available for OS X and UNIX.

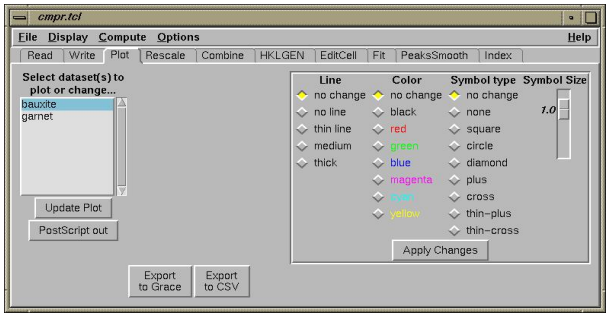

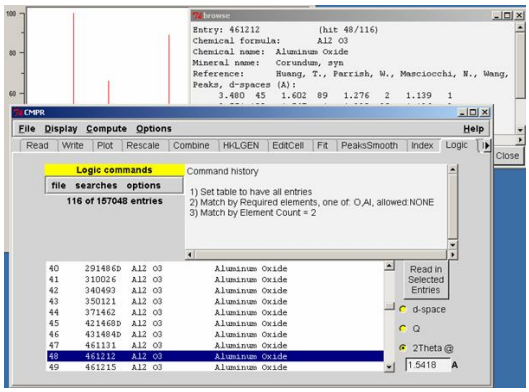

The Rescale panel offers many options for changing the way that data are displayed. One nice capability is that data sets collected at different wavelengths can be plotted as if they were collected at a common wavelength.

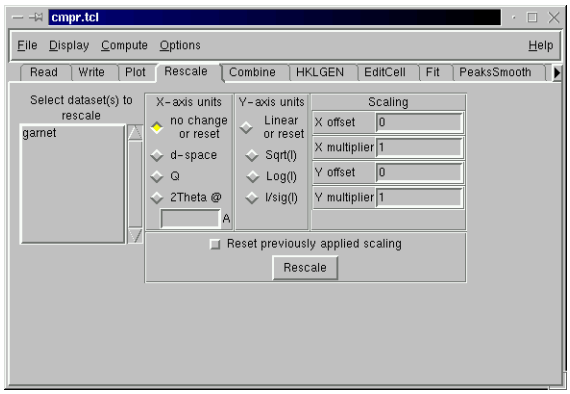

The Combine panel is used to add or subtract data sets. The data sets must be collected with the same point spacing. The experimental Interp panel, supplied by Dick Harlow, however, can be used to interpolate a dataset onto a new point spacing. Dick has also supplied the PeakSmooth panel, which smooths data, computes derivatives and also locates peaks.

The HKLGEN panel will generate a listing of reflection positions for a given unit cell and space group, but most readers will be more interested in the EditCell panel, where reflections can be generated and displayed for an arbitrary cell (see below). Note that this routine highlights extinct reflections and allows cell lengths to be modified using "sliders," so this is nice way to demonstrate aspects of powder diffraction crystallography.

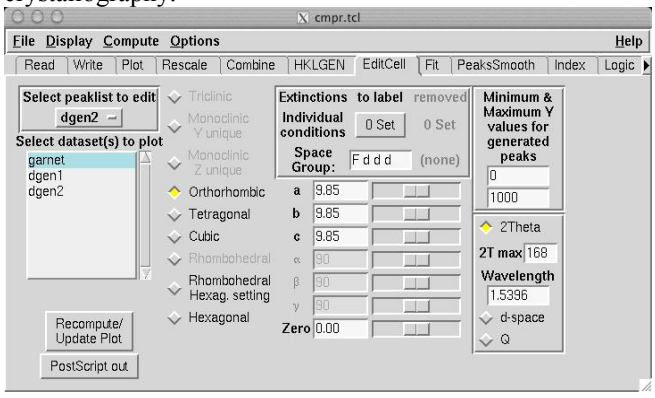

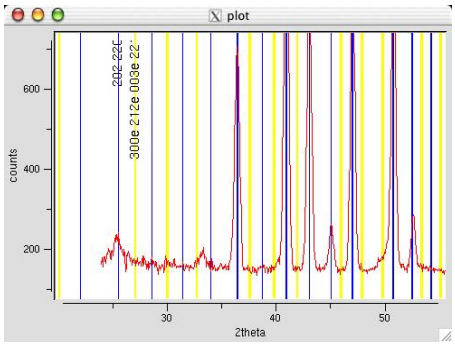

The Fit panel provides an interface to the Finger-Cox-Jephcoat peak fitting program GPLSFITA that allows peaks in a small range of a pattern to be fit. One good way to develop a list of peaks positions is step through the pattern, fitting peaks a section at a time. Thanks to the authors of the ITO, TREOR and DICVOL auto-indexing programs, who provided permission for their distribution codes within CMPR, the Index panel can be used to find unit cells that match a set of peak positions. Windows users will likely be better off using the more versatile CRYSFIRE indexing package, but for other platforms, CMPR may be easier than trying to put input together for each program by hand.

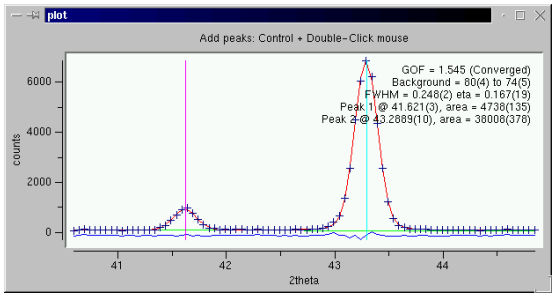

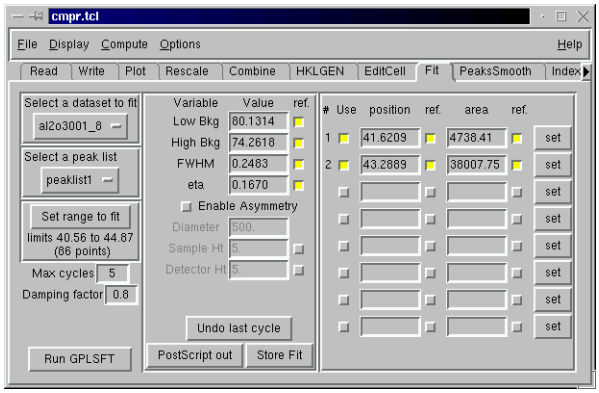

While there are many features I would like to add to CMPR, I do not expect have much time for this any time soon. I will attempt to repair bugs and assist others interested in adding new functionality to the program.

Standard disclaimer: neither the U.S. Government nor any author makes any warranty, expressed or implied, or assumes any liability or responsibility for the use of CMPR. Brand names cited here are used for identification purposes and do not constitute an endorsement by NIST.

Calendar of Events (2004)

Fifth Canadian Powder Diffraction Workshop (including neutron diffraction), 28th - 29th May 2004, University of Waterloo, Waterloo, Ontario, Canada. http://www.cins.ca/cpdw/

13th Annual CCP13/Fibre Diffraction & Non Crystalline Diffraction Workshop from 2-4 June 2004 at ILL/ESRF, Grenoble, France. http://www.ccp13.ac.uk/

2004 American Conference on Neutron Scattering College Park, MD, USA from June 6-10, 2004. http://www.ncnr.nist.gov/acns/

Polymorphism: Solvates and Phase Relationships. Erice, Italy, 9th-20th June 2004. http://crystalerice.org/Erice2004/Diversity.htm

Electron Crystallography: Novel Approaches to Structure Determination of Nanosized Materials 9-20 June 2004, Erice, Italy. http://crystalerice.org/Erice2004/electron.htm

The Joint Slovenian Croatian Crystallographic Meeting will be held in the Alpine region of Trenta, Bovec, Slovenia from 16-20 June 2004. http://rcul.uni-lj.si/~fn01leban/slkr13/

AsCA - Asian Crystallographic Association Meeting, June 27-30 2004 Hong Kong, China. http://www.ust.hk/asca04/

7th EMU School: Mineral behaviour at extreme conditions, Heidelberg, Germany, Summer 2005 http://www.univie.ac.at /Mineralogie/EMU/emusch_7.htm

XVI International School on the Physics and Chemistry of Condensed Matter Structural Aspects of Solids. Bialowieza, Poland, from 1st to 10th July, 2004, http://alpha. uwb.edu.pl/schoolXVI/

"Polymorphism in Liquid and Amorphous Matter" at the ESRF, in Grenoble (France) 7-9 July 2004.http://www.esrf.fr/Conferences/Polimat/

ACA - The American Crystallographic Association 2004 Meeting 17-22 July, Chicago, IL. http://www.uic.edu/orgs/aca2004/

22nd European Crystallographic Meeting in Budapest, Hungary from 26-31st August 2004. http://www.ecm22.mtesz.hu/

6th EMU School on Spectroscopic Methods in Mineralogy. Vienna, Austria. 30 August - 8 September 2004. http://www.univie.ac.at/Mineralogie/EMU_School/

EPDIC-IX, European Powder Diffraction Conference, Prague, Czech Republic, September 2 - 5 2004. http://www.xray.cz/epdic/

5th European Conference on Mineralogy and Spectroscopy (ECMS 2004). Vienna, Austria. 4-8 September 2004. http://www.univie.ac.at/Mineralogie/ECMS2004/

Solid State Chemistry 2004 , Prague, September 12-17, 2004.

Recent Advances in X-Ray Powder Diffraction 27 November - 2 December 2004, Assiut, Egypt http://www.geocities.com/egyptiansca/

Calendar of Events (2005)

Micro- and Mesoporous Mineral Phases: Mineralogical, Crystallographic and Technological aspects. 6-7 December 2004, Accademia Nazionale dei Lincei - Rome, Italy. http://www.lcm3b.uhp-nancy.fr/cims/ micromesoporous.htm

ACA- ACA Annual Meeting Walt Disney World, Florida, USA. 28 May-2 June 2005. http://www.hwi.buffalo.edu/aca/

XX Congress of the International Union of Crystallography Florence, Italy, August 23 – 31. 2005. http://www.iucr2005.it/

IUCr Computing School 18th to 23rd August 2005 in Siena, Italy, (prior to the Florence 2005 congress). http://www.iucr.org/iucr-top/comm /ccom/siena2005/

Calendar of Events (Sponsored by ICDD)

26-30 April 2004
ICDD, Newtown Square, Pennsylvania, U.S.A.
Practical X-ray Fluorescence Spectrometry
Covering basics of X-ray spectra, instrumentation design, methods of qualitative and quantitative analysis, specimen preparation, review of mathematical matrix correction procedures, applications for both wavelength and energy dispersive spectrometry and new developments in XRF.

7-11 June 2004
ICDD, Newtown Square, Pennsylvania, U.S.A.
Fundamentals of X-ray Powder Diffraction
Covering instrumentation, specimen preparation, data acquisition, and qualitative phase analysis.

14 – 18 June 2004
ICDD, Newtown Square, Pennsylvania, U.S.A.
Advanced Methods in X-ray Powder Diffraction
Emphasizing computer-based methods of data collection and interpretation, both for qualitative and quantitative phase analysis.

For further information contact:
Education Coordinator
International Centre for Diffraction Data
12 Campus Boulevard
Newtown Square, PA 19073-3273
Tel: +(610) 325-9814
Fax: +(610) 325-9823
E-mail: clinics@icdd.com
Web-site: www.icdd.com/education/clinics/

2-6 August 2004
Steamboat Springs, Colorado, U.S.A.
The 53rd Annual Denver X-ray Conference
The 53rd Denver X-ray Conference will be held at the Sheraton Steamboat Resort in Steamboat Springs, Colorado. The tradition of providing an international forum for discussions of state-of-the-art techniques and indications for future developments in X-ray analysis continues in the format of tutorial workshops, poster sessions, and technical sessions. In addition to providing sponsorship, the ICDD publishes the conference proceedings in CD-ROM format through the series *Advances in X-ray Analysis.* The 2004 tentative Program and *Call for Papers* are now available on the conference website.

For further information contact:
Conference Coordinator
International Centre for Diffraction Data
12 Campus Boulevard
Newtown Square, PA 19073-3273
Tel: +(610) 325-9814
Fax: +(610) 325-9823
E-mail: dxc@icdd.com
Web-site: www.dxcicdd.com

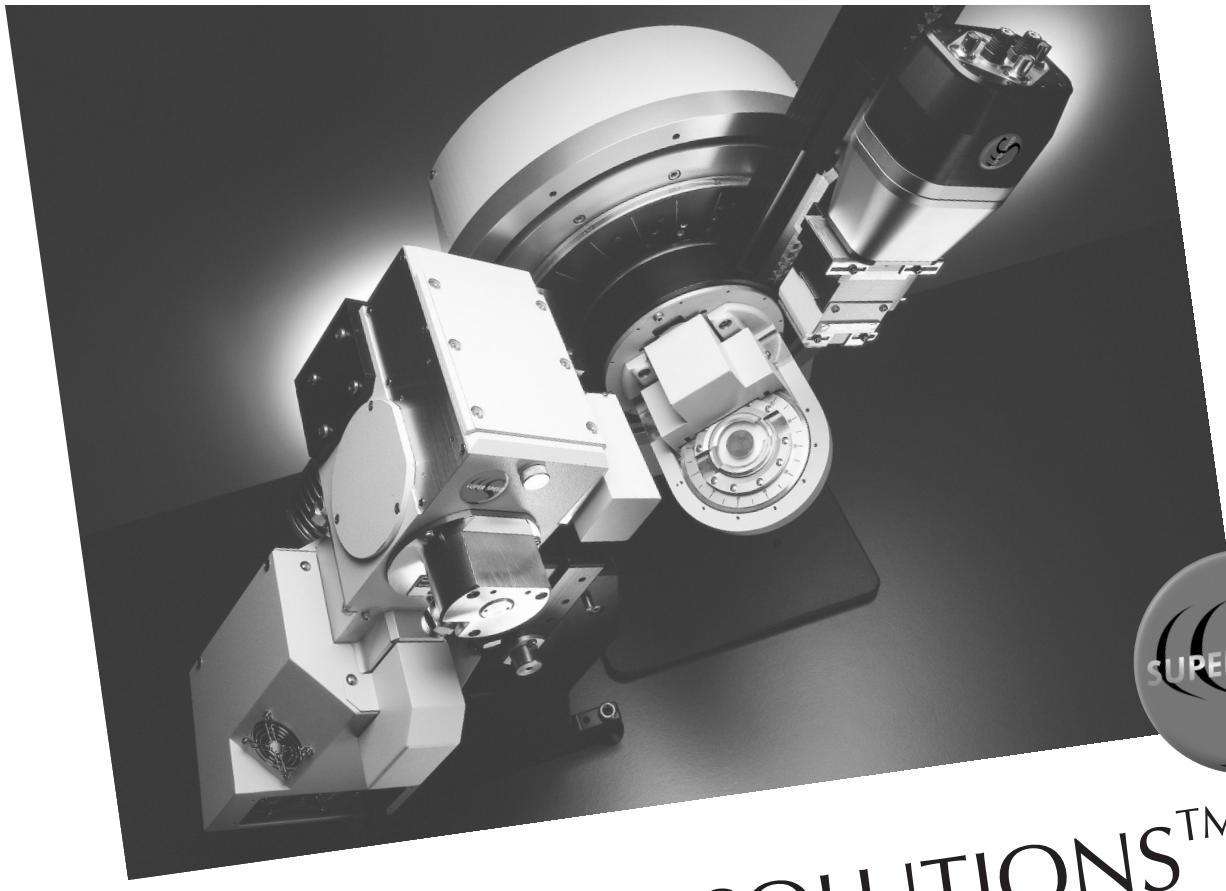

SUPER SPEED SOLUTIONS™

This stands for Speed, Power, and Perfection: 1000 times faster, 1000 times more information, and 1000 applications

- D8 ADVANCE SUPER SPEED –
  The fastest powder x-ray diffraction ever
- D8 DISCOVER SUPER SPEED –
  Thin film analysis on the way to the synchrotron
- D8 DISCOVER with GADDS SUPER SPEED –
  Microanalysis ready for takeoff
- NANOSTAR SUPER SPEED –
  Nanoanalysis in the fast lane

Are you interested? For more information:
www.superspeedsolutions.com

find out what's inside

BRUKER ADVANCED X-RAY SOLUTIONS

BRUKER axs

News from the
International Centre for Diffraction Data
(ICDD)

12 Campus Boulevard
Newtown Square, PA 19073-3273, U.S.A.
Phone: +610.325.9814
Fax: +610.325.9823

www.icdd.com
www.dxcicdd.com
E-mail: info@icdd.com

ICDD Annual Meetings

Mark your calendar!
Reserve the week of 22–26 March 2004 to attend the ICDD Annual Spring Meetings.
All are invited and most welcome.

This year's Plenary Session, scheduled for Tuesday, 23 March, will focus on Advanced Instrumentation. Advances in generator design, powerful high efficiency optics, fast and/or multidimensional detectors have resulted in increased design flexibility and new analysis capabilities in X-ray analysis. Leading experts in instrument design will discuss the technology behind these developments and their applications. Speakers include Martijn Fransen, PANalytical, Almelo, The Netherlands; Bob He, Bruker AXS, Madison, WI; and Hideo Toraya, Rigaku Corporation, Akishima, Japan. In addition, Pierre Villars will discuss the development of a new structural prototyping system used by the Linus Pauling File and proposed for the Powder Diffraction File.

Following the plenary, ICDD members, spouses, families, and guests are invited to tour the Philadelphia Museum of Art. Built in 1876, this great art institution is home to some of the most brilliant artistic achievements known throughout the world. This guided tour will offer a spectacular look at a sampling of the over 300,000 works of art sure to meet the varied interests of all in attendance.

Following the museum tour, ICDD will sponsor a poster session and reception at the host hotel, Best Western Concordeville Hotel and Conference Center. ICDD is soliciting poster presentations and their electronic abstracts for this event. Here's an opportunity to display and communicate your studies and research results. Posters relating to all aspects of X-ray analysis or work relating to ICDD are welcome.

Subcommittee, Committee, and Task Group meetings will follow on Wednesday and Thursday, 24 & 25 March.

2003 Denver X-ray Conference

The 52nd Annual Denver X-ray Conference was held in Denver, Colorado at the Denver Marriott Tech Center Hotel. The conference ran from 4–8 August, attracting 300 attendees and over 200 exhibit personnel. Most of the attendees were long-time supporters of the conference; however, approximately 10% of the attendees were first-time participants.

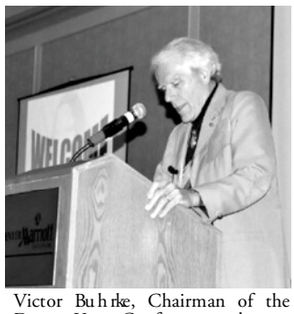

Victor Buhrke, Chairman of the Denver X-ray Conference, welcomes attendees at the Plenary Session.

Conference week began with 16 tutorial workshops, held on Monday and Tuesday. Instructors from all over the world gathered together to share their wisdom and skills. Topics included: Technical Communication, Optics, Rietveld Applications, Specimen Preparation–XRF, Alignment & Standards, Working Close to Detection Limits—XRF, Two-Dimensional XRD, Backscatter Electron Diffraction, Fundamentals of XRF, Quantitative Analysis, High Resolution—XRD and Basic TXRF.

Seventeen special sessions filled the remaining two and a half days of the conference, beginning with the Plenary Session, "X-ray Studies of Art & Archaeological Objects". Sessions covered subjects such as: New Developments in XRD & XRF Instrumentation, Rietveld Applications, High Resolution—XRD, Synchrotron Applications—XRF, Detectors & Sources, Synchrotron Applications XRD & Scattering, Stress Analysis, TXRF, X-ray Optics, Industrial Applications XRD, Quantitative XRF, Cement Analysis, Software, Pharmaceuticals, Catalysis and Problem Solving/Industrial Applications—XRF.

An awards presentation also took place during the Plenary Session to honor a variety of important contributions to the field of X-ray analysis. The 2003 Barrett Award was presented to Hugo M. Rietveld, Alkmaar, The Netherlands, recognizing the Rietveld Method of structure determination and its impact in XRD. John V. Gilfrich, Emeritus, SFA, Inc./NRL, Bethesda, MD was awarded the 2003 Jenkins Award, named after his good friend and colleague, Ron Jenkins, for his lifetime achievements in the advancement of the use of X-rays for material analysis. The 2003 Jerome B. Cohen Student Award was presented to Yukio Takahashi, Tohoku University, Sendai,

Bob Snyder (left) presented the 2003 Barrett Award to Hugo M. Rietveld (right).

Japan, for his paper, "Development and Application of Laboratory X-ray Fluorescence Holography Equipment". Frank McClune, ICDD, Newtown Square, PA, honored for his long and meritorious service to the ICDD, was presented the 2003 Distinguished Fellows Award.

John V. Gilfrich (left) received the 2003 Jenkins Award. Presented by Ray Goehner (right).

The 2004 Conference will be held 2-6 August 2004, in Steamboat Springs, Colorado. Review the *Call for Papers* by visiting the conference website at www.dxcicdd.com.

Powder Diffraction Journal

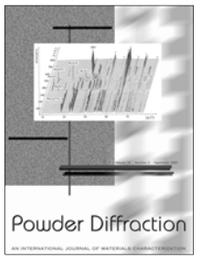

As publisher of *Powder Diffraction* and sponsor of the Denver X-ray Conference, ICDD has facilitated a partnership of these two services. The Program for the conference is now published in the June issue of *Powder Diffraction*, while the March issue will be devoted to select advance publications from *Advances in X-ray Analysis*, the proceedings series of the Denver X-ray Conference.

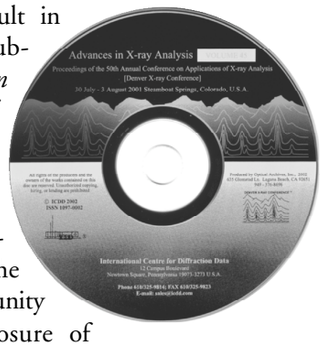

This collaboration will result in increased services for subscribers of *Powder Diffraction* as well as the authors of both *Powder Diffraction* and *Advances in X - ray Analysis*. Additionally, we anticipate that the benefits of this partnership will extend to the broader international community through the increased exposure of current developments in X-ray analysis.

ICDD Grant-in-Aid Workshops

Ekaterinburg, Russia was the location for an ICDD sponsored Grant-in-Aid Workshop, held 29 September–2 October 2003 at the Ural Branch of the Russian Academy of Sciences. The instructors for this workshop were Tom Blanton, Eastman Kodak Company, Evgeny Antipov and Andrei Mironov, both from Moscow State University.

Local organizers were Vladimir Zubkov and Alexander Tyutyunnik, both from the Institute of Solid State Chemistry, Russian Academy of Sciences.

A Grant-in Aid Workshop was also held in Nanning, Guangxi, PRC on 31 October 2003, in conjunction with the 8th National Chinese Symposium on X-ray Diffraction. Approximately 150 people attended the workshop. The instructors included Fangling Needham, ICDD; Lingming Zeng, Institute of Materials Science, Guangxi University; Shao-Fan Lin, Tianjin Institute of X-ray analysis; and Yuan Yuan Qiao, Central Laboratory, Nankai University.

New Product Releases

ICDD's current release of the Powder Diffraction File (PDF) includes 348,516 unique entries. Data from the PDF is available in the following ICDD products: PDF-2

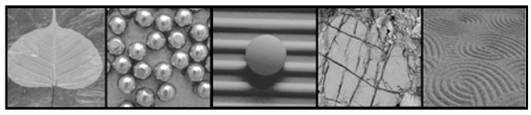

Release 2003, PDF-4/Full File 2003, PDF-4/Minerals 2003 and PDF-4/Organics 2004. Our PDF-4 databases are designed for rapid materials identification. They include indexes, display, query and sorting capabilities that allow the user to data mine the database correlating diffraction, bibliographic, unit cell and physical property data. The second edition of the organics file, PDF-4/Organics 2004, contains 218,194 entries including 70,933 new entries. This database is a practical results-oriented product designed for easy interface with diffractometers and data analysis systems from the world's leading software developers and manufacturers of X-ray equipment. PDF-4/Organics 2004 is targeted for the pharmaceutical and specialty chemical industries.

Further Information

To learn more about the ICDD, its products and services, please visit our web sites: www.icdd.com and ww.dxcicdd.com.

5th Canadian Powder Diffraction Workshop

2004 May 28-29

These two days of sessions are better described as a powder diffraction workshop being held in Canada than a "Canadian workshop".

Who should attend?

Anyone who is interested in or currently using powder X-ray, especially if you have not received formal training in X-ray powder diffraction, should consider attending. This includes students, laboratory technicians and scientists who use powder X-ray diffraction as a tool for wider research reasons.

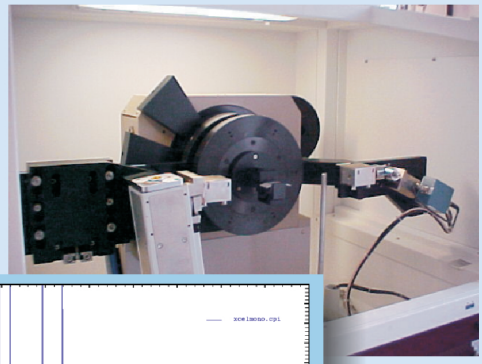

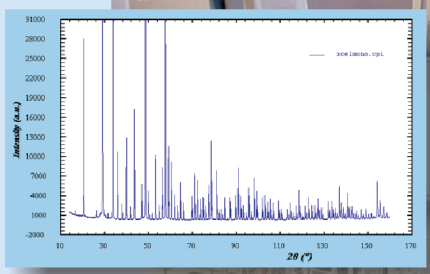

Lecture Titles Include:

Sample preparation, data collection considerations and phase identification using powder X-ray diffraction

Introduction to Powder Profile Refinement Profile Refinement with GSAS

Synchrotron Experiments

Why and when to use neutron powder diffraction

Using Rigid Bodies in GSAS

Using bond "restraints" and compositional / charge balance "restraints" in GSAS

Participants

Chair:
Professor Bruce Torrie,
University of Waterloo, Canada

Speakers:
Dr Robert Von Dreele,
Argonne National Laboratory, USA

Dr Angus Wilkinson,
Georgia Institute of Technology, USA

Dr Ian Swainson,
National Research Council Canada

Lachlan Cranswick,
National Research Council Canada

Check out the CPDW webpage for further information on the workshop and information about the Waterloo area for accompanying persons or contact Lachlan Cranswick at lachlan.cranswick@nrc.gc.ca

William G. Davis Centre
University of Waterloo
Waterloo, Ontario

Registration Costs

Students:
Cdn $125 (US~$100)

Academics and not-for-profit:
Cdn $150 (US~$120)

Commercial and Industrial:
Cdn $175 (US~$140)

Travel assistance for Canadian based students outside Ontario and Quebec is available, thanks to the Canadian Institute for Neutron Scattering.

www.cins.ca/cpdw

Canadian Institute for Neutron Scattering

University of Waterloo

CPD IUCr

NRC·CNRC

A preliminary announcement of the IUCr Commission on Crystallographic Computing

Siena 2005 - Crystallographic Computing School

Certosa di Pontignano, University of Siena, Italy
18th - 23rd August 2005

(just prior to the Florence IUCr 2005 congress)

http://www.iucr.org/iucr-top/comm/ccom/siena2005/

School Organisers: Prof Anthony Spek (Utrecht), Prof. Marcello Mellini (Siena), Prof. Alessandro Gualtieri (Modena), Dr Harry Powell (Cambridge), Lachlan Cranswick (NRC Chalk River)

Consultants: Dr David Watkin (Oxford), Dr Simon Parsons (Edinburgh)

Each day of the school is focussed on a different theme:

"principles & methods"
"joining things together"
"crystallographic implementations"
"selected topics in crystallography"
"special methods"

The City

Siena is described as one of the finest examples of a Medieval city. It is in the Italian province of Tuscany and has direct bus connection to Florence (1 hour) and Rome (3 hours).

The Venue

The Certosa di Pontignano has its origins as a medieval 14th century monastary. It is now run by the University of Siena. Attractively placed on the top of a hill, it is surrounded by vineyards; with a direct view to the town of Siena, and a famous Chianti winery.

School Aims

To have the crystallographic computing experts of the present, help train and inspire a generation of experts for the future. This will be achieved by the use of an excellent (and full) program of lectures, workshops and projects.

Università degli Studi di Siena

Registration Fees

L.E. 600 for ESCA members
L.E. 700 for Egyptians
L.E. 500 for accompanying persons
(Reduced in accordance with the decision of Supreme Council of Universities).
$ 450 for non-Egyptians
$ 250 for accompanying persons

Partial grants from IUCr are available for young scientists and postgraduate students.

The fees cover transportation from Cairo to Assiut and back, social activities and full board accommodation in double-bed rooms.

Payment can be made either directly to National Bank of Egypt, Dokki Branch, Account #01045003294 for local currency, and Account #11005003298 for foreign currency, or to the Secretary of Physics Department, Faculty of Science, Ain-Shams University. Dead time for receiving the registration fees is 1st Nov. 2004.

Use online registration or post your information (name, institution, adress, presentation & e-mail).

Mailing Address

Prof. Dr. Karimat El-Sayed
P.O.Box: 8014 Masaken Naser City, Cairo 11371.
E-mail : karima@frcu.eun.eg.
Web: www. geocities.com/egyptiansca

Key Information

International Travel

Visas must be obtained from the Egyptian Embassy. Arrival to Cairo should be arranged one day before departure to Assuit.

Gathering and Departure From Cairo

The trip to Assiut lasts about five hours. The Buses will leave Cairo to the Conference site in Assiut on Saturday 27th of November 2004 from two gathering points (will be anounced) at 7:00 am.

Organizing Committee

▪ *Yehia Abbas*	Suez Canal University
▪ *Naima. A. Ahmed*	National Research Centre
▪ *Salah Arafa*	American Univ. in Cairo
▪ *Ibrahim S. Farag*	National Research Centre
▪ *Mostafa Radwan*	Cairo Univ. (Fayoum)
▪ *Ahmed Ramadan*	Helwan University

Local Organizing Committee

▪ *Naser M. Afyfy*	Assiut University
▪ *Aamer A. El-Korashy*	Assiut University
▪ *Mohamed A. Gaffar*	Assiut University
▪ *Atef M. Abdalla*	Assiut University
▪ *Hisham M. Alattar*	Assiut University
▪ *Mohamed Almokhtar*	Assiut University

Scientific Committee

▪ *Y. Abbas*	Egypt
▪ *M. S. Ahmed*	Egypt
▪ *F. R. Ahmed*	Canada
▪ *N. A. Ahmed*	Egypt
▪ *S. Arafa*	Egypt
▪ *A. Le Bail*	France
▪ *R. B.Von Dreele*	U.S.A.
▪ *R. E. Dinnebier*	Germany
▪ *K. El-Sayed*	Egypt
▪ *I. S. Ahmed Farag*	Egypt
▪ *M. M. Radwan*	Egypt
▪ *A. A. Ramadan*	Egypt
▪ *J. Rodriguez-Carvajal*	France
▪ *J. Schneider*	Germany
▪ *A. M. Shamaah*	Egypt
▪ *R. Shirley*	U.K.

Prize

Farid Ramadan Ahmed Prize of L.E.500 will be given to the best poster.

THE EGYPTIAN SOCIETY OF CRYSTALLOGRAPHY AND ITS APPLICATIONS (ESCA)

الجمعية المصرية لعلم البلورات وتطبيقاته

NINTH INTERNATIONAL WORKSHOP OF CRYSTALLOGRAPHY

Recent Advances in X-Ray Powder Diffraction

27 November- 2 December 2004
Assiut, Egypt

Sponsored by:

* **Academy of Scientific Research and Technology, Egypt.**
* **Assiut University, Egypt.**
* **International Union of Crystallography (IUCr).**
* **The IUCr Commission on Powder Diffraction.**

The Workshop is Held Under The Auspices of

Prof. Dr. M. R. Mahmoud
President of Assiut University

Honorary Chairmanship

Prof. Dr. Ezzat A. Ahmed
Dean of Faculity of Science, Assiut University

Prof. Dr. M. Saleh Ahmed
Honorary President of ESCA

Chairmanship

Prof. Dr. Karimat El-Sayed
President of ESCA

Call for Papers

Participants who want to contribute with papers are welcomed. The submitted papers should cover work in the field of powder diffraction and its applications. The papers will be presented as posters. The authors should send an abstract on an A4 paper not later than 1st November 2004.

Basic Policy

The Organizing Committee will observe the basic policy of nondiscrimination and affirm the rights and freedom of scientists throughout the world to adhere or to associate in international scientific activity without regards to such factors as citizenship, relegion, creed, political stance, ethnic origin, race, colour, language age or sex in accordance with the statutes of the International Council for Science.

About Assiut

The Governorate of Assiut lies 350 Km south of Cairo and covering 120 Km along the Nile River. The name Assiut means the guardian of the road, meaning the guardian of the frontier of Upper Egypt. The name was first made of two syllables, sa- wat, in Hieroglyphic, and then was modified to suit the Arabic tongue and became Assiut. Assiut has rich and fascinating mixture of multicultural heritage, dating back as the Pre historic era (Dare Tasa/Sahel Selim El Hamamya - El Eqal Qably/El Badary). Then the Pharaonic times (Meer Tombs), the Greek and Roman times, the Coptic time (El Muharaq Monastery in al Qusiya), the Islamic time (Galal Addin Assiuti Mosque in Assiut city), up to the Modern times.

Objectives

During the last years fast developments in powder diffraction have been made. Advancement of the dedicated software combined with high resolution diffraction data increased the power of the powder method in structural and microstructural characterization. Accordingly, a regional Workshop is needed in order to allow researchers and post graduate students to be taught by experts in these growing fields. This Workshop will cover most of the recent developments in the field of powder diffraction. Lectures and hands on practical sessions covering many topics in the field will be given by highly specialized and eminent Professors.

Topics

1) High resolution powder diffraction: An indispensable tool in modern solid state science.
2) Structure prediction of inorganic compounds.
3) Indexing of powder diffraction using different programs (Crysfire, McMaille, ChekCell, etc).
4) *Ab-initio* structure analysis using different programs: EXPO (Direct method), ESPOIR (Reverse Monte Carlo method), etc.
5) Microstructural Rietveld analysis using different programs (GSAS, FULLPROF).
6) Rietveld quantitative multiphase analysis.

School Language

The language of the school will be English.